1-1-2012

Novel Roles for A-Type Lamins in Maintaining Genomic Stability

Abena Redwood
Washington University in St. Louis

WASHINGTON UNIVERSITY IN ST. LOUIS

Division of Biology and Biomedical Sciences

Molecular Cell Biology

Dissertation Examination Committee:
Susana Gonzalo, Chair
Didier Hodzic
Barry Sleckman
Sheila Stewart
Jason Weber
Zhongsheng You
Junran Zhang

Novel Roles for A-Type Lamins in Maintaining Genomic Stability

by

Abena B. Redwood

A dissertation presented to the
Graduate School of Arts and Sciences
of Washington University in
partial fulfillment of the
requirements for the degree
of Doctor of Philosophy

May 2012

St. Louis, Missouri

ACKNOWLEDGEMENTS

I would like to extend my most sincere gratitude to my thesis advisor, Susana Gonzalo, who has always gone beyond the call of duty to ensure not only my scientific success but also my personal well being. Susana's optimism, enthusiasm about science, and passion for teaching are only a few of the many attributes that made her a wonderful mentor. Her lighthearted spirit, consistent encouragement (and patience!) and genuine interest really impacted my time here. Words cannot express how grateful I am for this experience. ¡Muchisimos gracias!

My heartfelt appreciation goes to Ignacio Gonzalez-Suarez, David Grotsky and Martin Neumann, not only for making the lab a fun and positive environment to do science, but for always being willing to assist with experiments or techniques. I would like to especially thank Ignacio for patiently enduring the countless times I interrupted his experiments to ask questions about my own. I will fondly remember all the "lab field trips" and celebrations of birthdays, publications and grants.

I am thankful to Jason Weber, Sheila Stewart, Zhongsheng You, Junran Zhang, Barry Sleckman and Didier Hodzic who graciously served on my thesis committee. By offering invaluable feedback during joint lab meetings, sharing reagents and helping with numerous techniques, Sheila, Zhongsheng and Jun were instrumental to the development of my thesis. I would also like to acknowledge the Siteman Cancer Center for funding through the Cancer Biology Pathway Fellowship.

My experience in St. Louis would not have been the same without my friends. Special thanks to Pascale for being a super-friend, Hien, Deb & Tam for providing what seems to be our own laughing club, Esa for many amusing conversations and metro adventures, Marc for [always] entertaining my seemingly random musings, and Edwin for being supportive, understanding, and always interested/ing. I am deeply appreciative of the love and understanding that I have received

from my family, especially from my sisters Nyanda and Zahra, and my aunt Elaine. I thank my parents for encouraging me to follow my interests and most of all for being my continuous source of love and support.

This thesis is dedicated to my parents

Clive and Ivy Redwood

who taught me the value of life's intangible treasures.

TABLE OF CONTENTS

LIST OF FIGURES

SIGNIFICANCE AND OVERVIEW

Cancer remains among the leading causes of death worldwide. In 2008, the International Agency for Research on Cancer (IARC) estimated the global risk of being diagnosed with cancer before age 75 to be 21.2% and 16.5% for men and women respectively [1]. The IARC estimated the risk of dying from cancer before age 75 to be 13.4% and 9.1% for men and women respectively. The figures become even more daunting when we consider the statistics for economically developed countries like the United States of America, where males under age 75 have a 33.5% risk of being diagnosed with cancer, while women in the same category have a 26.7% risk [1]. Why is it that despite intense and prolonged cancer research over the last decades the incidence and mortality of cancer remains so high? Cancer, it turns out, is a multifaceted disease with the ability to stem from and/or affect almost any cell in the body. And with hundreds of trillions of cells in the human body [2], the real question becomes - why is the rate of cancer so low?

In an excellent review of the disease [3, 4], Hanahan and Weinberg described six features which a cell needs to acquire to become cancerous: (i) sustained stimulation of growth, (ii) resistance to tumor suppressor mechanisms, (iii) evasion of cell death, (iv) replicative immortality, (v) ability to activate angiogenesis and (vi) activation of metastasis and invasion. In a recent update they added four features that have consistently been associated with tumorigenesis: (a) evasion of immune destruction, (b) inflammation, (c) genomic instability and (d) deregulation of cellular energetics (Figure 1). Thus, it is undeniable that our own bodies do an enormous amount of work to ward of tumorigenesis and are extremely effective at doing so, at least while we are young. After age 40, the incidence of cancer dramatically increases [5] (Figure 2), indicating age as one of the single highest risk factors for cancer. Unfortunately, unlike dietary and environmental factors we are as yet unable to limit our exposure to age, so we must develop a better understanding of the relationship between age and cancer.

Research performed in the last few years has revealed important roles for the spatial and temporal organization of the genome on genome integrity and function [6, 7]. Alterations of

nuclear morphology are characteristic of aged cells and the gold standard for cancer diagnosis [8]. However, for the most part the functional interplay between genome organization and function is poorly understood both in normal tissue homeostasis and during tumorigenesis. A challenge in the field is to determine the molecular mechanisms involved in the organization of genome function, and how disruption of these mechanisms contributes to cancer and other diseases.

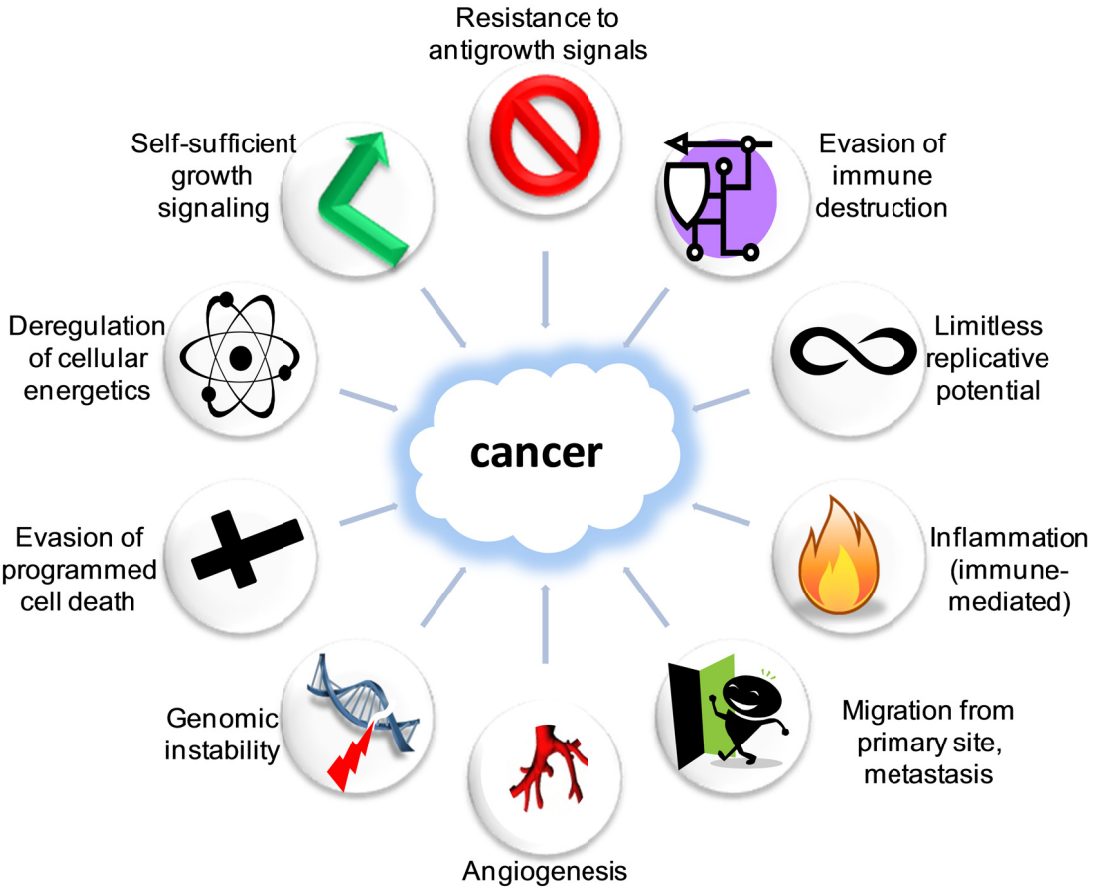

Figure 1 Characteristic features of cancer. Cells are subjected to strict regulation of growth, proliferation and survival. Cancer cells overcome these restrictions by acquiring key features: (i) evasion of apoptosis, (ii) aberrant regulation of cellular energetics , (iii) self-sufficient growth signaling, (iv) resistance to antigrowth signaling, (v) evasion of destruction by the immune system, (vi) activation of limitless replication potential, (vii) migration from primary site by metastasis, (viii) angiogenesis and (ix) genomic instability. Adapted from Hanahan and Weinberg, 2011 [3].

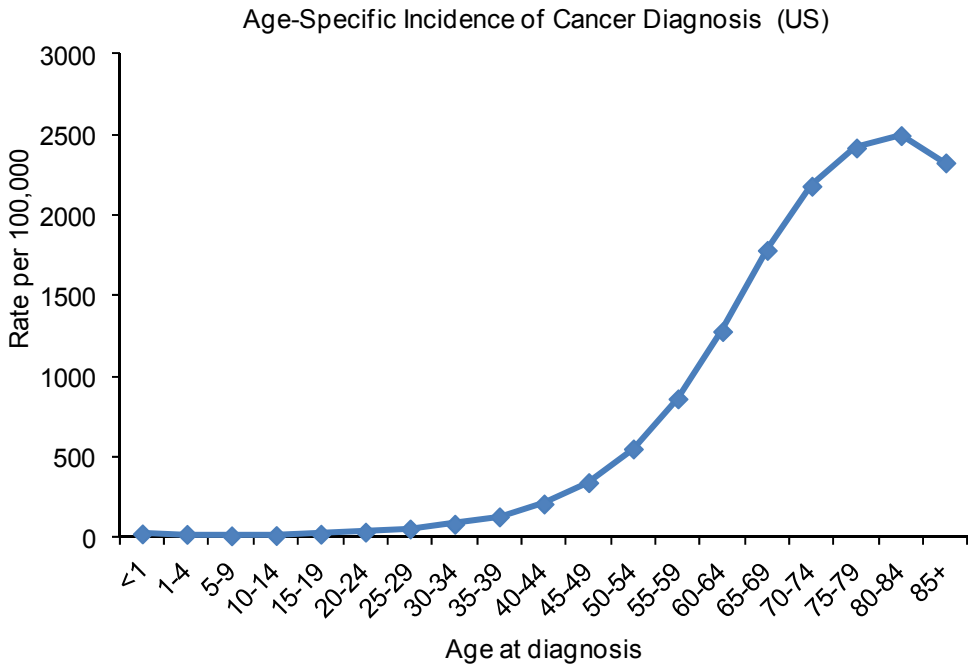

Figure 2. Age-specific incidence of invasive cancer in the US for the period of 1992 to 2008. Data from the National Cancer Institute's SEER (Surveillance and Epidemiology and End Results) program.

A-type lamins, key structural components of the nucleus, have been implicated in the maintenance of nuclear architecture and chromatin organization [7, 9]. Mutations in A-type lamins have been associated with defects in a number of nuclear processes, including DNA replication and repair, and gene transcription and silencing [10, 11]. In support of an important role for nuclear organization in pathogenesis, mutations in A-type lamins are associated with a wide variety of degenerative diseases which range from muscular dystrophies and lipodystrophies to premature aging syndromes [12, 13]. In addition, alterations in the expression of A-type lamins are associated with different cancers such as small cell lung carcinoma and gastrointestinal neoplasms [14-17]. Despite the prevalent link between A-type lamins and disease, the molecular mechanisms behind lamins-associated pathogenesis are poorly understood. Elucidation of these mechanisms would provide insight into how nuclear organization affects genome function and stability and the relationship between nuclear organization, cancer and other age-related diseases.

To advance the field, I have investigated the role of A-type lamins in the maintenance of genomic stability in mammalian cells. I present data showing novel functions for A-type lamins in the maintenance of the structure and nuclear distribution of telomeres, and the efficacy of the two major pathways of DNA double strand breaks repair, non-homologous end-joining (NHEJ) and homologous recombination (HR). Furthermore, I show that the mechanisms by which A-type lamins contribute to NHEJ and HR are distinct. A-type lamins maintain post-translational stabilization of 53BP1, which is an important NHEJ protein. In addition, A-type lamins maintain HR by regulating transcription of BRCA1 and RAD51, two essential HR factors. Importantly, the study of A-type lamins has led us to the discovery of a cysteine protease, cathepsin L, as a novel regulator of 53BP1 and the retinoblastoma tumor suppressor proteins. These findings are significant, because they reveal unexpected functions of A-type lamins and novel pathways that affect genomic stability. Our findings represent an important advance in understanding how nuclear organization affects genome function

BACKGROUND

(i) Genomic instability and tumorigenesis

Normal cells are subject to strictly controlled signaling mechanisms which ensure controlled growth, proliferation, and death if necessary. Tumors arise from cells that not only escape these controls, but also acquire the ability to stimulate growth of new blood vessels for nutrient supply, escape replicative mortality, and migrate from the primary site of formation to invade other tissues [3, 4]. Genomic instability -abnormal alterations in the structure or sequence of the genome- increases the likelihood of acquiring these characteristics [3]. In hereditary cancers, it commonly results from defective DNA damage repair due to germline mutations in DNA repair genes such as BRCA1, BRCA2 and WRN [18]. However, the cause of initial genomic instability in non-hereditary (sporadic) cancers is much less clear. Prior to therapy, sporadic cancers are not characterized by frequent mutations in DNA repair genes. Instead, the genomic instability is speculated to arise from other factors such as oncogenic mutations of caretaker genes like TP53 [18]. Defects in telomere biology and DNA damage repair are among the leading causes of genomic instability in cancer and aging.

(ii)Telomeres

Semi-conservative replication of DNA presents a unique problem for linear chromosomes. Since DNA polymerase moves in a 5' to 3' direction and requires RNA primers to begin synthesis, the very ends of the lagging strand DNA are not replicated (the "end replication problem") [19]. Thus, there is loss of genomic DNA with successive bouts of replication and cell division [19]. The presence of telomeres, highly conserved specialized nucleoprotein structures found at the end of linear chromosomes, helps to ameliorate this problem [20]. Telomeres serve a number of essential functions on chromosomes: (i) they buffer loss of genomic DNA due to the end replication problem, (ii) their specialized structure protects the ends of chromosomes from nucleolytic processing, (iii) they distinguish the ends of linear chromosomes from DNA double-strand breaks, and importantly (iv) they limit the replicative ability of the cell.

Normal somatic cells undergo telomere attrition with each round of cell division [21, 22]. When telomeres reach a critically short length, proliferation is halted as cells enter senescence, an irreversible state of cell cycle arrest [23, 24]. Cells that are able to bypass senescence continue dividing until the telomeres become so short as to trigger a second crisis, which is characterized by profound genomic instability that causes massive cell death[23]. Cancer cells acquire immortality by activating telomere lengthening mechanisms. 80-90% of cancers upregulate telomerase, a ribonucleoprotein enzymatic complex that is capable of performing de novo telomere extension [25-29]. Other cancers activate alternative lengthening of telomeres (ALT), a process which involves extension by recombination between telomere sister chromatids [30-33]. Telomere maintenance allows cancer cells to survive crisis [34] and attain unlimited replicative potential - immortalization [24, 35]. Inhibition of telomerase activity is under active research as a potential anticancer therapy [36-38].

While the length of the telomere is extremely important for its function, its tertiary structure is no less important. Human and mouse telomeres are composed of double stranded DNA (dsDNA) 5' to 3' TTAGGG repeats, capped off by a G-rich 3' overhang of single stranded DNA [39]. The G-rich overhang folds back onto the dsDNA and invades its complementary base pairing in a D-loop structure, forming a larger T-loop tertiary structure (Figure 3). Formation of the T-loop is facilitated by the shelterin complex which is composed of six proteins: the dsDNA binding TRF1 and TRF2, the ssDNA binding POT1, and the ancillary proteins TPP1, TIN2 and Rap1 [20, 40]. TRF1 and TRF2 bind directly to TTAGGG repeats and are present in the complex as homodimers. TPP1 and POT1 form a heterodimer with high affinity for the G-strand overhang, while TIN2 tethers TPP1/POT1 to TRF1 and TRF2, contributing to the stabilization of the complex [40-49]. All six proteins are necessary for maintenance of the tertiary structure, however TRF2 and TPP1-POT1 are notable for their role in preventing the telomeres from being recognized as DNA breaks by the DNA damage repair pathway. Removal of TRF2 or TPP1-POT1 shunts telomeres to the non-homologous end joining (NHEJ) DNA damage repair pathway [50, 51]. This results in end-to-end fusion of chromosomes, which leads to massive genomic instability in the

cell. In summary, a minimal length of telomeric repeats and proper binding of shelterin components is critical for the maintenance of telomere structure and function.

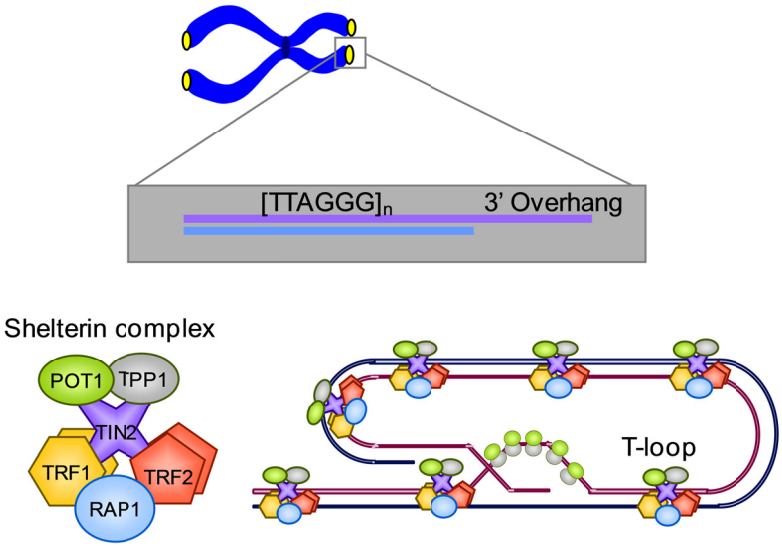

Figure 3. Mammalian chromosome and telomeres. Telomeres, specialized nucleoprotein structures at the ends of linear chromosomes, are composed of TTAGGG DNA repeats and bound by a specific group of proteins, the shelterin complex. Association of the shelterin complex facilitates formation of a distinct tertiary structure known as the T-loop, which is important for normal telomere function. Telomeres have a number of essential roles, including distinguishing the ends of our linear chromosomes from bona-fide DNA double strand breaks, and limiting the replicative potential of eukaryotic cells.

Along with the higher order conformation, telomere homeostasis is further regulated by epigenetic modifications. Telomeric chromatin is enriched in a number of heterochromatic features such as binding of HP1 (Heterochromatin Protein 1), and trimethylation of lysine 9 of histone H3 (H3K9me3) [52-54] and lysine 20 of histone H4 (H4K20me3) [55]. Loss of histone methyltransferase activities that regulate H3K9me3 or H4K20me3 at heterochromatin results in dramatic increases in telomere length in mouse embryonic fibroblasts [54]. Similarly, loss of DNA methylation at subtelomeric domains is associated with a telomere lengthening phenotype [56]. In addition disruption of HP1 binding to telomeres in human cells was associated with telomere erosion [57]. Recently, new components of telomeric heterochromatin have been identified. These are non-coding telomeric RNAs (TERRAs) that are transcribed by DNA-dependent RNA

polymerase II [58, 59]. TERRAs are emerging as inhibitors of telomerase activity and have been implicated in both the assembly of telomeric heterochromatin and regulation of telomere replication. Upregulation of TERRAs in *S. cerevisiae* resulted in telomere elongation and was associated with replication defects which resulted in increased sensitivity to hydroxyurea [60, 61]. Thus, the coordinated action of telomere length maintenance mechanisms and telomere binding proteins is essential for preserving the role of telomeres in ensuring genomic stability.

(iii)The DNA damage response (DDR)

Cells are constantly subjected to DNA damage from exogenous factors such as UV irradiation, and endogenous factors such as oxidative damage from metabolic processes, replication errors or aberrant activation of nucleases [62]. In addition to accidental DNA damage, some normal physiologic processes such as variable diversity and joining (VDJ) recombination and class switch recombination (CSR) in developing lymphocytes, involve deliberate formation of DNA breaks and require specific mechanisms of repair [63]. The presence of unrepaired double-strand breaks (DSBs) can be especially deleterious as it can trigger cell cycle arrest or even cell death when the damage is beyond repair [62]. Similarly, use of inappropriate repair mechanisms can cause genomic instability due to loss of genomic material or chromosomal translocation[64]. To counter the assaults on genomic integrity, cells have developed a DNA damage response pathway and a variety of specialized mechanisms for repair of DNA DSBs (Figure 4 and Table 1).

All organisms respond to DNA damage by launching the DNA damage response (DDR) [65, 66]. The DDR can be considered a signal transduction pathway where damaged DNA is detected by “sensors” that trigger the activation of a signaling cascade composed of protein kinases of the PIKK family – ATM (Ataxia telangiectasia mutated) and ATR (Ataxia Telangiectasia and Rad3 related) [67, 68]. The kinase cascade amplifies and transduces the initial DNA damage signal and triggers activation of “effector” proteins that activate cell cycle arrest or repair the damaged DNA. In mammalian cells, a DNA DSB is recognized by the MRN (Mre11/RAD51/Nbs1) sensor complex, which recruits ATM to the damage site. Once recruited, ATM undergoes

autophosphorylation and monomerization, and initiates the phosphorylation of a number of substrates implicated in different aspects of DNA repair such as Nbs1, the histone variant H2AX, and the tumor suppressor protein BRCA1. Additionally, ATM activates proteins involved in cell cycle arrest such as p53 and Chk2. This is particularly essential as it ensures that damaged DNA is repaired prior to DNA replication. Activation of the DDR results in repair of the DSB by either homology directed repair or non-homologous end-joining. The repair process generally includes processing of the end to remove damaged DNA, strand fill-in by DNA polymerases and finally ligation of opposite ends of the break [62, 69]. The extent of DNA end-resection during processing and the mechanism used for strand fill-in differ significantly between the two major forms of DSB repair - homology directed repair and non-homologous end-joining.

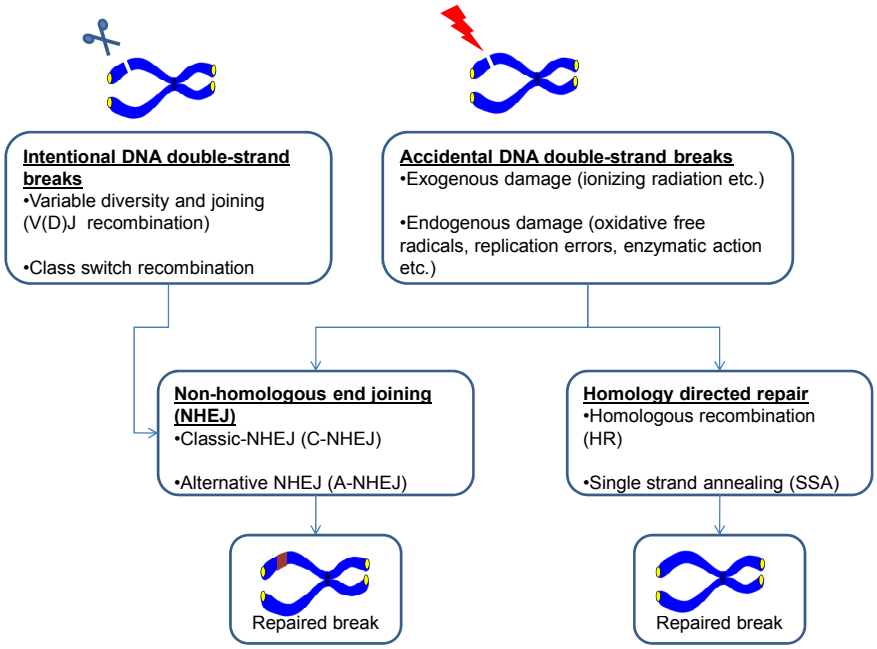

Figure 4. Mechanisms of DNA double strand break repair. Physiologic breaks such as those induced during immune cell development processes like V(D)J recombination and class switch recombination are targeted for repair by non-homologous end joining (NHEJ). Pathologic DSBs such as those occurring upon exposure to ionizing radiation, or free radical attack can be targeted for repair by NHEJ or by homology directed repair (HDR) depending on the cell cycle phase. As opposed to HR, NHEJ is error prone and likely to result in alterations in the genomic sequence at the site of repair. Indiscriminate use of either HR or NHEJ can cause genomic instability. Figure adapted from Lieber MR 2010 [63].

Table 1. Various causes of DNA double-strand breaks in eukaryotic cells. Adapted from Lieber 2010.

Causes of DNA Double Strand Breaks	
Physiological	V(D)J recombination, induced by RAG1/2
	Class switch recombination
Pathological	Ionizing radiation
	Reactive oxygen species
	Replication across a nick
	Enzymatic action at fragile sites
	Topoisomerase failures
	Mechanical stress

(iv) Homology directed repair (HDR)

Homology directed repair occurs under diploid conditions such as during meiosis or S/G2 phases of mitotic cells. Of the three types of HDR mechanisms -homologous recombination, single strand annealing and break-induced replication- homologous recombination is most frequently used [70]. Homologous recombination (HR) is possible during S/G2 phases of the cell cycle where DNA replication has produced sister chromatids to be used as templates for recombination. In the event of a DSB, there is extensive end resection of one strand of the DNA to reveal a 5' - 3' single strand overhang. ssDNA formed by end resectioning is coated with a ssDNA binding protein complex, RPA, which removes secondary structures on the DNA strand. Next, displacement of RPA on ssDNA by RAD51 forms the essential presynaptic filament, which facilitates the search for regions of homology, strand invasion and subsequent strand fill in by DNA polymerase [70-73]. The exact mechanism of DNA end resectioning in vertebrates remains unclear and seems to involve a number of different nucleases [73]. Recent studies have identified the mammalian protein CtIP as having an essential role in end resection, as depletion of CtIP leads to severe inhibition of the formation of ssDNA [74-79]. The role of CtIP in end resection relies on the ability of the phosphorylated form of the protein to interact not only with BRCA1,

which facilitates its recruitment to DSB sites [80, 81], but also with Mre11, a DNA damage sensor which possesses nuclease activity [73, 77, 82]. While the mechanism by which CtIP promotes end-resection is unclear, its recruitment is proposed to be a “switch” which facilitates end-resection of DSBs, in conjunction with MRN [79]. However the possibility remains that CtIP itself has nucleolytic activity, as has been shown for the S. cerevisiae homolog Sae2 [73].

BRCA1 functions as a tumor suppressor and mutations in the gene are commonly associated with breast and ovarian cancer [83-85]. The role of BRCA1 as a tumor suppressor stems from its essential role in facilitating formation of ssDNA during homologous recombination [86, 87]. BRCA1-deficient cells display significant reduction in the formation of ssDNA and subsequent recruitment of ssDNA binding proteins such as RPA and RAD51. Recent reports have established BRCA1 as a “competitor” against the NHEJ protein 53BP1 for DSB repair substrate [88-91]. These studies showed that loss of BRCA1 was associated with decreased HR and increased formation of aberrant chromosomal structures, and that this phenotype was reversed by decreasing 53BP1. The authors speculated that in the absence of BRCA1, DSBs that would normally be fixed by HR are retargeted for NHEJ by 53BP1, leading to ligation between incompatible DSBs which result in aberrant chromosome structures [90]. Removing 53BP1 is postulated to reduce this NHEJ pressure, which increases the competitive ability of HR. Thus, 53BP1-mediated NHEJ is a direct competitor of BRCA1-mediated HR. Activation of HR in the absence of sister chromatids could result in recombination between homologous regions of non-sister chromatids, which could cause loss of heterozygosity, or chromosomal translocations if non-allelic sequence templates are used [70]. Interestingly, Shibata A. et al. recently reported that NHEJ is used as the first attempt for DSB repair even during the G2 phase of the cell cycle of human fibroblasts [92]. The authors propose that components of THE NHEJ pathway are preferentially recruited to DSBs, but in the event of structural complexities at the lesion, the NHEJ proteins give way to HR.

(v) Non-homologous end joining (NHEJ)

NHEJ is dominant during G0/G1 and early S phase. It relies on ligation between DSB ends that have undergone minimal processing [93]. Upon recognition of a DSB, the Ku70/Ku80 heterodimer encircles the DNA end and helps to recruit DNA-dependent protein kinase catalytic subunit (DNA-PKcs), a member of the PIKK family of protein kinases. DNA-PKcs undergoes autophosphorylation and phosphorylates a number of proteins at the break site [63, 94]. Recruitment of the DNA processing enzyme Artemis follows activation of DNA-PKcs kinase activity. Artemis is important for the formation of 5'-phosphorylated ligatable DNA ends putatively through it's exo- and endonuclease activities [95-97]. Further processing such as gap-fill in by DNA polymerases (μ and λ) might be required to prepare the DNA ends for ligation [63]. Once compatible ends have been formed ligation occurs by a complex containing XRCC4, a ku interacting protein, and the ligating enzyme DNA ligase IV. The ligation step is significantly different from HR, as it requires neither significant end-resection nor homologous sequences for strand fill-in by DNA polymerase.

The ku70/80 heterodimer can interact with and recruit nucleases, polymerases and the ligase complex in any order [63]. This allows flexibility in the sequence of processing events at the DSB site, with the result that a single DSB can yield different DNA sequences at the region of ligation. For example, a break that is processed by a nuclease and then a polymerase will be different from one that is processed by a nuclease and then a DNA ligase. Further diversity might occur from recruitment of polymerase μ, which is capable of template-independent DNA synthesis for strand fill-in. Thus, unlike HR, NHEJ is inherently associated with alterations of the DNA sequence at the site of repair. While NHEJ is more error prone than HR it is essential not only for the timely repair of pathogenic DSBs, but also for endogenous processes which involve deliberate formation/repair of DSBs, such as class switch recombination (CSR) and variable diversity and joining recombination (VDJ) in lymphocytes [98-100]. Mutations in NHEJ genes are associated with increased radiosensitivity as well as immunodeficiency syndromes [101, 102].

Along with this “classic” form of NHEJ (C-NHEJ), recent work has begun to demonstrate the importance of a less understood pathway designated “alternative-NHEJ” (A-NHEJ) pathway [93, 103, 104]. A-NHEJ is distinct from C-NHEJ in its requirement for short regions of microhomology between ligatable ends of DNA [93, 105]. A-NHEJ relies on CtIP-mediated resection of DNA to reveal short regions of homology, which then undergo ligation primarily mediated by DNA ligase III [104, 106]. Unlike homologous recombination, DNA that is resected during A-NHEJ does not undergo strand fill-in from a homologous sequence, so there is permanent loss of DNA sequence, making it a potentially more deleterious pathway than C-NHEJ or HR. In line with this idea, A-NHEJ was reported to play a primary role in the formation of chromosomal translocations in mouse embryonic stem cells [103].

(vi) p53 Binding Protein 1 (53BP1)

53BP1 was initially discovered in 1994 in a yeast two-hybrid screen as a p53-interacting protein [107]. Since its discovery it has been demonstrated to play significant roles in DSBs repair pathways with a primary role in NHEJ of long-range DNA breaks and an indirect role as a suppressor of other pathways of DSBs repair [108-112]. 53BP1 is necessary for efficient repair of non-pathogenic “long-range” DSBs such as those that occur during V(D)J recombination or class-switch recombination in immune cell development and maturation [51, 98-100, 113]. Maturation of the immune system B and T lymphocytes involves generation of DSBs by RAG1 and RAG2 endonucleases at recombination signal sequences on different gene segments (Variable, Diversity and Joining). Ligation of the DSBs produces the heavy and light immunoglobulin chains during maturation. 53BP1 was shown to be necessary for joining between distal (long-range) sequences, but dispensable for short range end-joining. Consistent with these roles, 53BP1$^{-/-}$ mice suffer a significant reduction in the formation of B & T cell lineage cells [100]. Similarly, 53BP1 is necessary for long range DSBs end joining which occurs in class switch recombination during B cell activation, and also in the processing of telomeres that are rendered deprotected by loss of the TRF2 shelterin complex component [51, 98]. The mechanism by which 53BP1

promotes end-joining between distal DSBs is unclear, but thought to involve promotion of synapsis, chromatin relaxation and possibly regulation of the mobility of DSBs [114, 115].

A number of unresolved questions remain regarding the role of 53BP1 in repair of different forms of DNA DSBs. For example, 53BP1 is immediately recruited to DSBs induced by ionizing radiation (IR), however loss of 53BP1 has only a mild effect on the repair of IR-induced breaks. Furthermore, the necessity for 53BP1 seems to depend on the amount of DSBs that are present, such that 53BP1 has a bigger impact on the repair of low levels of DSBs, putatively through its ability to promote recruitment of the MRN complex (which then promotes ATM recruitment) via binding of Rad50 to the BRCT domain of 53BP1 [111, 114, 116]. It is speculated that high levels of IR-induced DSBs can sufficiently stimulate MRN recruitment and activation of ATM, while low levels stimulate only a mild DDR, and thus require assistance from 53BP1 [114]. Recent work demonstrating a specific role for 53BP1 in late-repairing heterochromatic DSBs has begun to shed light on these issues, showing why 53BP1 might only be required for repair of a subset of IR-induces breaks. A.T. Noon and colleagues [114] demonstrated that 53BP1 promotes localization of phosphorylated KAP-1 (pKAP-1, KRAB Associated Protein-1) at late repairing heterochromatic DSBs that were induced by IR. pKAP-1 promotes repair of heterochromatic DSBs by inhibiting the function of CHD3, an ATP dependent chromatin remodeling enzyme which promotes nucleosome compaction [117]. Thus, 53BP1 plays a significant role in repair of breaks in heterochromatic regions of the genome by affecting chromatin structure.

Recent work revealed that 53BP1 suppresses HR and A-NHEJ putatively by binding to DSBs and inhibiting end-resection [90, 118]. Further work is required to clarify the exact mechanism of inhibition; however the implication of 53BP1 in other repair pathways is exciting, as it suggests novel approaches for cancer therapy. A number of elegant studies recently demonstrated that loss of 53BP1 can reverse some of the phenotypes associated with BRCA1 deficiency [89-91]. In particular, cells double null for BRCA1 and 53BP1 exhibit a much lower degree of genomic instability and have increased survival when treated with DNA damaging

agents. These studies demonstrate that loss of 53BP1 is “synthetically viable” with BRCA1 loss [88]. The current view is that loss of BRCA1 results in defective end-resection of DNA DSBs. In this context, accumulation of 53BP1 at the breaks promotes NHEJ.

The interplay between 53BP1 and the HR pathway is functionally important, as it could contribute to the development of resistance of BRCA1-mutated cancers to treatment with DNA damaging agents. A major breakthrough in the treatment of BRCA1-mutant tumors was the finding that these types of tumors are very sensitive to poly(ADP-ribose) polymerase inhibitors (PARPi) [119, 120]. The targets of PARPi are PARP1 and the closely related PARP2 proteins, which are activated at sites of DNA breaks to catalyze the formation of poly(ADP-ribose) polymers both on themselves as well as other substrates [121-124]. Inhibition of PARP activity hinders repair of single stranded DNA breaks, which are converted to DSBs if encountered by a replication fork during DNA synthesis in S-phase. [120, 125]. Since DSBs are primarily repaired by HR during S-phase, lack of BRCA1 impairs repair of these DSBs and leads to activation of cell cycle arrest and/or cell death. Thus, treatment of BRCA1-mutated cells with PARPi is a way to selectively induce death. Despite the promising results of phase 2 trials the first phase 3 clinical trial with iniparib, the most advanced PARPi, was disappointing as it did not improve patient survival [126]. Given that double deficiency of BRCA1 & 53BP1 in mouse cells promotes resistance to PARPi, it is likely that loss of 53BP1 is one of the key mechanisms activated by BRCA1-mutated tumors to develop resistance to PARPi. This is supported by the fact that there is decreased 53BP1 expression in a subset of BRCA1-associated breast cancers and that loss of 53BP1 is associated with a decreased likelihood of survival in breast cancer patients [88, 89]. Thus, 53BP1 is a key player in DNA damage repair and genomic stability, directly through its role in NHEJ and indirectly through its crosstalk with the HR pathway.

(vii) Aging and tumorigenesis

The likelihood of being diagnosed with cancer increases exponentially with age, up until age 75 (Figure 2) [5], making age one of the greatest “risk factors” for cancer. In recent years, a number of studies addressed whether or not age actually contributes to tumorigenesis or is merely associated with it. This question has posed difficult to answer, as cancer and aging are characterized by many of the same features such as genomic instability, cellular senescence, autophagy and alterations in telomere biology [127]. Intriguingly, a number of human diseases present with mutations in factors that are involved in DNA replication and the DDR pathways [128] (See table 2). A whole body of evidence indicates that mutations in factors involved in DNA replication, the DDR pathway or mechanisms of DNA repair result in premature aging and increased cancer susceptibility [128-130].

Mutations in the gene coding for Werner protein (WRN) give rise to Werner Syndrome, a premature aging disease which associates with increased risk of cancer, especially carcinomas and sarcomas [130]. WRN is a member of the RecQ family of DNA helicase and displays both helicase and exonuclease activity, which are necessary for DNA replication. Patients afflicted with Werner Syndrome present with premature aging which begins to manifest in early adulthood with features such as grey hair, wrinkled skin, bone loss, diabetes type II and atherosclerosis. Cells from these patients are characterized by increased chromosomal instability and prolonged S-phase [131, 132]. A report on cells from a Werner Syndrome patient indicated abnormalities in nuclear shape, such as nuclear invaginations and protrusions, suggesting possible defects in nuclear organization [133]. Interestingly, several heterozygous mutations in the LMNA gene, which codes for the nuclear structural proteins lamin A and lamin C, also cause a similar phenotype, Atypical Werner Syndrome, which features premature aging, bone loss and diabetes [134-136]. However, there have been no reports on genomic instability in LMNA-associated Atypical Werner Syndrome to date.

Table 2. A number of diseases that manifest premature aging are associated with mutations in genes involved in the DNA damage response pathways.

Premature Aging Syndromes Associated with Mutations in DNA Repair Genes
Ataxia Telangiectasia (ATM)
Werner Syndrome (WRN)
Bloom Syndrome (BLM)
Dyskeratosis Congenita (DKC1, TERC)
Aplastic Anaemia (TERC, TERT)
Fanconi Anemia (Fanc genes)
Nijmegen Breakage Syndrome (NBM)

Another interesting link between A-type lamins and premature aging is manifested by the most severe premature aging disease, Hutchinson-Gilford Progeria Syndrome (HGPS) [137-140]. HGPS arises due to a mutation in the LMNA gene which results in production of a mutant protein, progerin. Children with HGPS appear normal at birth but within a year they begin to manifest characteristic features of aging such as shortened stature, craniofacial disproportion, alopecia (hair loss), osteoporosis and abnormal distribution of fat. These children die very young, usually by their early teens, due to severe atherosclerosis and cardiovascular complications. Interestingly, progerin has also been shown to accumulate in cells from aged individuals, further implicating A-type lamins in aging and tumorigenesis. Along these lines, HGPS fibroblasts undergo faster telomere attrition than their normal counterparts and have global defects in the epigenetic marks characteristic of constitutive heterochromatin [22, 141]. Given the commonalities between aging and cancer and the link between A-type lamins and premature aging, we speculate that the molecular mechanisms responsible for the pathogenesis of LMNA mutations might be similar to those involved in cancer and physiological aging.

(viii) A-type lamins: structure and distribution

A-type lamins are type V intermediate filaments found exclusively in the nuclei of differentiated cells [12, 142, 143]. The major products of the LMNA gene are lamin A and its smaller splice variant lamin C, which lacks 92 amino acids at the C-terminus. Minor products of the LMNA gene are lamin AΔ10 and lamin C2, a testis specific protein [144]. A-type lamins are expressed only in differentiated cells and are absent during embryogenesis up until mouse embryonic day 12, where tissue-specific expression becomes apparent [145]. While most adult tissues express A-type lamins a few, including cells of the immune system such as B and T lymphocytes, cells isolated from the bone marrow, and pancreatic islets, show little to no expression [146].

Within the nucleus, A-type lamins form coiled-coil filaments that are juxtaposed to the inner nuclear membrane as a filamentous mesh that interacts with locally distributed proteins such as integral nuclear membrane proteins, B-type lamins and lamins-associated proteins (LAP) [144]. A fraction of lamin A/C extends throughout the nucleoplasm where they also interact with numerous proteins involved in cell cycle regulation, including Rb and PCNA [147-149]. Initial translation of the LMNA transcripts yields mature lamin C and a premature form of lamin A, prelamin A, which undergoes extensive post-translational processing to yield the mature form. Prelamin A contains a C-terminus CAAX motif which is targeted for farnesylation for attachment to the inner nuclear membrane. Following farnesylation, the Zmpste24 enzyme cleaves prelamin A at a specific site within the C-terminus. This cleavage relieves lamin A of its farnesylation and produces mature lamin A. A-type lamins are thought to play a scaffolding role for tethering chromatin to specific sub-compartments, which in turn serves to organize nuclear processes [7, 9, 12, 150]. In fact, depletion of A-type lamins or expression of mutant forms of the proteins leads to defects in chromatin remodeling and in the 3D organization of the genome, as exemplified by loss of heterochromatin from the nuclear periphery [13, 151].

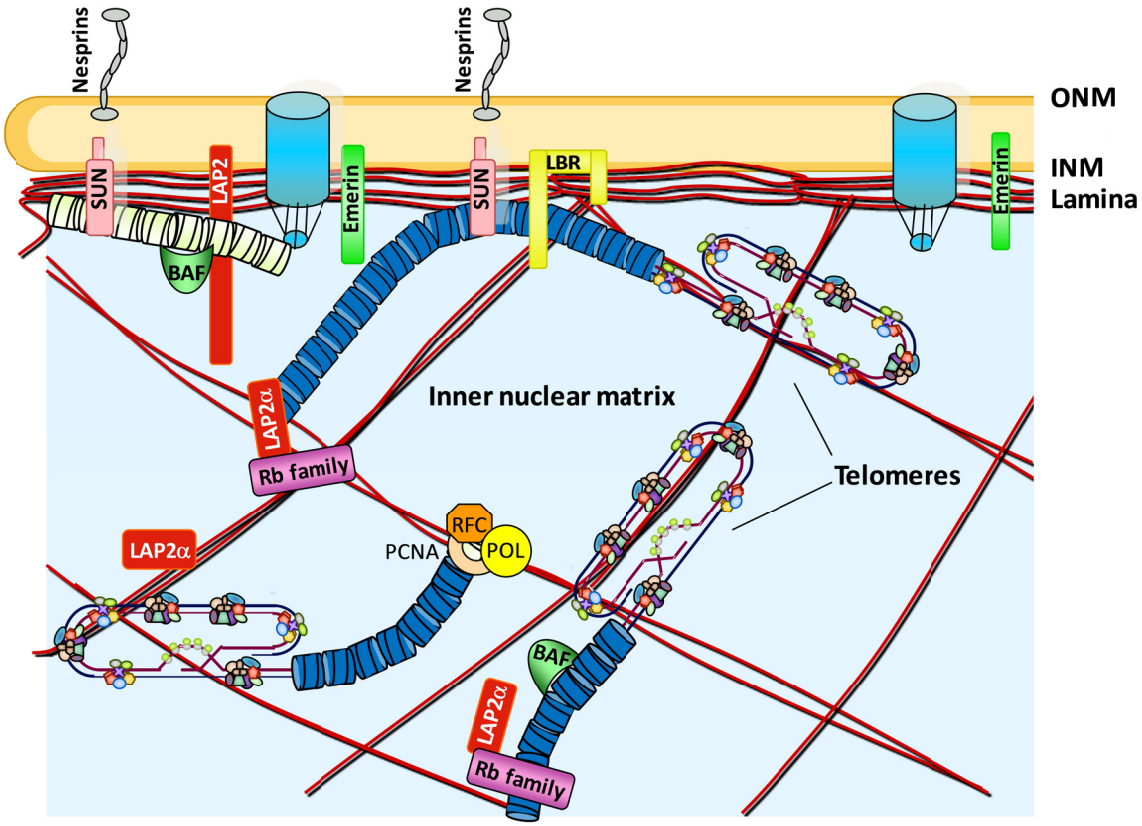

Figure 5. Nuclear distribution of A-type lamins. A-type lamins (in red) form a filamentous meshwork juxtaposed to the inner-nuclear membrane, where they interact with different membrane proteins, such as emerin and SUN proteins. Additionally, they extend throughout the nucleoplasm where they also interact with a variety of proteins, such as those of the retinoblastoma family and PCNA. A-type lamins also associate directly with DNA and chromatin.

Interestingly, changes in the expression of A-type lamins are observed in leukemias, lymphomas, small cell lung and ovarian cancer, as well as colon carcinoma, often associated with poor prognosis [14-17]. The cellular mechanisms affected by these malignancy-associated alterations of A-type lamins are only beginning to be unraveled. In recent years, various lines of evidence have linked lamins-associated diseases with increased genomic instability. In particular, the expression of A-type lamins mutant isoforms has been associated with defective DNA repair in mouse fibroblasts [152, 153].

(ix) A-type lamins and disease

Alterations in the processing of lamins A/C, either through mutations in the LMNA gene or the processing enzymes, can lead to pathogenesis. In particular, mutations in the LMNA gene are associated with a number of degenerative diseases, collectively termed laminopathies, which are divided into two broad non-exclusive categories: diseases that affect striated muscle (muscular dystrophies) and diseases that affect adipose tissue (lipodystrophies) and bone [12, 142, 154]. The muscular dystrophies are characterized by wasting or lack of development of muscular tissue and include autosomal dominant emery-dreyfuss muscular dystrophy (AD-EDMD), limb-girdle muscular dystrophy 1B (LDMD1B) and dilated cardiomyopathy (DCM). Diseases of the adipose tissue and bone feature hyperlipidemia, aberrant distribution of white adipose tissue, and sometimes abnormal bone structure in diseases such as familial partial lipodystrophy (FPLD) and mandibuloacral dysplasia (MAD). In an overlapping phenotype, mutations in A-type lamins can feature defects in both adipose tissue and bone structure, as well as defects in striated muscle, as seen in HGPS, a severe premature aging disease. HGPS is caused by a single mutation (1824C>T, G608G) which results in activation of a cryptic splice site within the LMNA gene, leading to removal of the Zmpste24 cleavage site [140, 155]. This aberrant version of lamin A (known as progerin) is still farnesylated, however absence of the Zmpste24 cleavage site prevents further processing and it accumulates at the nuclear membrane, causing abnormalities in the nuclear shape such as nuclear blebbing and invagination [139].

(x) Mouse models of laminopathies

In an effort to understand the pathogenesis behind LMNA mutations, several groups have developed mouse models of various laminopathies [156]. These mouse models of laminopathies have ranged from deletion of the LMNA gene ($Lmna^{-/-}$) or a lamin A-processing enzyme ($Zmpste24^{-/-}$) to introduction of various mutations in the LMNA gene [151, 157]. The different mouse models reproduce varying spectrum of human laminopathies. The $Lmna^{-/-}$ and $Zmpste24^{-/-}$ mice have been most extensively characterized. $Zmpste24^{-/-}$ mice are normal at birth up until 4

weeks, after which they present decreased growth rate, size, abnormal posture, muscular dystrophy and loss of subcutaneous fat [157, 158]. These mice eventually succumb to death within 20 weeks due to dilated cardiomyopathy and heart failure. The Lmna$^{-/-}$ mice are very similar to the Zmpste24$^{-/-}$, showing growth retardation, lipodystrophy, muscular dystrophy, cardiac and skeletal myopathy and death within 8 weeks [151]. Most of what we currently understand about the role of A-type lamins in pathogenesis has been gleaned from studies in the mouse models of laminopathies.

A-type lamins function in a number of nuclear processes, including positioning of nuclear pore complexes, interaction with chromatin, DNA synthesis and transcription [10, 11, 159]. However, the exact molecular mechanisms behind the function of lamins in these processes remain undefined. Studies from the Zmpste24$^{-/-}$ mice as well as cells from HGPS patients have shed some light on the mechanisms which might contribute to pathogenesis. Bone marrow cells from the Zmpste24$^{-/-}$ mice have increased genomic instability, characterized by chromosome breaks and presence of γ-H2AX foci, while fibroblasts from HGPS patients and Zmpste24$^{-/-}$ mice have alterations in the DDR [152, 160]. At a molecular level, HGPS and Zmpste24$^{-/-}$ MEFs showed delayed recruitment of 53BP1 to DNA repair foci upon treatment with ionizing radiation, and delayed disappearance of these foci [152]. Interestingly, Zmpste24$^{-/-}$ MEFs are thought to have enhanced NHEJ, based on their increased ability to efficiently re-join a linearized plasmid after transient transfection. Zmpste24$^{-/-}$ MEFs also showed impaired recruitment of RAD51 to sites of DNA damage leading to a delayed checkpoint response and defective DNA repair, suggestive of impaired HR [152]. In additional support of a role for A-type lamins in the DDR, ectopic expression of mutant forms of lamin A in the presence of wild-type lamin A/C was sufficient to inhibit formation of γ-H2AX-labeled DNA repair foci in response to mild doses of cisplatin or UV irradiation [161]. All these reports suggest that unprocessed prelamin A and truncated lamin A act in a dominant negative fashion to perturb DNA damage response and repair.

(xii) A-type lamins and cancer

Aberrant nuclear morphology and changes in the nuclear lamina are emerging as characteristic features of cancer cells [8]. This suggests that factors that are important determinants of nuclear architecture might be relevant for understanding tumorigenesis. In fact, the expression of A-type lamins has been shown to be altered in a number of malignancies including small cell lung carcinoma (SCLC) and certain types of gastrointestinal neoplasms [14, 17, 162, 163]. Furthermore, A-type lamins are implicated in a variety of pathways that are involved in genomic instability and tumorigenesis. One of the most notable pathways involves the stabilization of the retinoblastoma tumor suppressor proteins pRb and p107 by A-type lamins. Using cells from wild-type and $Lmna^{-/-}$ mice, Johnson et al. (2004) demonstrated interaction between A-type lamins and pRb, and that loss of A-type lamins leads to increased proteasomal degradation of pRb and p107 [148]. Given the significant roles of pRb and p107 as bona-fide tumor suppressors [164], the mechanism by which they are regulated is of relevance to this field. However, studies attempting to understand the mechanism of lamins-dependent pRb/p107 degradation have only managed to demonstrate that MDM2 and gankryin, the pathways currently known to regulate their stability, are not involved in this process [165]. Thus loss of A-type lamins leads to degradation of pRb/p107 by a mechanism that has remained elusive.

Given that A-type lamins are strongly implicated in aging and are emerging to be relevant for cancer, we hypothesized that they are involved in the maintenance of genomic stability. To test this hypothesis we investigated various components of genomic instability, such as alterations in telomere biology, chromosomal structure and the efficacy of DNA damage repair pathways in lamin A/C-proficient or deficient mouse and human cells. Strikingly, we found that lamin A/C-deficiency was associated with gross abnormalities in telomere structure and nuclear organization, as well as significant inhibition of the two major pathways of DNA DSBs repair. Our studies reveal a novel relationship between A-type lamins and both NHEJ and HR: A-type lamins promote NHEJ through stabilization of 53BP1, whereas they promote HR by transcription of BRCA1 and RAD51 genes. Furthermore, these studies have led to the discovery of new

pathways that are involved in the regulation of 53BP1 and the retinoblastoma pocket family proteins, and that are activated in disease states independently of A-type lamins.

RESULTS

CHAPTER ONE

Loss of A-Type Lamins Affects Telomere Homeostasis and Genomic Stability in Mammalian Cells

ABSTRACT

Research performed in the last few years has revealed important roles for the spatial and temporal organization of the genome on genome function and integrity. A challenge in the field is to determine the molecular mechanisms involved in the organization of genome function. A-type lamins, key structural components of the nucleus, have been implicated in the maintenance of nuclear architecture and chromatin structure and have a prevalent connection to disease. Mutations in the LMNA gene are linked to a wide variety of degenerative disorders termed laminopathies, whereas changes in the expression of lamins are associated with tumorigenesis. However the molecular pathways affected by alterations of A-type lamins and how they contribute to disease are poorly understood. To gain insight into the mechanisms that contribute to pathogenesis, we determined whether loss of A-type lamins affects overall genomic stability and telomere homeostasis in LMNA knockout mouse fibroblasts. Intriguingly, we find that loss of A-type lamins alters the nuclear distribution of telomeres and is also associated with telomere attrition, defective assembly of telomeric heterochromatin, and increased chromosomal instability. This study reveals new functions for A-type lamins in the maintenance of genomic integrity and suggests that alterations of telomere biology may contribute to the pathogenesis of lamin-related diseases.

1.1 Altered nuclear organization of telomeres

Three dimensional (3D) analysis of telomere positioning indicates that mammalian telomeres are distributed throughout the entire nuclear volume in G0/G1/S phases of the cell cycle, whereas they assemble into a telomeric disk at the center of the nucleus during G2 in preparation for mitosis [166]. The molecular mechanisms that ensure proper nuclear localization of mammalian telomeres and their relevance in telomere metabolism remain undefined. Interestingly, the 3D positioning of telomeres is altered in tumor cells [167] and in senescent cells presenting defects in the nuclear lamina [168], suggesting a relationship between nuclear

distribution of telomeres and alterations of telomere metabolism observed during senescence and immortality.

To determine whether A-type lamins have a role in the nuclear compartmentalization of telomeres, we compared the distribution of telomeres between wild-type ($Lmna^{+/+}$) mouse embryonic fibroblasts (MEFs) and MEFs devoid of A-type lamins ($Lmna^{-/-}$). MEFs were analyzed after spontaneous immortalization in culture. Cells were subjected to 3D telomere fluorescence *in situ* hybridization (3D-FISH), imaged and analyzed for telomere distribution (Figure 6A). The distances of each telomere to the nuclear edge was determined using the TeloView program [169]. We found a clear difference in telomere distribution between the two genotypes (Figure 6B), such that lamins-deficient cells had a shift in the localization of telomeres towards the nuclear periphery. By calculating the cumulative distribution of telomere intensities we show that approximately 20% of telomere signals were found at the very edge of the nucleus (≤0.4 μm) in both genotypes (Figure 6C). However, although the remaining 80% of telomeres in $Lmna^{-/-}$ cells accumulated within a distance of 1.75 μm from the edge, telomeres in $Lmna^{+/+}$ MEFs were more dispersed throughout the nucleoplasm.

These results clearly show that A-type lamins participate in the correct distribution of telomeres throughout the entire nuclear volume, with a significant shift in distribution towards the nuclear periphery and away from the nuclear centre upon loss of A-type lamins. Fluorescence-activated cell sorting analysis carried out on proliferating $Lmna^{-/-}$ and $Lmna^{+/+}$ immortalized fibroblasts indicated that changes in telomere distribution were not due to differences in cell-cycle profiles between genotypes [170]. In addition, chromatin immunoprecipitation (ChIP) assays performed using lamin A/C antibody showed binding of lamins to telomeres [170], suggesting that tethering of telomeres to the lamins scaffold might regulate their nuclear distribution.

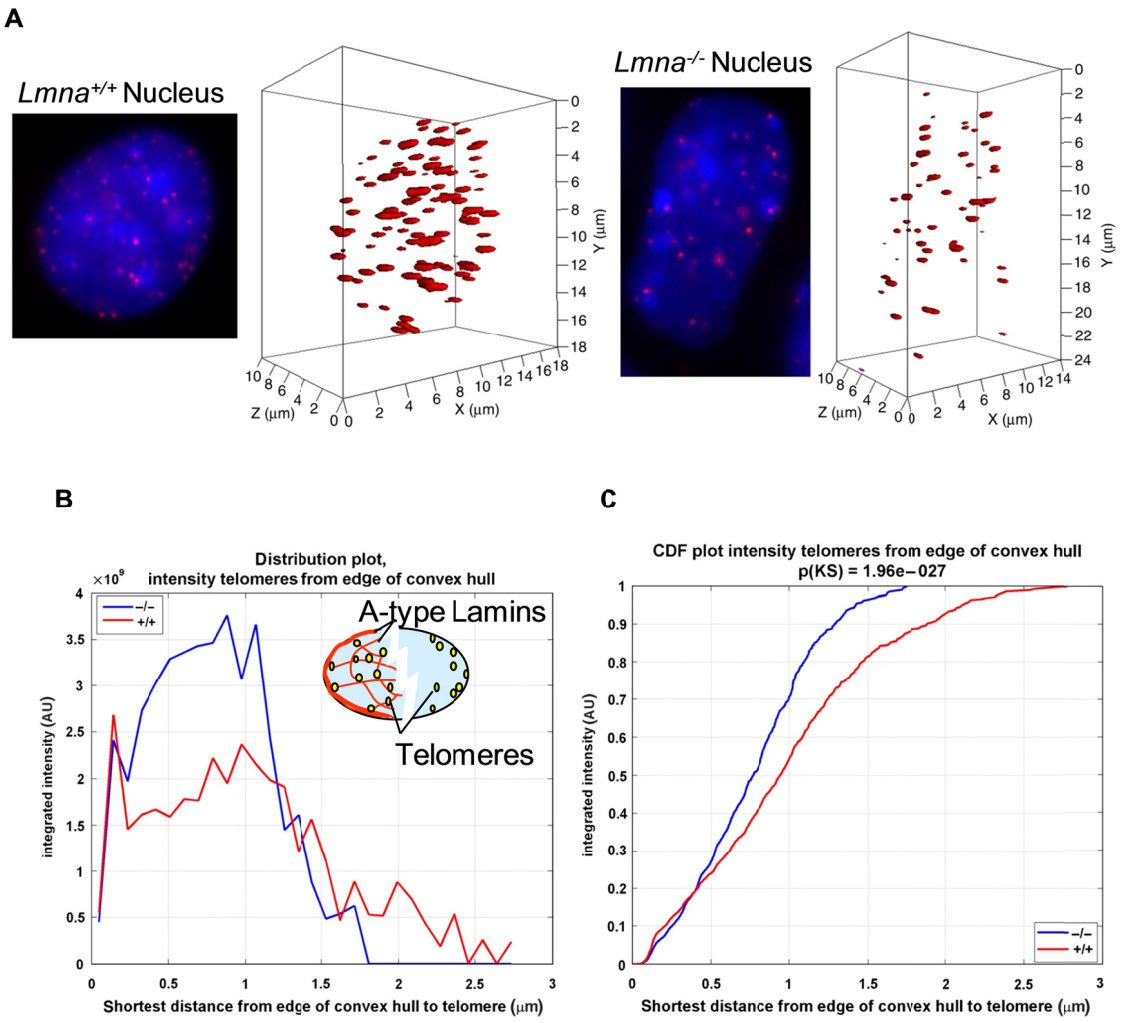

Figure 6. Altered distribution of telomeres in Lmna$^{-/-}$ cells. (A) Representative reconstructed images of nuclei from Lmna$^{+/+}$ and Lmna$^{-/-}$ MEFs processed by 3D FISH with a fluorescent telomere probe (shown in red). DAPI counterstained DNA is shown in blue. 3D telomere distribution throughout the nuclear space is shown. **(B)** Distribution plot of the intensity of telomere signals with respect to distance of signals from the edge of nuclei. Integrated intensity represents sum intensity of all telomeres at a distance from edge ≤ to X. **(C)** Cumulative distribution function (CDF) showing integrated intensity in relation to distance from nuclear edge. Integrated intensity is defined as: (sum intensity of telomeres at a distance from edge ≤ to X)/(sum intensity of all telomeres). No changes in the pool of telomeres between the two genotypes were observed at the very edge of nuclei. In contrast, higher pools of telomeres were found at all peripheral distances in Lmna$^{-/-}$ MEFs, when compared with Lmna$^{+/+}$ MEFs. 3D FISH was carried out three times. Telomeres in 85 nuclei of Lmna$^{-/-}$ MEFs and 81 nuclei of Lmna$^{+/+}$ MEFs were analyzed.

1.2 Telomere attrition in lamins-deficient cells

To determine whether changes in telomere distribution upon loss of A-type lamins are accompanied by alterations of telomere metabolism, we compared telomere length between multiple sets of $Lmna^{+/+}$ and $Lmna^{-/-}$ MEFs of early passage (pre-senescent). Analysis by terminal restriction fragment (TRF) [171] showed faster migration of telomeres in all five $Lmna^{-/-}$ lines compared to $Lmna^{+/+}$ lines, indicating a moderate but highly consistent telomere shortening upon loss of A-type lamins (Figure 7A). These results were confirmed by quantitative fluorescence In situ hybridization (Q-FISH) [171] of metaphase nuclei using a telomeric probe. While mean telomere lengths of $Lmna^{+/+}$ lines ranged between 37.6 and 40.8 kb, with an average telomere length of 39.0 kb, all five lines of $Lmna^{-/-}$ MEFs presented lower mean telomere length than any of the $Lmna^{+/+}$ lines, ranging between 34.0 and 35.2 kb, with an average telomere length of 34.6 kb (Figure 7B). To determine whether these differences were statistically significant, we carried out a two-sided t-test considering the mean from each of the cell lines to be an independent sample of either $Lmna^{+/+}$ or $Lmna^{-/-}$ genotype. We found that the mean telomere length is significantly different between these two genotypes ($P=0.0003$). In addition, TRF analysis of adult fibroblasts from $Lmna^{-/-}$ mice also showed a more pronounced telomere shortening phenotype [170].

To test whether acute depletion of A-type lamins would also lead to telomere attrition, we lentivirally transduced wild-type MEFs with constructs carrying shRNA specific for depletion of A-type lamins (shLmna) or shRNA specific for luciferase (shLucif) as control. Transduction using shLmna led to undetectable levels of lamin A/C (Figure 7C). Telomere length analysis by Q-FISH revealed a marked decrease in telomere length after only five passages of the cells in culture (Figure 7D). Most importantly, reintroduction of either lamin A, lamin C, or both, by retroviral transduction of A-type lamins-depleted cells rescued the telomere shortening phenotype to varying degrees (Figure 7D). Overall, reintroduction of lamins led to a significant increase in average telomere length, as well as a decrease in the pool of short telomeres and an increase in the pool of long telomeres.

A

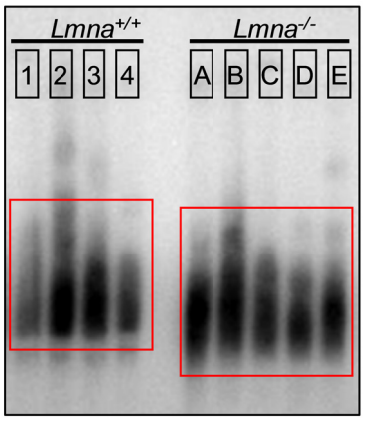

B

Lmna$^{+/+}$	Telomere length (kb)	*Lmna*$^{+/+}$	Telomere length (kb)
1	39.5 ± 20.4	A	35.2 ± 17.8
2	38.3 ± 19.8	B	35.0 ± 16.8
3	40.8 ± 20.9	C	34.1 ± 16.4
4	37.6 ± 18.1	D	34.0 ± 16.0
		E	34.7 ± 17.7
Avg	39.0 ± 19.0	Avg	34.6 ± 17.0*
*p=0.0003			

C

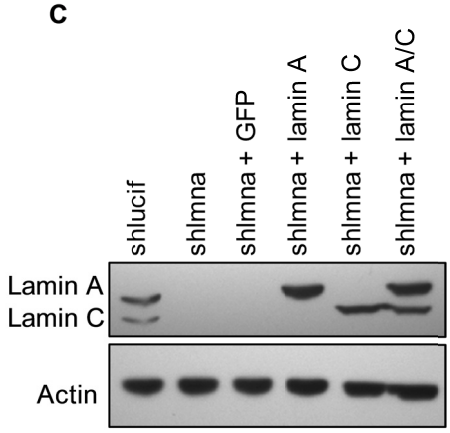

D

	Telomere length	%tel < 10 kb	%tel > 80 kb
shLucif	43.1 ± 23.5	4.7	7.2
shLmna	38.3 ± 22.4	7.6	5.0
shLmna + GFP	39.6 ± 23.4	7.2	5.6
shLmna + Lam A	43.5 ± 24.7	4.8	7.2
shLmna + Lam C	46.5 ± 24.3	4.4	10.2
shLmna + Lam A/C	47.9 ± 25.7	3.1	11.1

Figure 7. Defective maintenance of telomere length upon loss of A-type lamins. (A) Representative TRF analysis of several independent Lmna$^{+/+}$ (1–4) and Lmna$^{-/-}$ (A–E) MEF lines of early passage (passages 3–5). Note the faster migration of telomeres in all Lmna$^{-/-}$ lines when compared with Lmna$^{+/+}$ lines, indicating telomere shortening. **(B)** Telomere length distribution (expressed as average ± s.d.) in Lmna$^{+/+}$ (1–4) and Lmna$^{-/-}$ (A–E) MEFs as determined by Q-FISH. The individual values for each of the samples are shown. Q-FISH was carried out three times. For each experiment, at least 20 metaphases were analyzed in every MEF line. **(C)** Western blot to detect the levels of lamin A/C on lentiviral transduction of wild-type MEFs with constructs carrying shRNA specific for lamin A/C (shLmna) or an shLucif control, as well as cells expressing lamin A, lamin C, or both. **(D)** Q-FISH analysis to measure telomere length in MEFs after depletion of A-type lamins (compare shLmna and shLucif) and rescue with expression of lamin A, lamin C or both lamin A and C. *Represents P-value of statistical significance.

These data indicate that A-type lamins play a key role in the control of telomere length. However, we do not know the mechanism behind the telomere shortening phenotype observed in A-type lamins-deficient cells. The levels of telomerase activity and the binding of the shelterin complex components TRF1 and TRF2 were not affected by the loss of A-type lamins [170]. Similarly, we did not observe any evidence of aberrant recombination at telomeres, which could explain the loss of telomeric sequences [170]. It is possible that the binding of other shelterin complex components or DNA repair factors with a function at the telomere could be defective in LMNA null cells. Alternatively or concomitantly, loss of A-type lamins might hamper the accessibility of telomerase or other proteins implicated in telomere metabolism, especially factors implicated in telomere replication. While the mechanisms remain unclear, our data clearly show that A-type lamins have a key role in the maintenance of telomere length homoeostasis.

1.3 Abnormal heterochromatin assembly

Maintenance of the heterochromatic structure of telomeres is important for telomere length homoeostasis [56, 172]. A common feature in fibroblasts from HGPS patients and from old individuals expressing progerin is the global alteration of histone marks characteristic of constitutive heterochromatin [173, 174], however the effect on telomeres is unknown. To investigate whether loss of A-type lamins affects the assembly of telomeric heterochromatin, we carried out ChIP assays using antibodies recognizing well-established heterochromatic marks, H3K9me3 and H4K20me3. Although we found no changes in H3K9me3 levels, we observed a significant decrease in telomeric H4K20me3 levels in $Lmna^{-/-}$ MEFs (Figure 8A). Interestingly, these defects were phenocopied by pericentric heterochromatin (Figure 8B), supporting the idea that alterations of A-type lamins function affect the epigenetic status of constitutive heterochromatin [174]. Notably, the changes reported here are different from those described in HGPS cells, indicating different functional implications of mutation or silencing of the LMNA gene. The epigenetic defects of $Lmna^{-/-}$ MEFs were confirmed by western blot analysis, which showed a marked reduction in global H4K20me3 levels but no changes in H3K9me3 (Figure 8C). Additionally we found significant decreases in the expression of non-coding telomeric RNAs

(TERRAs) in Lmna$^{-/-}$ cells [170]. Telomere attrition and increased signal free ends are opposite to what would be expected in cells with low levels of TERRAs. However decreased TERRAs represents yet another alteration in the homeostasis of telomeres in Lmna$^{-/-}$ cells.

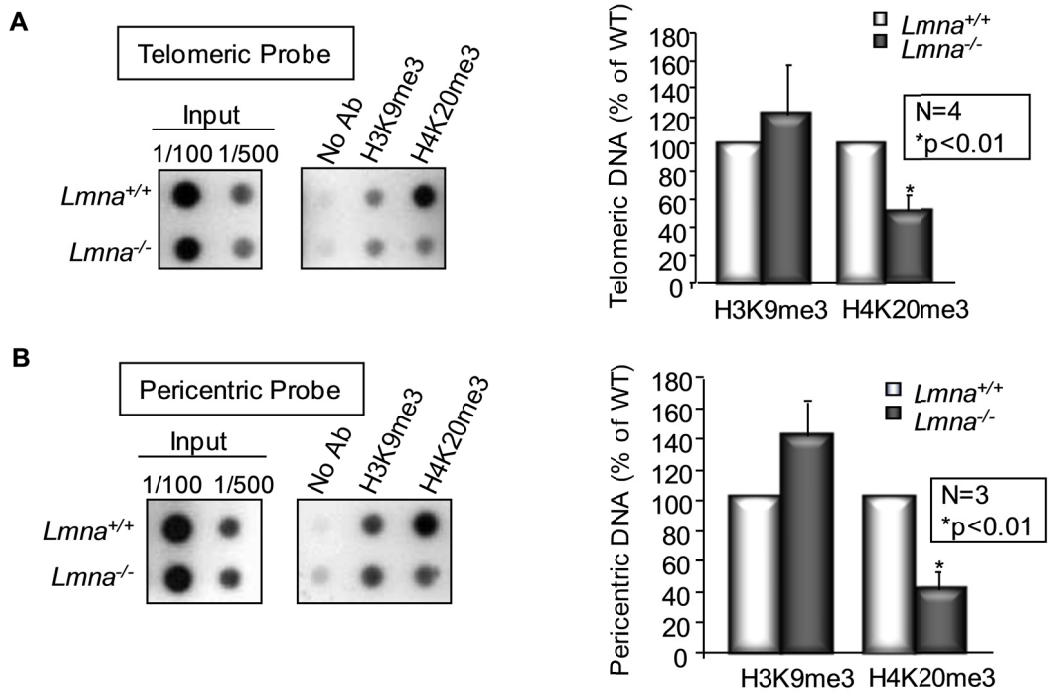

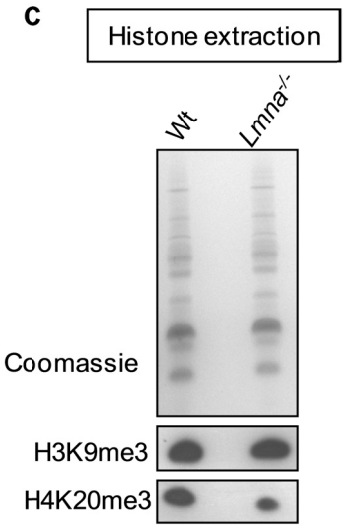

Figure 8. Alterations of telomeric heterochromatin structure in Lmna$^{-/-}$ MEFs. **(A)** Chromatin immunoprecipitation (ChIP) with antibodies recognizing heterochromatic marks H3K9me3 and H4K20me3. Immunoprecipitated DNA was hybridized to a telomeric probe. The graph shows the quantification of immunoprecipitated telomeric repeats after normalization to input signals in four independent experiments. **(B)** Immunoprecipitated DNA was hybridized to a probe recognizing major satellite repeat sequences characteristic of pericentric heterochromatin. The graph shows the quantification of major satellite repeats signal after normalization to input signals in three independent experiments. **(C)** Western blots showing global levels of H3K9me3 and H4K20me3 in MEFs. The immunoblots show no changes in the levels of H3K9me3, but a significant decrease in global H4K20me3 levels on loss of A-type lamins.*Represents P-value of statistical significance. R.U. stands for relative units.

1.4 Increased genomic instability

Next, we evaluated the presence of genomic instability in Lmna$^{-/-}$ cells. We determined the frequency of loss of telomeric signals (signal-free ends), chromosome/ chromatid breaks and end-to-end fusions, as well as the presence of aneuploidy in pre-senescent Lmna$^{+/+}$ and Lmna$^{-/-}$ MEFs (Figure 9). We found a threefold increase in the number of signal-free ends (Figure 9A) and a twofold increase in chromosome and chromatid breaks (Figure 9B) in Lmna$^{-/-}$ MEFs, indicating increased genomic instability. This finding was supported by an increased number of nuclei with basal DNA damage, as indicated by a twofold increase in cells presenting γ-H2AX-labeled foci upon loss of A-type lamins (Figure 9C).

In normal cells, inappropriate recombination between telomeres of sister chromatids can serve to lengthen one telomere at the expense of another [175]. To test whether aberrant recombination involving telomeric repeats contributed to the loss of telomere signals in Lmna$^{-/-}$ MEFs, we carried out chromosome orientation fluorescence in situ hybridization (CO-FISH) [175]. This technique allows the differential labeling of leading and lagging strands of telomeres. In the absence of recombination events between telomeric sequences, only one telomere at each chromosome end is labeled with either the leading or the lagging strand probe. If recombination occurs, the labeling is split between both sister telomeres, giving rise to telomeres labeled with both the leading and lagging strand probes. CO-FISH results indicated that loss of A-type lamins did not lead to increased telomeric recombination events [170]. Thus, alternative mechanisms are responsible for the loss of telomere signals upon loss of A-type lamins.

In addition to telomeric instability, karyotype analysis showed an increase in the numbers of cells with abnormal chromosome dosage in Lmna$^{-/-}$ MEFs (Figure 9D). Since earlier studies had shown that reduced Rb family function leads to aneuploidy partly due to defects in centrosome duplication [176], we tested if loss of A-type lamins was leading to errors in centrosome duplication. This was done by quantifying the centrosome numbers in Lmna$^{+/+}$ and Lmna$^{-/-}$ MEFs by performing immunofluorescence staining of γ-tubulin. Lmna$^{-/-}$ cells had an

increase in the number of cells presenting centrosome amplification [170], suggesting that this contributes to the aneuploidy observed in Lmna$^{-/-}$ cells. Overall, these results show increased genomic instability on loss of A-type lamins.

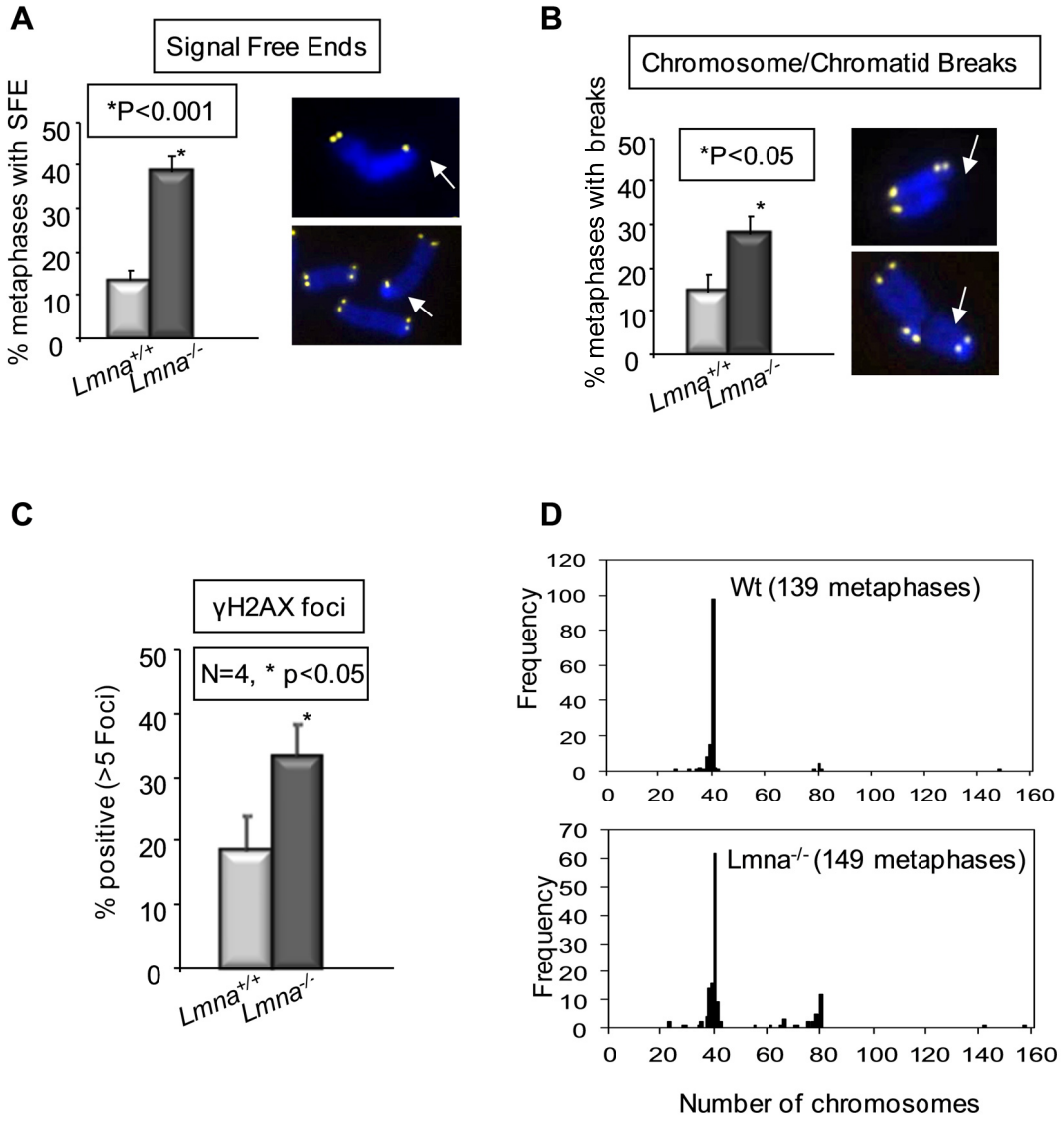

Figure 9. Genomic instability in lamin A/C-deficient cells. Lmna$^{+/+}$ and Lmna$^{-/-}$ MEFs were prepared for FISH and metaphases evaluated for the presence of chromosomal instability. **(A)** Lmna$^{-/-}$ MEFs displayed a higher frequency of chromosomes that did not have telomeric signal (signal-free ends) and **(B)** higher frequency of chromosome and chromatid breaks. **(C)** Consistent with the presence of genomic instability, Lmna$^{-/-}$ MEFs also had more persistent DNA damage signaling, as assessed by the presence of γ-H2AX foci. **(D)** Karyotype analysis of more than 100 metaphases shows a clear increase in the number of metaphases with an aberrant number of chromosomes in Lmna$^{-/-}$ MEFs.*Represents P-value of statistical significance.

1.5 DISCUSSION

Understanding the cellular functions of A-type lamins is a highly topical subject because of their implication in a number of disease states, including laminopathies, aging and cancer. In particular, reduced expression of A-type lamins is emerging as a factor contributing to tumorigenesis [14, 15, 162]. Our results indicate that A-type lamins play a fundamental role in the maintenance of telomeres and genomic stability. We have shown that loss of A-type lamins leads to a variety of alterations in telomere biology: (i) nuclear decompartmentalization of telomeres, (ii) impaired maintenance of telomere length homoeostasis, and (iii) defects in telomere chromatin architecture. In addition, we found that loss of A-type lamins resulted in an increase in basal levels of DNA damage (γ-H2AX foci), increased frequency of chromosome and chromatid breaks, and aneuploidy. Given that alterations of telomere biology is one of the hallmarks of cancer and aging, we suspect that the observed alterations upon loss of A-type lamins are contributing to the pathogenesis of lamin-related diseases, especially premature aging syndromes such as HGPS and tumoral processes characterized by the silencing of the LMNA gene.

Various lines of evidence indicate that the nucleus is compartmentalized and that changes in the spatial organization of chromatin affect nuclear functions [6, 10, 11]. The importance of telomere compartmentalization for telomere function has been clearly shown in yeast [177]. To date, the mechanisms regulating the nuclear distribution of mammalian telomeres remain to be identified. In addition, how the nuclear localization of mammalian telomeres influences telomere biology is unknown. Lamins, which are absent in yeast, can bind directly to DNA and core histones, which attributes them a major role in tethering chromatin to specific sub-nuclear compartments [178, 179]. Our results show that A-type lamins associate with telomeres and contribute towards their proper nuclear localization.

In normal cells, A-type lamins are highly enriched at the nuclear periphery and are also found throughout the nucleoplasm [180]. We thus reasoned that loss of A-type lamins could lead to the detachment of telomeres from the nuclear periphery. In contrast, we found that the

localization of telomeres shifted towards the nuclear periphery in the absence of A-type lamins. This raises the possibility that the nuclear periphery represents a default pathway for telomere localization. In this model, A-type lamins would have an active role in the localization of telomeres throughout the nucleoplasm in mammalian cells. A recent study showing that alterations of the nuclear lamina during senescence are associated with increased aggregation of telomeres at the nuclear periphery supports this model [168]. It remains to be investigated whether tumor cells with silenced LMNA gene also present alterations in telomere compartmentalization and telomere structure, length, and function. These types of studies will provide insights into the mechanisms altered upon loss of A-type lamins, which could contribute to tumorigenesis.

The profound impact that loss of A-type lamins has on different aspects of telomere biology suggests that the nuclear compartmentalization of telomeres could be fundamental for telomere metabolism. Our results do not indicate that changes in telomerase activity, binding of the shelterin complex components TRF1/ TRF2, or aberrant recombination are the cause of the telomere shortening in $Lmna^{-/-}$ cells. It is possible that the accessibility of telomerase and/or activities participating in telomere metabolism is reduced on disruption of the scaffold for nuclear organization provided by A-type lamins. Studies aimed at elucidating the impact of loss of A-type lamins on telomere replication, and on the binding of other shelterin complex components or DNA repair factors to telomeres will be fundamental to understanding the mechanisms behind the alterations in telomere biology described here.

In addition to the effect on telomere biology, loss of A-type lamins impacts on other molecular mechanisms, such as stabilization of Rb and ING tumor suppressors [148, 181, 182]. Alterations in these tumor suppressors could contribute to the telomere phenotypes in $Lmna^{-/-}$ MEFs and to the genomic instability that drives cancer and aging. While reduced Rb family function is likely to be responsible for histone modifications defects in $Lmna^{-/-}$ cells, we showed that the telomere-shortening phenotype and the decrease in density of TERRAs are Rb independent [183].

Along with changes in telomere metabolism, Lmna$^{-/-}$ cells were also characterized by increased chromosomal instability as manifested by chromosome and chromatid and chromatid breaks, and loss of telomeric signal from chromosomes. These cells also had a higher basal level of DNA damage, which we detected as γ-H2AX foci. The increase in signal-free ends was particularly interesting because they suggested the presence of deprotected telomeres in the Lmna$^{-/-}$ cells. Deprotected telomeres are potent inducers of the DNA damage response and undergo processing as DSBs by the non-homologous end-joining (NHEJ) pathway. Processing of telomeres by NHEJ results in fusions between telomeres of different chromosomes however there was no increase in the frequency of end-to-end fusions in the Lmna$^{-/-}$ cells, indicating defective NHEJ in these cells. In the next section we investigate the efficacy of NHEJ in lamins-deficient cells, and the molecular mechanisms by which loss of A-type lamins could contribute to the genomic instability.

CHAPTER TWO

53BP1-Dependent Non-Homologous End-Joining is Suppressed in Lamins-Deficient Cells

ABSTRACT

A-type lamins are emerging as regulators of nuclear organization and function. Changes in their expression are associated with cancer and mutations are linked to degenerative diseases -laminopathies-. Although a correlation exists between alterations in lamins and genomic instability, the molecular mechanisms remain largely unknown. In the previous chapter we showed that loss of A-type lamins leads to alterations in the homeostasis and nuclear distribution of telomeres in mouse cells. Cells lacking A-type lamins had increased genomic instability with increased basal DNA damage signaling, chromosome and chromatid breaks, and loss of telomeric signal (signal-free ends). Despite the presence of signal-free ends, lamins-deficient cells did not exhibit any changes in the frequency of chromosome end-to-end fusions, suggesting an inhibition of the non-homologous end-joining (NHEJ) pathway. Here, we determined if A-type lamins are required for efficient NHEJ of DNA double-strand breaks (DSBs) using deprotected telomeres as a model of long-range DSBs, and ionizing radiation-induced breaks as a model of short range DSBs. Strikingly, we find that loss of A-type lamins significantly inhibits NHEJ of both types of DSBs. We demonstrate that the mechanism behind deficient NHEJ is degradation of 53BP1, an important NHEJ protein. Importantly, reconstitution of 53BP1 in lamins-deficient cells is sufficient to rescue both long-range and short-range NHEJ. These findings are significant as they uncover previously unknown mechanisms by which A-type lamins contribute to genomic stability and offer new avenues for development of therapy for laminopathies and cancer.

2.1 Suppression of long-range NHEJ in lamin A/C-deficient cells

First, we artificially induced telomere deprotection by expression of a dominant negative telomere binding protein, TRF2$^{\Delta B\Delta M}$, by retroviral transduction of Lmna$^{+/+}$ and Lmna$^{-/-}$ MEFs. Expression of TRF2$^{\Delta B\Delta M}$ has been established to induce telomere dysfunction, which leads to chromosome end-to-end fusions in the presence of an intact NHEJ repair pathway [50, 184] (Figure 10). NHEJ processing of deprotected telomeres leads to the recruitment of DNA repair proteins to the telomeres, which can be visualized as “telomere induced foci” (TIF) when

subjected to immunofluorescence techniques [51, 185, 186]. The ability of Lmna$^{-/-}$ MEFs to form TIFs upon expression of TRF2$^{\Delta B\Delta M}$ was evaluated by carrying out Immuno-FISH using a γ-H2AX antibody and a telomeric probe. Expression of TRF2$^{\Delta B\Delta M}$ (Figure 11A) led to the formation of γ-H2AX-labeled TIF in both Lmna$^{+/+}$ and Lmna$^{-/-}$ MEFs (Figure 11B), which suggests that the initial step in the sensing of DSBs (dysfunctional telomeres) is intact upon loss of A-type lamins. There was equal induction of γ-H2AX as measured by formation of foci and western blot to detect protein level (Figure 11C and D).

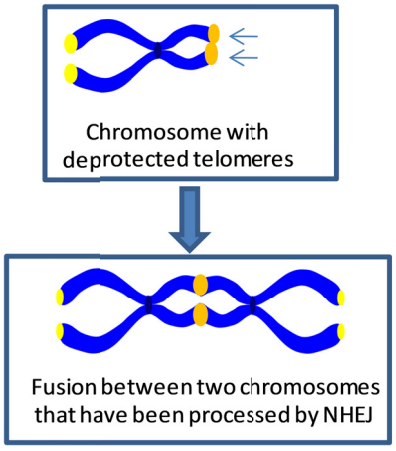

Figure 10. Expression of TRF2$^{\Delta B\Delta M}$ induces telomere deprotection, which leads to processing by the NHEJ DNA repair pathway to result in telomere end-to-end chromosome fusions.

Despite the ability of Lmna$^{-/-}$ MEFs to sense DNA damage, the processing of dysfunctional telomeres by NHEJ was significantly hindered by the loss of A-type lamins. Expression of TRF2$^{\Delta B\Delta M}$ in Lmna$^{+/+}$ MEFs, resulted in chromosome fusions in ~50% of metaphases, consistent with previous reports (Figure 11E), but only ~12% of metaphases presented fusions in the Lmna$^{-/-}$ MEFs. This suggested severe defects in the processing of DSBs by the NHEJ pathway. To test if this relationship was maintained in human cells, we depleted A-type lamins from U2OS cells using two separate short hairpins, and induced telomere deprotection by retrovirally expressing TRF2$^{\Delta B\Delta M}$ (Figure 12A). Consistent with the results in MEFs, expression of TRF2$^{\Delta B\Delta M}$ led to the formation of end-to-end fusions in 42% of metaphases (average of 3.7 fusions per metaphase) in cells with a control short hairpin, versus only 17.5% or 27% of metaphases in cells expressing either shlmna A or shlmna B (average of 0.6 or 1 fusion per

metaphase, respectively) (Figure 12B). These results indicated conservation of the role of A-type lamins in the processing of deprotected telomeres by NHEJ in mouse and human cells.

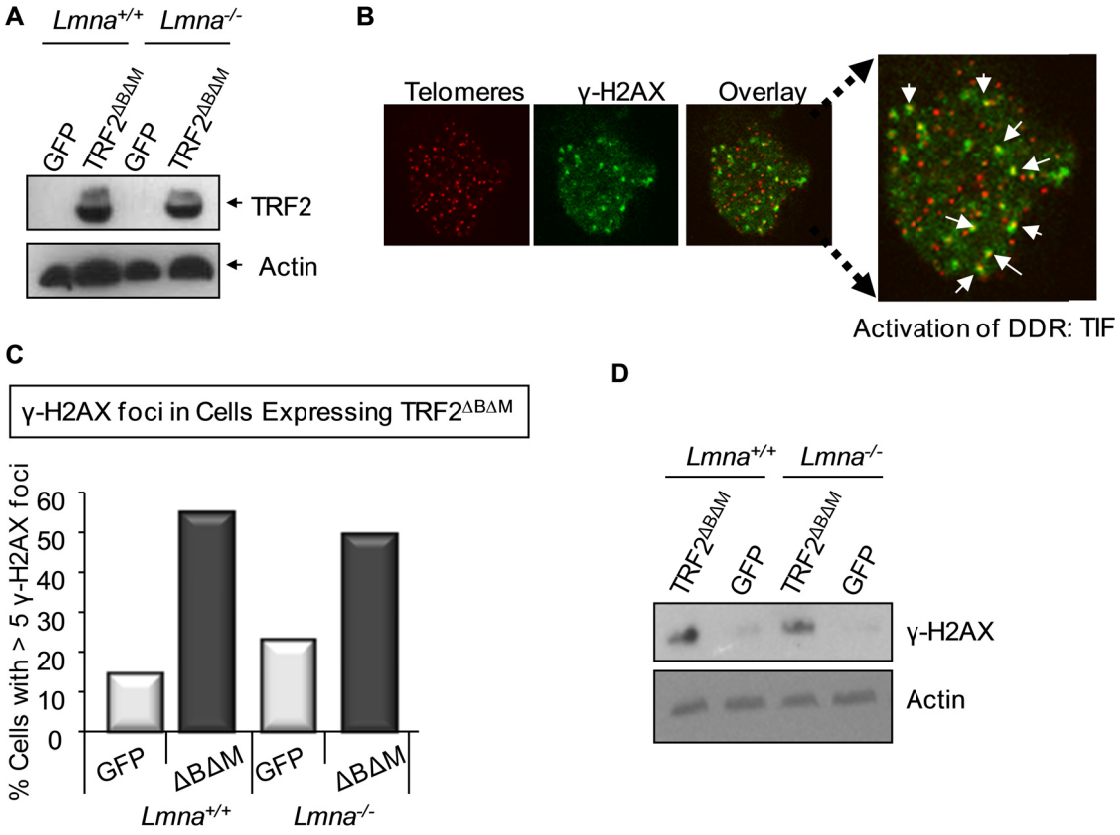

Figure 11. Defective non-homologous end joining (NHEJ) of deprotected telomeres in Lmna$^{-/-}$ cells. (A) Expression of the dominant negative shelterin complex component, TRF2$^{\Delta B\Delta M}$, by retroviral transduction in Lmna$^{+/+}$ and Lmna$^{-/-}$ cells. **(B)** Representative image from the immuno-FISH assay to detect the co-localization of telomeres (red) with γ-H2AX DNA damage foci (green), TIFs in cells that are expressing TRF2$^{\Delta B\Delta M}$. **(C)** Quantification of TIFs upon expression of TRF2$^{\Delta B\Delta M}$ in Lmna$^{+/+}$ and Lmna$^{-/-}$ cells indicates similar activation of the DNA damage response in both cell lines. Expression of GFP was used as a negative control. **(D)** Western blot showing equal levels of γ-H2AX in Lmna$^{+/+}$ and Lmna$^{-/-}$ cells expressing TRF2$^{\Delta B\Delta M}$**(E)** NHEJ of deprotected telomeres is significantly decreased in Lmna$^{-/-}$ cells, as evaluated by the frequency of end-to-end telomere fusions in cells expressing TRF2$^{\Delta B\Delta M}$.

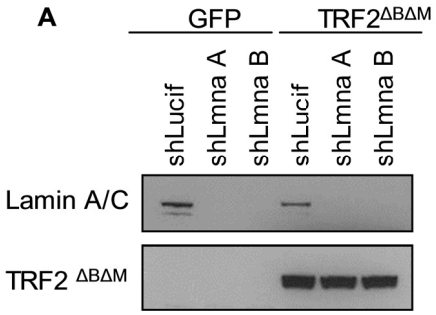

Figure 12. Defective NHEJ of deprotected telomeres in lamins-deficient human cells. (A) U2OS cells were depleted of lamin A/C using two separate shRNAs (shLmnaA and shLmnaB) and retrovirally transduced with TRF2$^{\Delta B\Delta M}$ or GFP as a control. **(B)** Quantification of the resulting telomere end-to-end fusions shows a severe decrease in the frequency of fusions in both shLmna A and shLmna B cells, indicating conservation of the phenotype between human and mouse cells.

B

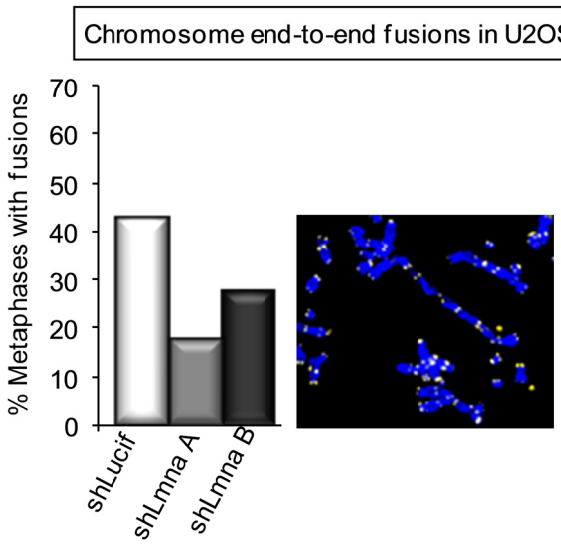

Average fusions per metaphase

	GFP	TRF2$^{\Delta B\Delta M}$
shLucif	0	3.7
shLmna A	0	0.6
shLmna B	0	1

2.2 A-type lamins stabilize 53BP1

To gain insight into specific steps of NHEJ that are affected by loss of A-type lamins, we tested whether the cellular levels of key components of the DDR pathway were altered in $Lmna^{-/-}$ MEFs. First, we monitored the levels γ-H2AX and 53BP1, which have a function in the sensing of dysfunctional telomeres. While there was no difference in the level of H2AX in lamins-deficient cells, we confirmed our previous observation of increased γ-H2AX in $Lmna^{-/-}$ MEFs, indicating increased basal DNA damage upon loss of A-type lamins (Figure 13A). In addition, we observed a marked decrease in the levels of 53BP1 in $Lmna^{-/-}$ MEFs when compared with $Lmna^{+/+}$ cells by both western blot and immunofluorescence (Figure 13A). Consistent with the $Lmna^{-/-}$ MEFs, acute depletion of A-type lamins in U2OS cells by shRNAs also led to a significant decrease in 53BP1 protein (Figure 13B). Importantly, reconstitution of either lamin A, lamin C, or both lamin A and lamin C into lamins depleted cells rescued the levels of 53BP1 (Figure 13C).

To determine if other DDR proteins were affected by loss of A-type lamins, we monitored the levels of a variety of proteins with different roles in the DDR pathway and in DNA repair in lamins-deficient cells. Unlike 53BP1, we detected no significant differences in the cellular levels of MDC1, ATM, DNA-PK, Mre11, Nbs1, Ku70, and ERCC1 (Figure 13D). In addition, we found no differences in the global levels of TRF1, TRF2, and POT1— proteins with a key structural function in telomeres (data not shown), which suggested that the defect in telomeric NHEJ is not likely to be due to differences in the shelterin complex at the telomeres. These results indicate that depletion of A-type lamins preferentially affects 53BP1 levels.

To investigate if the regulation of 53BP1 was occurring at the transcriptional level we monitored the levels of 53BP1 transcripts by real-time quantitative PCR (Q-PCR). As shown in Figure 14A, no differences in the levels of 53BP1 transcripts were detected between the two genotypes, which suggested that A-type lamins were involved in regulating 53BP1 protein stability. Interestingly, incubation of $Lmna^{+/+}$ and $Lmna^{-/-}$ MEFs with the proteasome inhibitor MG132 partially rescued the levels of 53BP1, implicating the proteasome pathway in degradation

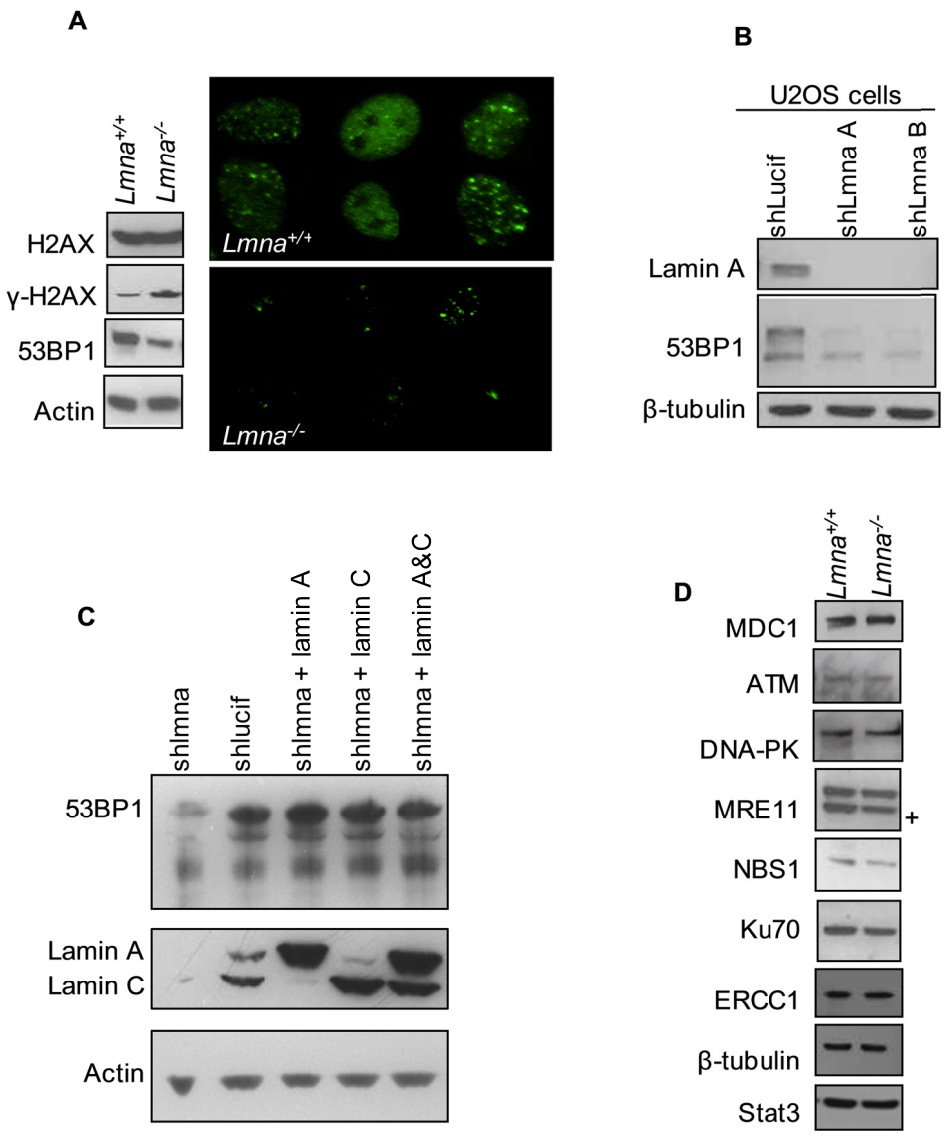

Figure 13. Decreased 53BP1 in lamin A/C-deficient cells. (A) Western blots (left) showing cellular levels of factors involved in the initial sensing of DNA damage. No changes in H2AX levels, but an increase in γH2AX levels was observed in Lmna$^{-/-}$ MEFs. In contrast, a marked decrease in 53BP1 protein levels was observed in Lmna$^{-/-}$ MEFs by western blot and immune-fluorescence. Images were acquired under equal exposure conditions. **(B)** Acute depletion of lamin A/C leads to a decrease in 53BP1, which can be rescued by re-introduction of lamin A, lamin C, or both lamin A and C. **(C)** Depletion of lamin A/C in U2OS cells with two separate shRNAs also leads to decreased levels of 53BP1 protein. **(D)** Westerns blots showing that the levels of MDC1, ATM, DNA-PK, Mre11, Nbs1, Ku70, and ERCC1 remain unchanged in Lmna$^{-/-}$ MEFs. Immunoblotting with β-tubulin and Stat3 were performed as control for loading.

of 53BP1 (Figure 14B). We hypothesized that similar to what has been reported for Rb family members, A-type lamins might stabilize 53BP1 protein levels by preventing their degradation by the proteasome [148]. While treatment with MG132 increased 53BP1 in lamins-deficient cells it was not sufficient to restore the levels to that of wild-type cells. This indicated that additional mechanisms were involved in degradation of 53BP1 in these cells. This additional mechanism of degradation was later shown by our group to be the result of a cysteine protease, cathepsin L, which is upregulated in lamins-deficient cells [187].

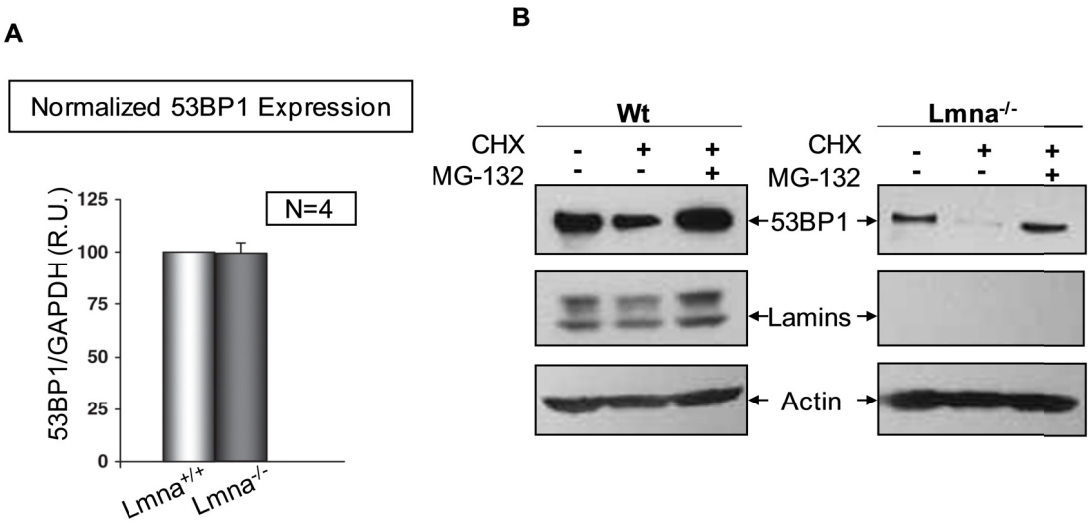

Figure 14. Mechanism of reduced 53BP1 in Lmna$^{-/-}$ cells. (A) Quantitative real-time PCR indicates normal levels of 53BP1 mRNA transcripts in Lmna$^{-/-}$ cells. Levels were normalized to GAPDH transcript levels. The average of four independent experiments is shown. **(B)** Western blot of Lmna$^{+/+}$ and Lmna$^{-/-}$ cells treated with cycloheximide (CHX) to inhibit protein synthesis and/or MG132 to inhibit proteasomal degradation.

2.3 53BP1 rescues long-range NHEJ in lamins-deficient cells

To determine the contribution of 53BP1-deficiency to the NHEJ defect in lamins deficient cells we performed 53BP1 rescue experiments in human cells. U2OS cells were retrovirally transduced with 53BP1 or an empty vector (EV) control followed by lentiviral transduction with a shRNA specific for depletion of A-type lamins (shLmna) or a shRNA control (shCtrl) (Figure 15A). Next, we retrovirally transduced cells with a dominant negative of the telomere binding protein TRF2 (TRF2$^{\Delta B\Delta M}$) to induce telomere deprotection. To quantify the resulting end-to-end fusions, we scored metaphases based on four different categories of increasing chromosome fusions ranging from “less than 5 chromosomes fused” (category 1) to “more than half of the chromosomes fused” (category 4) (Figure 15B and C). In cells that express A-type lamins and have normal levels of endogenous 53BP1 (EV/shCtrl/TRF2$^{\Delta B\Delta M}$), 53% of metaphases were scored in category 1 and 31% in category 4 (Figure 15D). In contrast, lamin A/C-depleted cells (EV/shLmna/TRF2$^{\Delta B\Delta M}$) exhibited an overall decrease in the extent of end-to-end fusions (66% category 1 and only 14% category 4). Most importantly, reconstitution of 53BP1 into lamin A/C-depleted cells (53BP1/shLmna/TRF2$^{\Delta B\Delta M}$) resulted in a rescue of chromosome fusions (36% category 1 and 40% category 4). As a control, we monitored fusions in cells transduced with an empty vector instead of TRF2$^{\Delta B\Delta M}$ (53BP1/shLmna/EV). As expected, 100% of metaphases belong to category 1, indicating that 53BP1 expression itself does not induce fusions (data not shown). We conclude that the effect of A-type lamins in NHEJ of dysfunctional telomeres is due to their ability to stabilize 53BP1 protein.

Cathepsin L (CTSL), a cysteine protease which is upregulated upon loss of A-type lamins, was demonstrated by our group to participate in degradation of 53BP1 in lamins-deficient cells [187]. CTSL is a cysteine protease from the papain family that is ubiquitously expressed in mouse and human tissues. Like other proteases, it is synthesized as a zymogen which undergoes autoproteolytic processing within the lysosomal/endosomal compartment to release the mature active form [188]. Though its activity is enhanced by low pH in the lysosome, CTSL can also be found in other cellular organelles, where it can selectively process other targets at

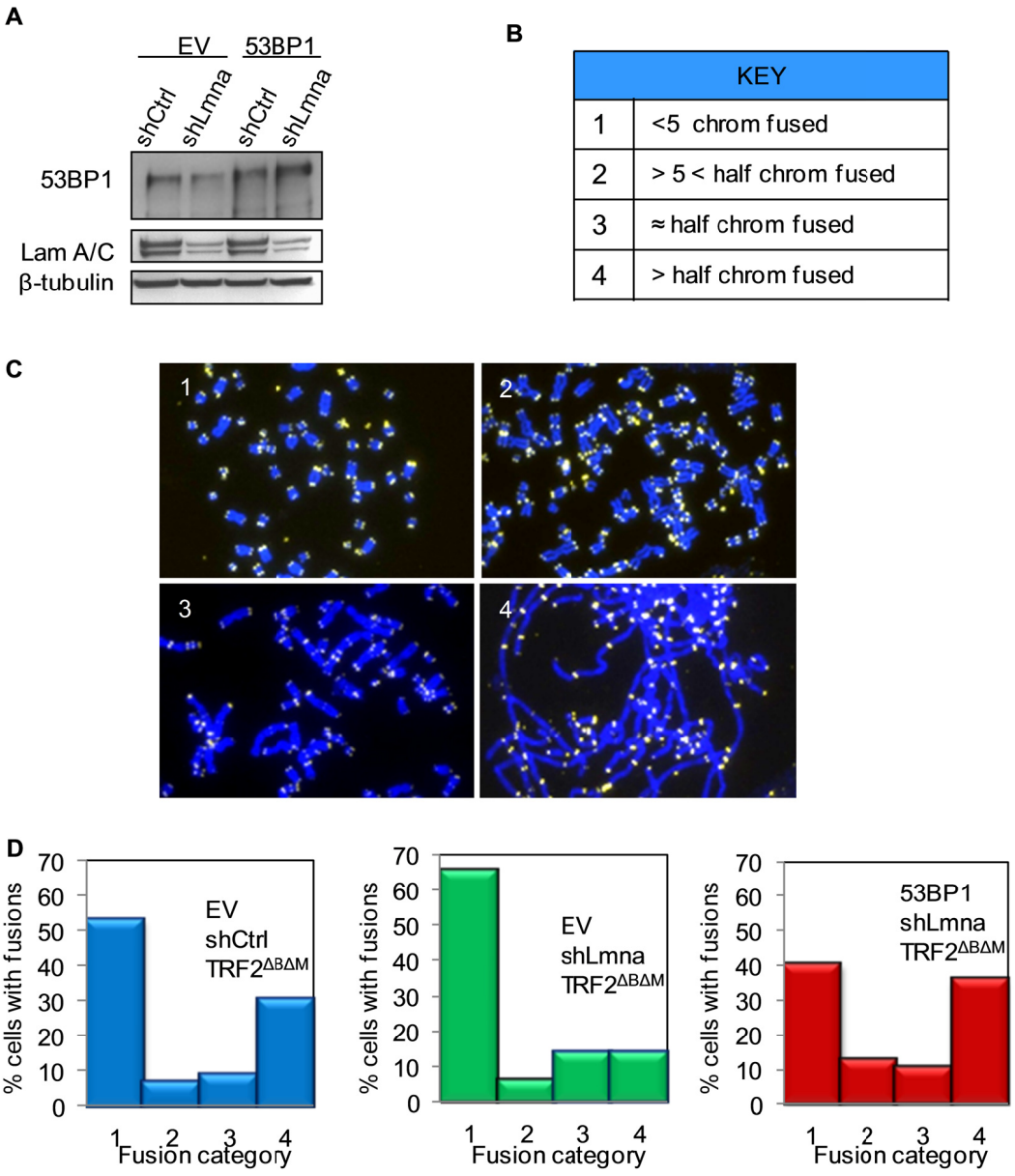

Figure 15. Defects in NHEJ of dysfunctional telomeres are rescued by ectopic reconstitution of 53BP1. (A) Levels of 53BP1 and A-type lamins in U2OS cells after ectopic expression of 53BP1 (EV, empty vector control), followed by lentiviral transduction with shLmna or shCtrl. β-tubulin was used as loading control. Note how ectopic expression of 53BP1 prevents the decrease in protein levels upon depletion of A-type lamins. **(B)** Key of the different categories of metaphases based on the extent of chromosome end-to-end fusions induced by expression of $TRF2^{\Delta B\Delta M}$. **(C)** Representative images of the different categories are shown. **(D)** Histograms showing the percentage of metaphases belonging to each category from the different cell lines. left panel: cells transduced with EV, shCtrl and $TRF2^{\Delta B\Delta M}$. Middle panel: cells transduced with EV, shLmna and $TRF2^{\Delta B\Delta M}$. right panel: cells transduced with 53BP1, shLmna and $TRF2^{\Delta B\Delta M}$. 79–88 metaphases were analyzed per condition.

less acidic or even neutral environments [189]. CTSL can be secreted to the extracellular matrix where it is known to degrade some of its components under physiological conditions –i.e. favoring bone resorption in osteoclasts [189]. Increased extracellular CTSL has been reported in numerous types of cancer and is often associated with increased invasiveness and metastasis [190-192]. More recently, CTSL was found inside the nucleus, where in a more regulated fashion it processes specific nuclear components such as histone H3 tails during stem cell differentiation and the transcription factor CDP/Cux during cell cycle progression [193, 194].

Previous studies demonstrated that 1,25(OH)2D3 (vitamin D) inhibits CTSL activity in colon cancer cells [195, 196]. Interestingly, treatment of lamin A/C-deficient cells with vitamin D is sufficient to inhibit activity of CTSL activity and results in increased levels of endogenous 53BP1 [187]. To determine if restoration of endogenous 53BP1 was sufficient to rescue TRF2$^{\Delta B\Delta M}$ induced telomere fusions we treated lamins-deficient cells with vitamin D and scored telomere fusions (Figure 16). Wild-type MEFs with either a control shRNA (shGFP) or shRNA targeting A-type lamins (shLmna) were retrovirally transduced with TRF2$^{\Delta B\Delta M}$ or an empty vector control. Cells were treated vitamin D or with a vehicle control (bovine growth serum, BGS) for 24hours prior to collecting metaphases for analysis of telomere fusions by FISH. As expected, treatment of shGFP cells with vitamin D had no effect on 53BP1 levels while similar treatment of shLmna cells led to a significant increase in levels of 53BP1 (Figure 16A). Consistent with our previous findings, the frequency of TRF2$^{\Delta B\Delta M}$ -induced fusions in shGFP cells treated with BGS was ~40% while the shLmna cells of the same treatment had fusions in less than 10% of the metaphases (Figure 16B and C). Remarkably, treatment of shLmna/TRF2$^{\Delta B\Delta M}$ cells with vitamin D was sufficient to increase the frequency of fusions to ~30%. Along with our overexpression data, these results provide conclusive evidence that A-type lamins mediate NHEJ processing of deprotected telomeres *via* their ability to stabilize 53BP1

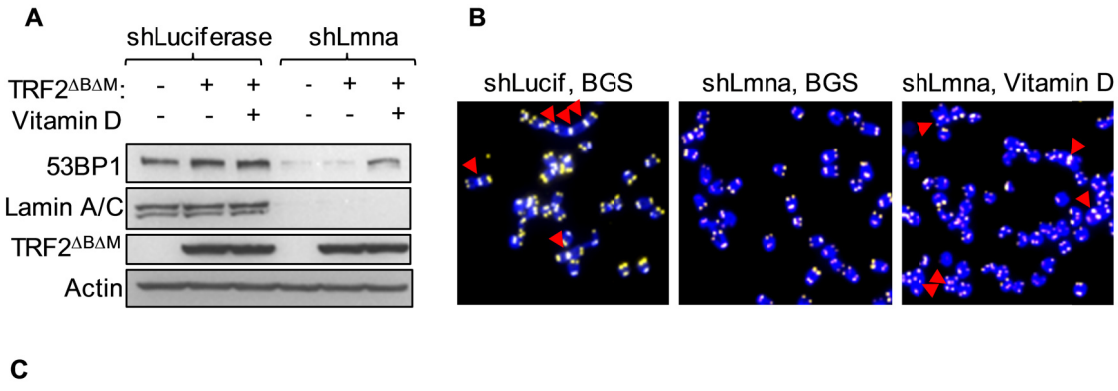

Figure 16. Defects in NHEJ of dysfunctional telomeres are rescued by recovery of endogenous 53BP1. (A) Western blots of 53BP1 and lamins upon expression of TRF2$^{\Delta B\Delta M}$ in cells proficient or deficient in A-type lamins (lentivirally transduced with shControl or shLmna, respectively). The two cell lines were treated with vitamin D or vehicle control (BGS) for 24 h. Actin was used as a loading control. **(B)** Representative images of metaphase spreads from the different samples analyzed. Telomeres are labeled with a specific PNA probe (yellow). Chromosomes are stained with DAPI (blue). Red arrows indicate fusions. **(C)** Quantification of the percentage of metaphases presenting chromosome end-to-end fusions in cells treated with either vitamin D or BGS after retroviral transduction with TRF2$^{\Delta B\Delta M}$. vitamin D treatment restores 53BP1 levels and normal processing of dysfunctional telomeres in lamins-deficient cells, leading to increased number of fusions. WT MEFs retrovirally transduced with TRF2$^{\Delta B\Delta M}$ were used as a positive control. A minimum of 20 metaphases were analyzed per sample.

2.4 Response of lamins-deficient cells to IR-induced DNA DSBs

By investigating the role of A-type lamins in NHEJ of deprotected telomeres, we revealed a novel pathway that might be affected by laminopathic mutations and/or alterations in the expression of A-type lamins. However, despite their tremendous usefulness as models of long-range DSBs, deprotected telomeres are significantly different from the intrachromosomal breaks that might arise due to genotoxic insult to the cell. Telomeric DNA consists of TG-rich repeats, is highly heterochromatinized, bound by a distinct group of sequence/structure specific proteins (shelterin complex), and adopts a very specific tertiary structure. In fact, specific components of the shelterin complex strongly affect recognition of telomeres by the DSB repair pathway and the specific mechanism used to process them. Although many of the processes that contribute to repair of normal intrachromosomal DSBs are also necessary for processing of deprotected telomeres, repair of deprotected telomeres involves additional steps, such as maneuvering of the shelterin complex to provide access to DDR proteins. As such, our findings on A-type lamins and telomeric NHEJ could not automatically be extrapolated to repair of other forms of DSBs. To develop a more inclusive understanding of DSB repair in lamins-deficient cells we investigated the global repair of DSBs, which we induced by treating asynchronous cells with ionizing radiation.

One of the earliest responses to DNA DSBs is phosphorylation of H2AX (γ-H2AX) in the surrounding chromatin [197, 198] followed by recruitment of 53BP1 to the demarcated site [199]. These changes occur within minutes of exposure to IR and can be visualized as foci by immunofluorescence. IR-induced foci (IRIF) are highly organized structures and are strictly regulated during the course of the DNA damage response [200]. Changes in the kinetics of formation and resolution of DNA repair foci are used as an indication of alterations in the DDR pathway [69]. Here, we tested whether loss of A-type lamins alters the cellular response to IR by evaluating the formation/resolution of γ-H2AX and 53BP1 IRIF. $Lmna^{+/+}$ and $Lmna^{-/-}$ MEFs were treated with 0.5 Gy of IR and immunofluorescence assays performed to label γ-H2AX and 53BP1 IRIF at different times post-IR. Cells presenting more than 5 foci were scored as positive for

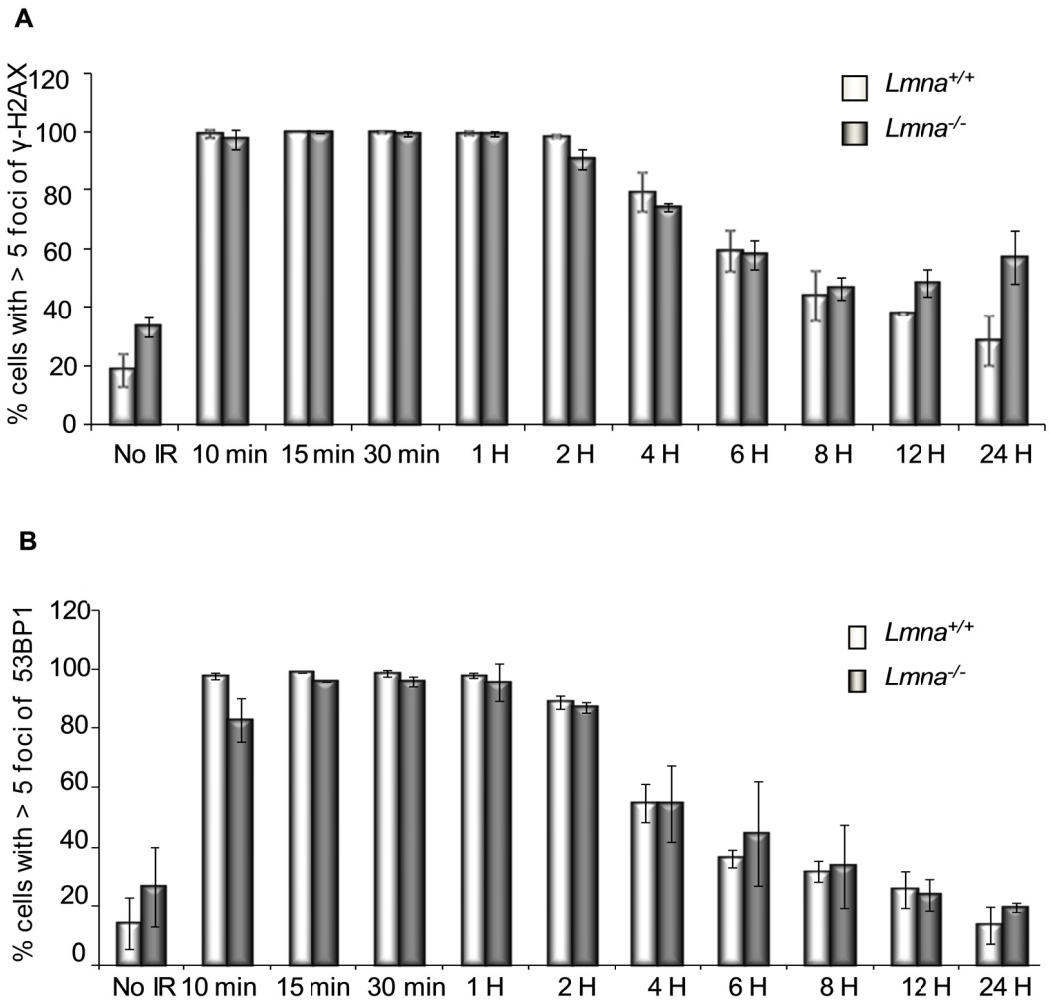

Figure 17. Spatio-temporal formation and resolution of DNA repair foci induced by ionizing radiation. Lmna$^{+/+}$ and Lmna$^{-/-}$ MEFs were irradiated with 0.5 Gy or left untreated. Cells were fixed at different times post-IR (from 10 min to 24 h) and subjected to immunofluorescence (IF) with an antibody recognizing **(A)** γH2AX or **(B)** 53BP1. Cells presenting more than 5 foci were scored as positive for responding to IR. A total of 200–300 cells were scored per time point and per experiment. The average ± standard deviation of three independent experiments is shown.

responding to IR. In agreement with our previous studies, untreated Lmna$^{-/-}$ MEFs had a higher percent of cells that scored positive for γ-H2AX foci (Figure 17A). However both genotypes sensed IR-induced damage similarly, so that nearly 100% of MEFs had formed γ-H2AX foci by 10 min post-IR. Resolution of γ-H2AX foci (starting at 4hrs post IR) was also grossly similar in both genotypes. However at 24h post-IR the Lmna$^{+/+}$ cells had reverted to basal levels of DNA

damage while the Lmna$^{-/-}$ cells still exhibited residual γ-H2AX IRIF, which indicated an incomplete response to the DNA damage. Given the decreased 53BP1 in lamin A/C-deficient cells, we determined if the kinetics of 53BP1 IRIF was altered in the Lmna$^{-/-}$ and Lmna$^{+/+}$ cells. As with γ-H2AX IRIF, nearly 100% of the cells in both genotypes responded to IR by forming 53BP1-labeled foci, and the overall kinetics of formation and resolution of 53BP1 DNA repair foci was similar in both genotypes (Figure 17B).

While the ability of cells to form 53BP1 IRIF was unaffected by the absence of A-type lamins, we observed a profound and consistent decrease in the intensity of fluorescence of 53BP1 IRIF in Lmna$^{-/-}$ MEFs with respect to Lmna$^{+/+}$ controls at all times post-IR (Figure 18 and data not shown). Striking differences in intensity were observed at 30 min, 1 h, and 2h after IR. By 24 h, 53BP1 protein was dispersed throughout the nucleus in Lmna$^{+/+}$ cells, mirroring the localization of the protein in cells that were not irradiated. In contrast, Lmna$^{-/-}$ fibroblasts still displayed decreased 53BP1 intensity, and there were changes in its nuclear distribution so that rather than having a disperse distribution, it had accumulated in a few large foci. Since the intensity of labeling with γ-H2AX foci was indistinguishable between Lmna$^{+/+}$ and Lmna$^{-/-}$ cells throughout the time course of the experiments, we conclude that the difference in 53BP1 accumulation in Lmna$^{-/-}$ cells is specific to that protein and not due to widespread changes in the DDR proteins.

Large 53BP1 nuclear bodies, similar to what we observed, were recently shown to colocalize with OPT (Oct-1, PTF, transcription) domains in G1 BJ fibroblasts [201]. These 53BP1-OPT domains were characterized by low levels of transcriptional activity and co-localized with γ-H2AX and MDC1. The authors proposed that the 53BP1-OPT bodies mark damaged DNA, particularly fragile chromosome sites, where replication is incomplete. In support of this model, treatment of cells with low levels of aphidicolin, which induces DNA damage at fragile sites [202], but not hydroxyurea increased the formation of 53BP1-OPT bodies. Future studies will determine if the large 53BP1 foci we observe upon treatment of Lmna$^{-/-}$ with IR colocalize with OPT

domains. This would indicate that either (i) fragile sites in Lmna$^{-/-}$ cells have increased susceptibility to ionizing radiation as compared to those in Lmna$^{+/+}$ cells or (ii) Lmna$^{-/-}$ cells do not fully arrest in response to DNA damage, allowing some unrepaired breaks to carry over into S-phase. The former is supported by the fact that there are gross changes in the epigenetic features of chromatin in Lmna$^{-/-}$ cells which could render the chromatin more "delicate", while the latter is supported by the fact that cell cycle control is deregulated in the Lmna$^{-/-}$ cells due to alterations in Rb proteins.

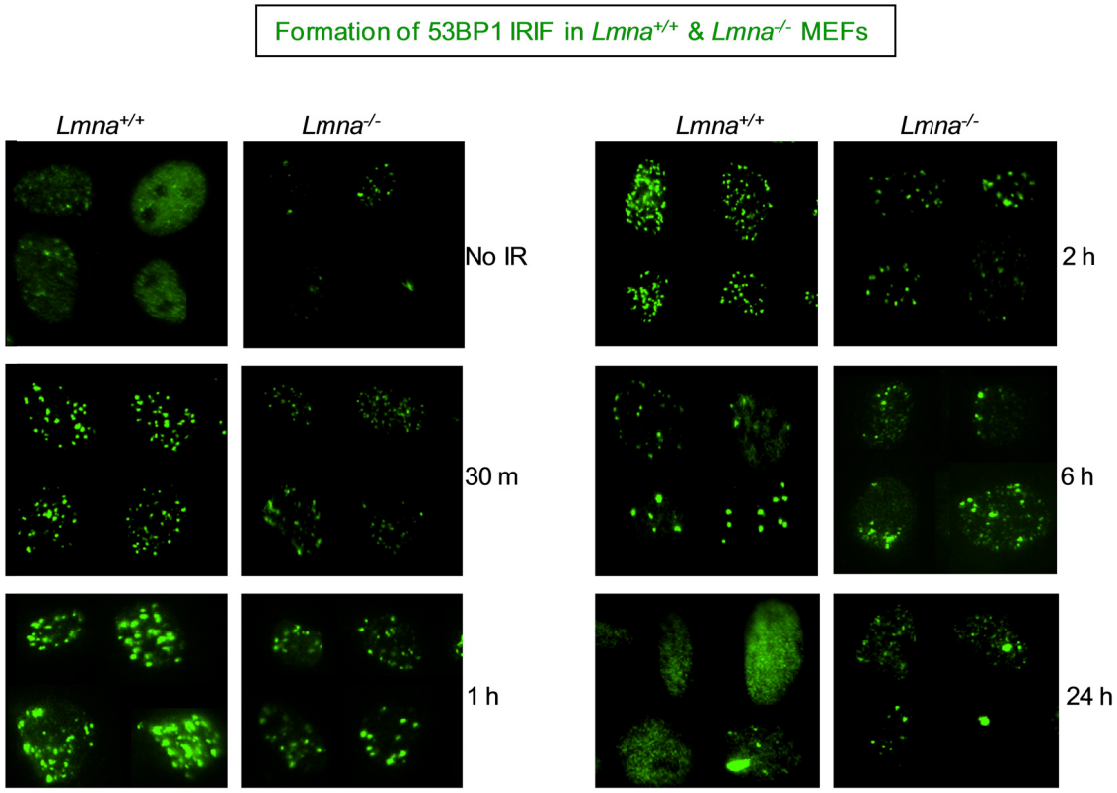

Figure 18. Decreased accumulation of 53BP1 at IRIF in Lmna$^{-/-}$ MEFs. Lmna$^{+/+}$ and Lmna$^{-/-}$ MEFs were irradiated with 0.5 Gy or left untreated. Cells were fixed at different times post-IR (from 30 min to 24 h) and subjected to immunofluorescence (IF) with an antibody recognizing 53BP1. Pictures of fields selected randomly were taken under the same conditions of exposure. Representative images of four cells per condition are shown in each panel.

Given the differences in accumulation of 53BP1 at the IRIF and the role of 53BP1 in NHEJ, we speculated that decreased accumulation of 53BP1 at the break sites might affect downstream effectors of the DDR pathway. In a previous model, Fernandez-Capetillo et al. suggested that phosphorylation of H2AX induces an increase in the local concentration of 53BP1

around damaged DNA/chromatin, which serves as a platform for interaction with different DDR factors [109]. Defects in γ-H2AX and 53BP1 were predicted to result in impaired activation of downstream effectors of the signaling and repair of DNA damage. Based on this model, we decided to investigate if decreased accumulation of 53BP1 in $Lmna^{-/-}$ cells affects downstream signaling in the DDR pathway. A central event in IR-induced DDR is ATM -dependent phosphorylation of p53 at Ser15. Phosphorylation of p53 activates checkpoints that slow cell cycle progression until the damage is repaired. Despite significant decreases in 53BP1 at IRIF, $Lmna^{-/-}$ fibroblasts could robustly phosphorylate p53 at Ser15 in response to IR (Figure 19) indicating that the loss of A-type lamins did not hinder the activation of this downstream DDR effector. Furthermore, there was normal induction of p21 in lamins-deficient cells (data not shown). These results indicate that the loss of A-type lamins does not hinder the activation of the DDR pathway.

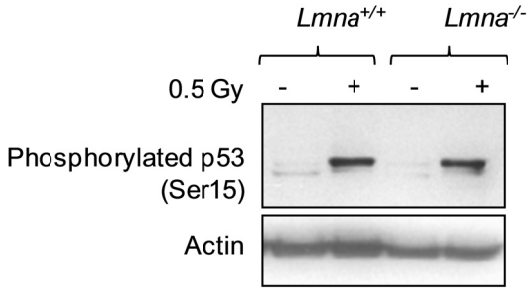

Figure 19. Phosphorylation of p53 in $Lmna^{+/+}$ and $Lmna^{-/-}$ MEFs treated with IR. Cells were treated with 0.5 Gy IR and total cell lysates collected 30 minutes post-treatment. Immunoblotting with antibodies recognizing phosphorylated p53 at Ser15 indicates no difference in activation of the p53 pathway in lamins-deficient cells.

2.5 Defective repair of IR-induced DSBs in lamins-deficient cells

To determine the functional significance of decreased 53BP1 at IRIF in Lmna$^{-/-}$ cells, we evaluated repair of IR-induced DSBs by performing neutral comet assays. Asynchronously growing Lmna$^{+/+}$ and Lmna$^{-/-}$ MEFs were treated with 8 Gy of IR, cells were collected at different times post-IR, and the extent of DNA DSB repair evaluated by single cell gel electrophoresis under neutral conditions [203]. Single cell gel electrophoresis results in a comet-shaped distribution of DNA as fragments migrate away from the center of the nucleus. The comet head contains high-molecular weight and intact DNA, and the comet tail contains the leading ends of migrating fragments (Figure 20a). Olive moment, a quantification of the amount of DNA and its distribution in the tail, is a measure of unrepaired DNA breaks [203]. When compared to wild-type MEFs, lamin A/C-deficient cells had a higher olive moment at all times tested post-IR (Figure 20b). This indicated that DNA DSB repair was substantially compromised by loss of A-type lamins.

The repair of DSBs after IR usually follows bimodal kinetics with fast and slow repair phases [69]. There is substantial evidence implicating classical NHEJ as the major mechanism used during the fast phase of DSBs repair, and alternative NHEJ or HR in the slow phase of repair [204, 205]. This bimodal form of DNA DSBs repair is clearly observed in Lmna$^{+/+}$ fibroblasts, such that the fast phase occurred within 60 minutes post-IR, followed by a relatively slow phase of DSBs repair onwards (Figure 20B). However, Lmna$^{-/-}$ fibroblasts did not display this fast phase of repair, requiring up to 150 minutes to repair the damage that could be repaired within 30 - 60 minutes by the wild-type cells (Figure 20B). This indicated that the involvement of A-type lamins in NHEJ extends beyond the scope of deprotected telomeres, being also applicable to the repair of IR-induced DSBs.

To determine if 53BP1 could rescue the defective fast-phase of repair of IR-induced DSBs in Lmna$^{-/-}$ MEFs, cells were retrovirally transduced with a 53BP1 construct or an empty vector control (Figure 21A) and neutral comet assays were performed. While Lmna$^{-/-}$ fibroblasts

transduced with the empty vector still presented defects in the fast phase of DNA repair (Figure 21B), reconstitution of 53BP1 into Lmna$^{-/-}$ fibroblasts completely restored the fast-phase repair of DNA DSBs repair (Figure 21B). Furthermore, overexpression of 53BP1 in Lmna$^{+/+}$ fibroblasts did not lead to a further increase in the ability of these cells to repair DSBs (Figure 21B). Collectively, our data on NHEJ-mediated DSB repair (IR-induced breaks and deprotected telomeres) strongly suggest that the mechanism by which A-type lamins affects NHEJ is indirect, occurring *via* stabilization of the 53BP1 protein. In further support of this finding, treatment of lamins-deficient cells with vitamin D (which increases 53BP1 levels by inhibiting the activity of cathepsin L) was also shown to restore the fast phase of repair [187].

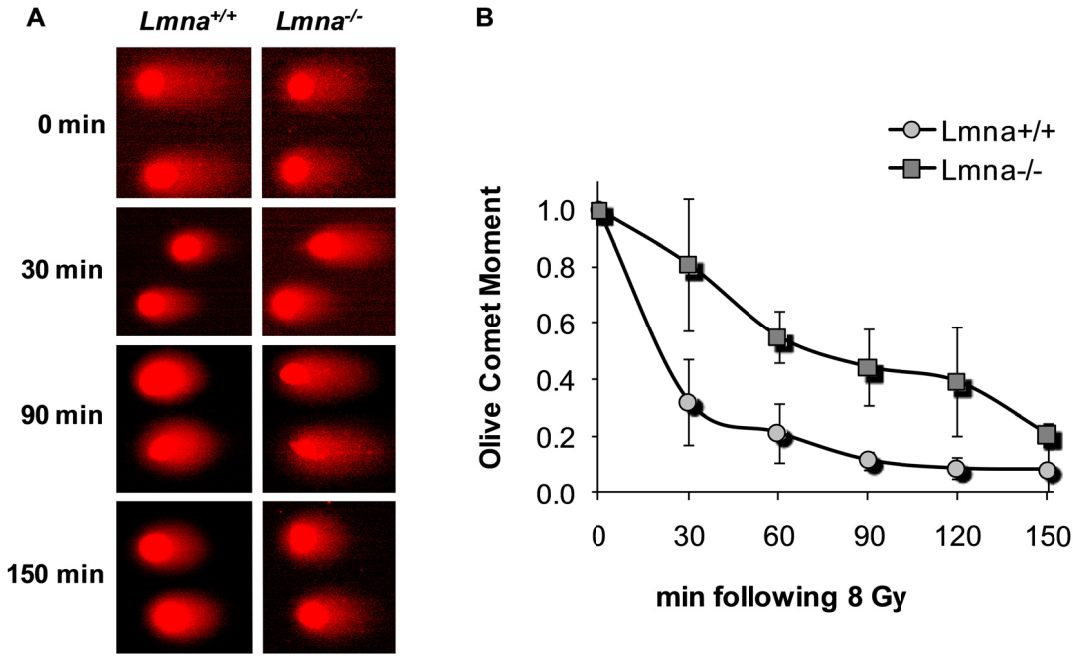

Figure 20. Defective repair of IR-induced DNA DSBs upon loss of A-type lamins. Asynchronously growing Lmna$^{+/+}$ and Lmna$^{-/-}$ MEFs were irradiated with 8 Gy. At different times post-irradiation (0, 30, 60, 90, 120 and 150 min) cells were collected and neutral comet assays were performed. **(A)** Representative images of the comets. Note the presence of comet tails immediately after IR, and how the tails decrease with time, indicating active repair of DSBs. **(B)** Kinetics of repair of IR-induced DSBs as assessed by Olive Comet Moment, a measure of unrepaired DNA. A total of 25 to 30 cells were analyzed per sample in each experiment. The average ± standard deviation of 4 independent experiments is shown.

.

Interpretation of these results is complicated by the fact that previous reports have indicated dispensability of 53BP1 for repair of short-range DNA DSBs, along with our data showing that depletion of 53BP1 in wild-type MEFs did not inhibit the fast-phase of repair (Figure 21C). We reason that 53BP1 deficiency in lamin A/C-deficient cells is not solely responsible for the observed defects in the fast-phase of repair. Rather, it is the combined deficiency of A-type lamins and 53BP1 which is responsible for the shift in the kinetics of DNA DSBs repair towards a slower operating mechanism. This slower form of repair could represent a lower efficiency of C-NHEJ or activation of an alternative mechanism of repair in lamins-deficient cells. In either case the fact that reconstitution of 53BP1 restores normal kinetics of repair of IR-induced DNA DSBs supports a role for 53BP1 in promoting C-NHEJ repair and inhibiting alternative mechanisms of DNA DSBs repair.

2.6 DISCUSSION

Previous studies had shown that expression of mutant lamin A isoforms leads to alterations in the DDR and defective repair, which translate into increased sensitivity to DNA-damaging agents [152, 173, 206]. Prior to our studies the effect of complete loss of A-type lamins on DNA repair mechanisms remained unknown. By demonstrating that TRF2$^{\Delta B\Delta M}$ -induced telomere fusions require A-type lamins, we provided the first link between loss of A-type lamins and defective NHEJ repair. The fact that mutations in the LMNA gene were previously associated with increased NHEJ [152] indicates yet another functional difference between mutation and loss of A-type lamins. In light of a report showing that loss of 53BP1 inhibits processing of dysfunctional telomeres by NHEJ [51], we hypothesized that destabilization of this protein in lamins-deficient cells was in part responsible for the observed phenotype. In support of this hypothesis, our reconstitution experiments clearly demonstrate that destabilization of 53BP1 upon loss of A-type lamins is responsible for the defects in the processing of dysfunctional telomeres by NHEJ. Interestingly, the telomeric NHEJ elicited by TRF2$^{\Delta B\Delta M}$ requires 53BP1 and DNA ligase IV, indicating it as C-NHEJ, whereas the NHEJ elicited by removal of Tpp1-Pot1a/b, another shelterin

complex protein, is independent of 53BP1 and instead requires the A-NHEJ protein CtIP [207]. Future experiments will determine if A-type lamins function in A-NHEJ of deprotected telomeres.

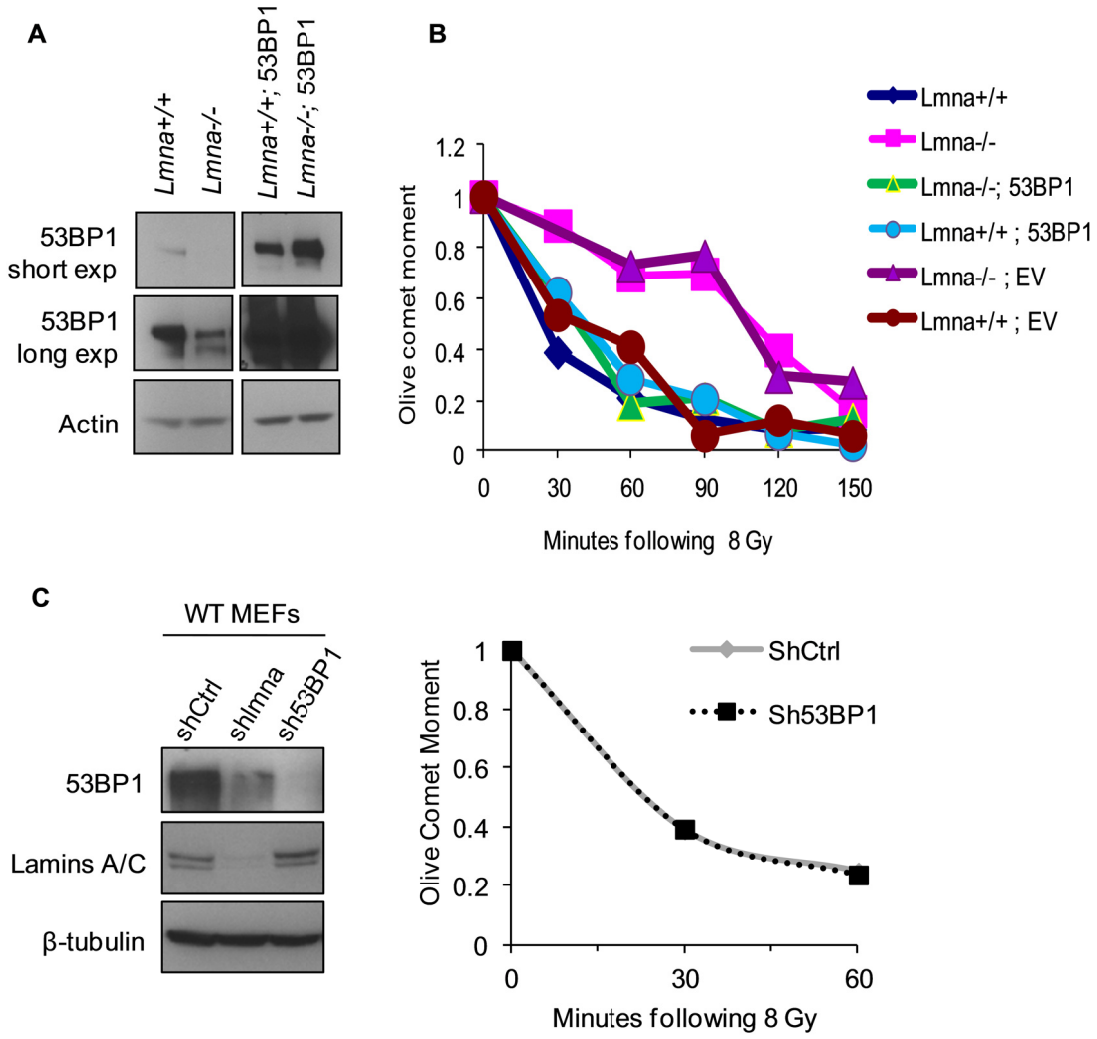

Figure 21. 53BP1 rescues fast-phase repair of IR-induced DSBs in Lmna$^{-/-}$ cells. (A) Western blots to monitor the levels of 53BP1 protein in Lmna$^{+/+}$ and Lmna$^{-/-}$ MEFs retrovirally transduced with empty vector (EV) control or a 53BP1-expressing vector. Short and long exposures of 53BP1 are shown. Actin levels are used as loading control. **(B)** Kinetics of repair of IR-induced DSBs as assessed by Olive Comet Moment in Lmna$^{+/+}$ and Lmna$^{-/-}$ MEFs retrovirally transduced with an EV or a vector encoding 53BP1. Approximately 25 to 30 cells were analyzed per sample, normalized, and the mean calculated. Reconstitution of 53BP1 in Lmna$^{-/-}$ cells rescues fast-phase repair, as opposed to expression of an empty vector control. **(C)** Comet assays performed on wild-type MEFs with or without 53BP1 demonstrate that loss of 53BP1 (left panel) alone does not affect fast-phase repair of IR-induced DNA DSBs (right panel).

In addition to the role of A-type lamins in long-range NHEJ, our studies demonstrate their participation in short-range DSBs repair, as exemplified by the defects in the fast-phase of repair of IR-induced DSBs. In mammalian cells DNA DSB repair occurs mainly by NHEJ and HR. NHEJ is faster and more efficient than HR, but at the expense of low fidelity. Analysis of kinetics of repair of IR-induced DNA DSBs has revealed two types of NHEJ. C-NHEJ represents the fast component of DSB rejoining and relies on DNA-PK and the XRCC4/DNA Ligase IV complex [205, 208]. Although DNA-PK deficiency retards repair of DNA DSBs, damage is eventually repaired by a slower operating mechanism, possibly A-NHEJ [204]. Given the dominance of the slow phase repair in lamins-deficient cells we speculate that it might represent an upregulation of A-NHEJ in lieu of decreased C-NHEJ. Interestingly reconstitution of 53BP1 in lamins-deficient cells was sufficient to rescue the fast-phase repair of IR-induced DNA damage. While a whole body of evidence indicates that 53BP1 participates in long-range DNA end-joining processes, such as class switch recombination, V(D)J recombination, and chromosome end-to-end fusions, the role of 53BP1 in short-range DSB repair is not clear [99]. Depletion of 53BP1 from wild-type cells resulted in no change in their ability to complete the fast-phase of repair IR-induced DSBs. The fact that 53BP1 was able to rescue fast-phase repair in $Lmna^{-/-}$ cells suggests that the role of 53BP1 in repair of IR-induced DSBs in wild-type cells is masked by a functional redundancy, which is lost in A-type lamins-deficient cells. We speculate that loss of A-type lamins activates compensatory mechanisms that repair DSBs with slower kinetics. Restoration of 53BP1 in this context would then alter the balance between different DSBs repair pathways, tilting it in favor of the fast-phase C-NHEJ. Future studies will address whether loss of A-type lamins is associated with upregulation of other repair pathways, such as A-NHEJ.

Given the well established contribution of genomic instability to aging and cancer, identifying the molecular mechanisms involved in maintaining genomic integrity is of utmost importance. DNA DSBs repair, which occurs mainly by NHEJ and HR, is critical for maintaining genomic stability. We have demonstrated that the structural nuclear proteins A-type lamins preserve the integrity of the genome in part by maintaining the ability of cells to repair DNA DSBs

by NHEJ. We also provide evidence that the mechanism which allows A-type lamins to promote long-range (dysfunctional telomeres) and short-range (IR-induced DNA DSBs) classical-NHEJ is the stabilization of 53BP1.

CHAPTER THREE

Repression of Homologous Recombination in Lamins-Deficient Cells

ABSTRACT

In the previous chapters, we demonstrated a significant inhibition of the non-homologous end-joining (NHEJ) pathway in lamins-deficient human and mouse cells. Lamins-deficient cells exhibit decreased levels of 53BP1, an important NHEJ protein, due to post-translational degradation. Increasing the levels of 53BP1 in lamins-deficient cells by exogenous expression or inhibiting the degradation of the endogenous protein was sufficient to rescue NHEJ. To attain a more complete understanding of how A-type lamins affect repair of DNA double strand breaks, we investigated whether A-type lamins could affect homologous recombination (HR). Based on the idea that different DSB repair pathways compete for repair substrate and recent reports showing that 53BP1 is a potent inhibitor of HR, we hypothesized that decreased 53BP1 in lamin A/C-depleted cells would lead to increased HR. Surprisingly, we find that depletion of lamins significantly compromises HR by a mechanism involving transcriptional downregulation of BRCA1 and RAD51. Furthermore, we show that repression of BRCA1 and RAD51 requires p130, and occurs in the context of decreased Rb and p107 protein levels. It was previously established that loss of A-type lamins leads to proteasomal degradation of Rb and p107; however the exact mechanism by which they become targeted for degradation remained an enigma. We provide evidence that the cysteine protease Cathepsin L, which is upregulated in lamins-deficient cells contributes to degradation of Rb and p107. In line with the DNA repair defects, lamins-deficient cells exhibit increased radiosensitivity. This study demonstrates that A-type lamins promote genomic stability by maintaining the levels of proteins with key roles in DNA DSBs repair by NHEJ and HR, and reveals an unprecedented role for Cathepsin L in regulating Rb and p107.

3.1 Decreased HR in lamins-deficient cells

To evaluate the proficiency of HR in lamins-deficient cells, we used a chromosomally integrated reporter substrate, DR-GFP, in MCF-7 cells that were depleted of A-type lamins [209]. The DR-GFP substrate consists of two tandem GFP sequences that have both been mutated to abrogate expression of GFP, and an Isce-I recognition site in one sequence. Transient

expression of the I-SceI endonuclease produces a DSB at the recognition site. Repair of this break by intragenic HR with the downstream GFP sequence as the homology substrate results in restoration of a functional GFP gene. Thus, expression of GFP is a readout of successful HR in these cells.

While shRNA depletion of A-type lamins in MCF-7 DR-GFP cells led to a substantial reduction in 53BP1 (Figure 22A), contrary to our expectations, there was a 40% reduction in HR in these cells when compared to their shcontrol counterparts (Figure 22B). As a positive control for the DR-GFP assay similar experiments were performed in parallel in cells expressing the viral oncoprotein E6, which is known to cause increased homologous recombination (Figure 22C). Thus, the combined loss of A-type lamins and 53BP1 resulted in a phenotype that was inconsistent with only 53BP1 deficiency, suggesting that the loss of A-type lamins affected additional events during HR.

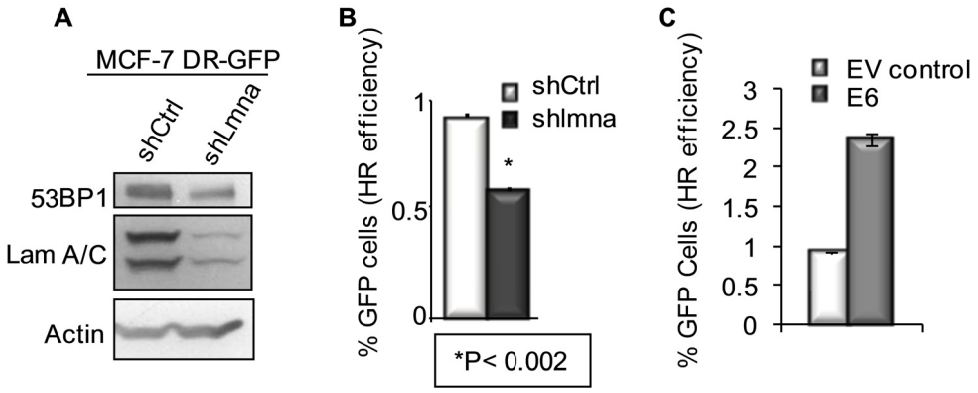

Figure 22. A-type lamins promote homologous recombination. (A) Western blots showing decreased 53BP1 protein upon depletion of A-type lamins in human cells (MCF-7) carrying an HR reporter construct (DR-GFP). **(B)** Percent of GFP-positive MCF7-DR-GFP cells resulting from homologous recombination of I-SceI-induced DSBs. Depletion of A-type lamins leads to a 40% reduction in HR. **(C)** As a positive control for Isce-I induced HR using the DR-GFP assay, we found that inactivation of p53 by retroviral transduction of MCF-7 DR-GFP cells with the viral oncogene E6 leads to increased HR, as previously reported[210].

3.2 Deficient recruitment of HR proteins to IRIF

To elucidate the molecular mechanisms behind HR defects in lamins-deficient cells, we monitored recruitment of RAD51, an essential HR protein, to IRIF. We treated lamin A/C proficient and deficient MCF-7 DR-GFP cells with 8 Gy of IR and performed immunofluorescence to detect RAD51 foci 6 h post-IR. We found a significant decrease in the formation of RAD51 foci, such that only 27% of shLmna cells scored positive for RAD51 IRIF, as opposed to 64% of the shCtrl cells (Figure 23A and C). To ensure that our results were not cell type- or shRNA sequence-specific, we performed acute depletion of A-type lamins in wild-type MEFs, using a mouse-specific shRNA. Consistently, loss of A-type lamins led to a decrease in the formation of RAD51 IRIF (Figure 23B). Next, we determined if upstream steps in the HR pathway were affected by monitoring the formation of RPA IRIF. RPA binds to single stranded DNA (ssDNA), which is formed during end-resection in homologous recombination, and can also be visualized as foci by immunofluorescence staining. The presence of RPA foci is generally considered an indication of successful DNA end-resection. As with the RAD51 IRIF we found a significant reduction in the formation of RPA IRIF in the lamins-depleted cells (Figure 23D).

Interestingly, monitoring the levels of RAD51 by western blot revealed a marked decrease of the protein in lamins-depleted cells. (Figure 24A). In contrast, global levels of RPA were not affected by depletion of A-type lamins (Figure 24B). This indicated that another critical upstream step in the HR process was affected. Since the formation of RPA foci reflects the presence of ssDNA, we reasoned that DNA end-resection could be affected by loss of A-type lamins. Based on the importance of BRCA1 in the formation of ssDNA we investigated whether BRCA1 protein levels were also being affected by depletion of A-type lamins. We were surprised to find that like RAD51, depletion of A-type lamins from MCF-7 cells was associated with a significant reduction in BRCA1 protein levels (Figure 24B).

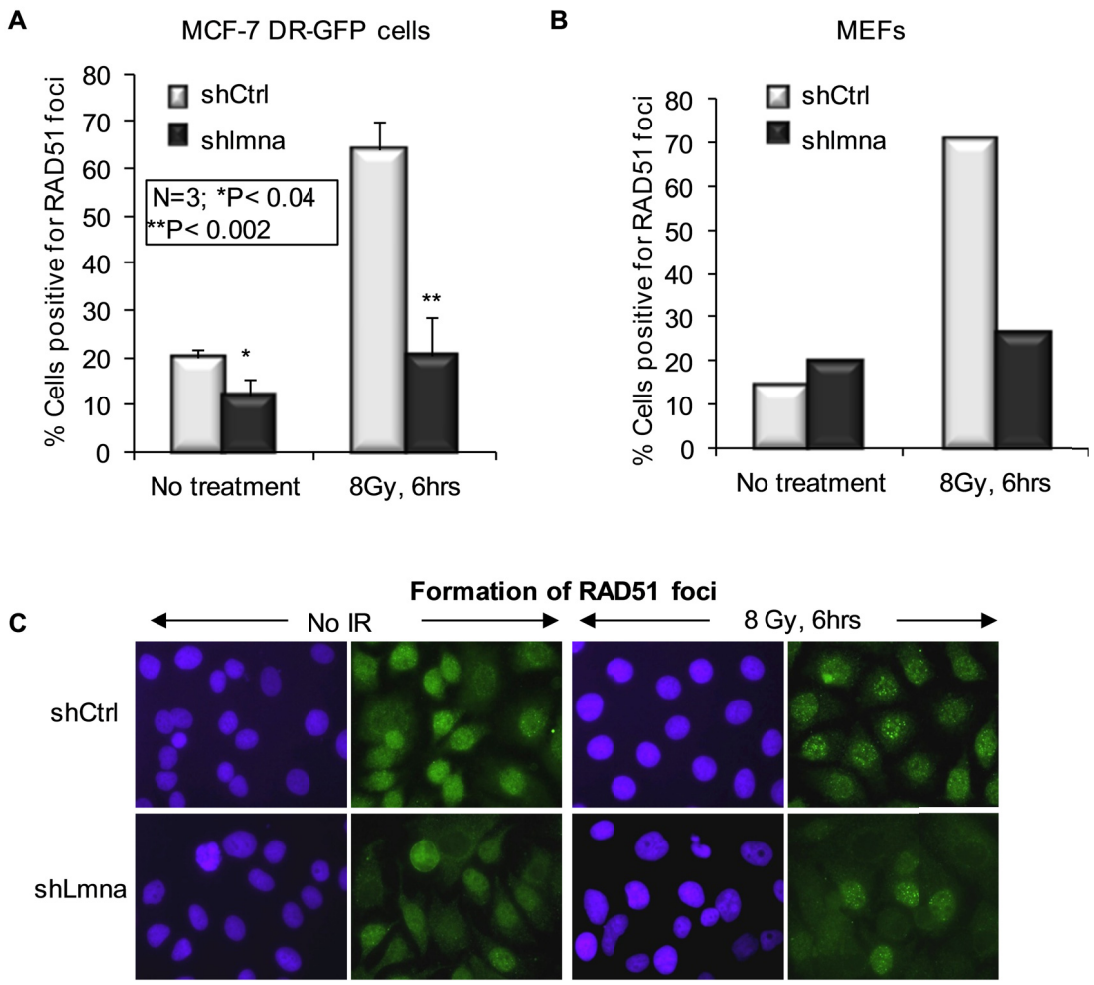

Figure 23. Loss of A-type lamins leads to decreased formation of IR-induced RAD51 foci. Cells were lentivirally transduced with a control shRNA or shLmna, treated with 8Gy IR and allowed to recover for 6 hrs before immunofluorescence experiments to monitor formation of RAD51 foci. **(A)** Graph shows the percentage of MCF-7 DR-GFP cells positive for RAD51 foci (more than 10 foci in the nucleus). 200 cells per condition were analyzed per experiment. The average ± standard deviation of 3 independent experiments is shown. **(B)** MEFs that are depleted A-type lamins also display a significant reduction in their ability to form RAD51 IRIF. **(C)** Representative images of RAD51 foci in MCF-7 DR-GFP cells. Blue images show DAPI stained nuclei, green shows RAD51 immunofluorescence. **(D)** Percent of cells positive for formation of RPA2 foci.

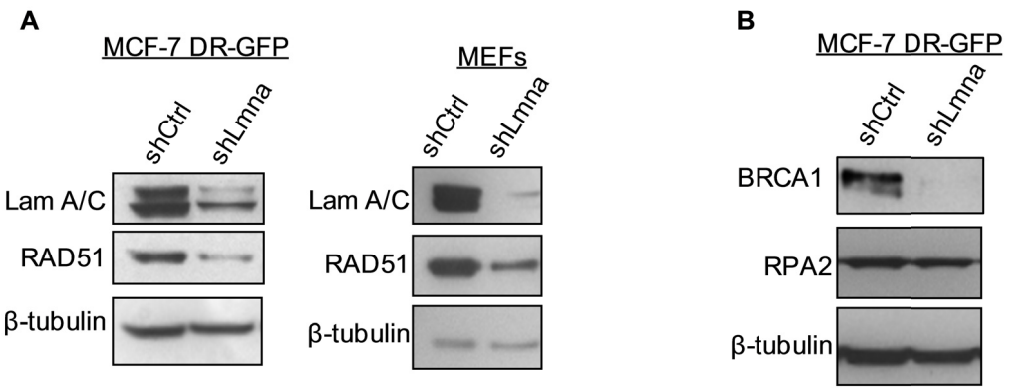

Figure 24. Decreased expression of RAD51 and BRCA1, but not RPA2 in lamin A/C-depleted cells. (A) Western blots showing the decrease in global levels of RAD51 upon depletion of A-type lamins in both MCF-7 DR-GFP cells and MEFs. β–tubulin was used as a loading control. **(B)** BRCA1, an essential HR protein, is also severely decreased in lamins-deficient cells. However this effect is not observed in another important HR protein RPA2.

To determine the mechanism behind decreased RAD51 and BRCA1 protein expression, we performed qRT-PCR to determine if their mRNA levels were affected. Unlike 53BP1, decreased RAD51/BRCA1 was associated with significant decreases in mRNA levels (Figure 25A). This decrease in mRNA level was not a general occurrence for HR proteins, as the mRNA levels of RPA2 were not significantly affected. A similar decrease in RAD51 transcript levels was also observed in MEFs depleted of A-type lamins (Figure 25B).

Previous studies indicated that under certain stress conditions cells downregulate the expression of RAD51 and BRCA1 genes *via* transcriptional repression by E2F4/p130 complexes that bind to E2F sites in their promoters [211, 212]. The co-regulation of BRCA1 and RAD51 observed upon loss of A-type lamins, together with the fact that lamins deficiency induces profound decreases in pRb and p107 levels with only minor effects in p130 ([148] and Figure 26A) led us to hypothesize that this E2F4/p130 repressive complex might participate in the repression of RAD51 and BRCA1 genes. To test if p130 was required for the transcriptional downregulation of RAD51 upon loss of A-type lamins, we depleted lamins in cells double null for pRb and p107 (DKO: $Rb^{-/-}$;$p107^{-/-}$) and in cells null for all three Rb family members (TKO: $Rb^{-/-}$

;p107$^{-/-}$;p130$^{-/-}$). Depletion of A-type lamins in DKO cells - proficient in p130 - led to a marked decrease in RAD51 protein levels (Figure 26B). In contrast, depletion of A-type lamins in TKO cells did not result in downregulation of RAD51 levels, indicating that p130 is required for downregulation of RAD51 upon loss of A-type lamins.

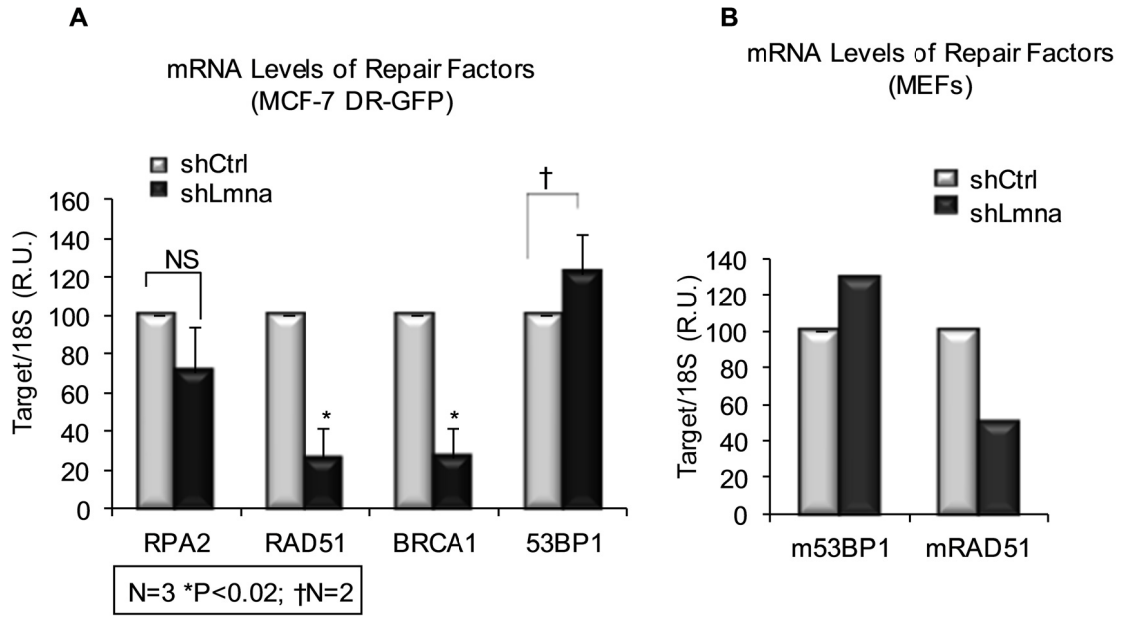

Figure 25. Decreased transcription of RAD51 and BRCA1, but not RPA2 or 53BP1 in lamin A/C-depleted cells. (A) qRT-PCR to determine the mRNA transcript levels of RPA2, RAD51, BRCA1, and 53BP1 in MCF-7 cells. Note that loss of A-type lamins leads to a significant reduction in transcripts of RAD51 and BRCA1, but not RPA2 or 53BP1. Shown are the averages and standard deviations from three different experiments. **(B)** qRT-PCR in MEFs demonstrates a similar decrease in RAD51 mRNA but not 53BP1 upon loss of lamin A/C.

To further investigate the role of E2F4/p130 in RAD51 repression in lamin A/C deficient cells, we determined if depletion of A-type lamins would promote formation of the p130/E2F4 repressive complex by performing co-immunoprecipitation studies. Total cell lysates from wild-type MEFs were subjected to immunoprecipitation with an E2F4 antibody, and the presence of p130 monitored by western blot. While depletion of A-type lamins did not affect the global levels of E2F4 (Figure 26A and C), it promoted the formation of p130/E2F4 complexes, as shown by the increase in p130 co-immunoprecipitated with the E2F4 antibody (Figure 26C). The same results were obtained upon depletion of A-type lamins in DKO cells, proficient in p130 (Figure 26D).

Thus, we conclude that depletion of A-type lamins promotes the ability of p130 to form repressor complexes with E2F4, which in turn leads to downregulation of RAD51 and BRCA1 genes, resulting in defective repair of DNA DSBs by HR.

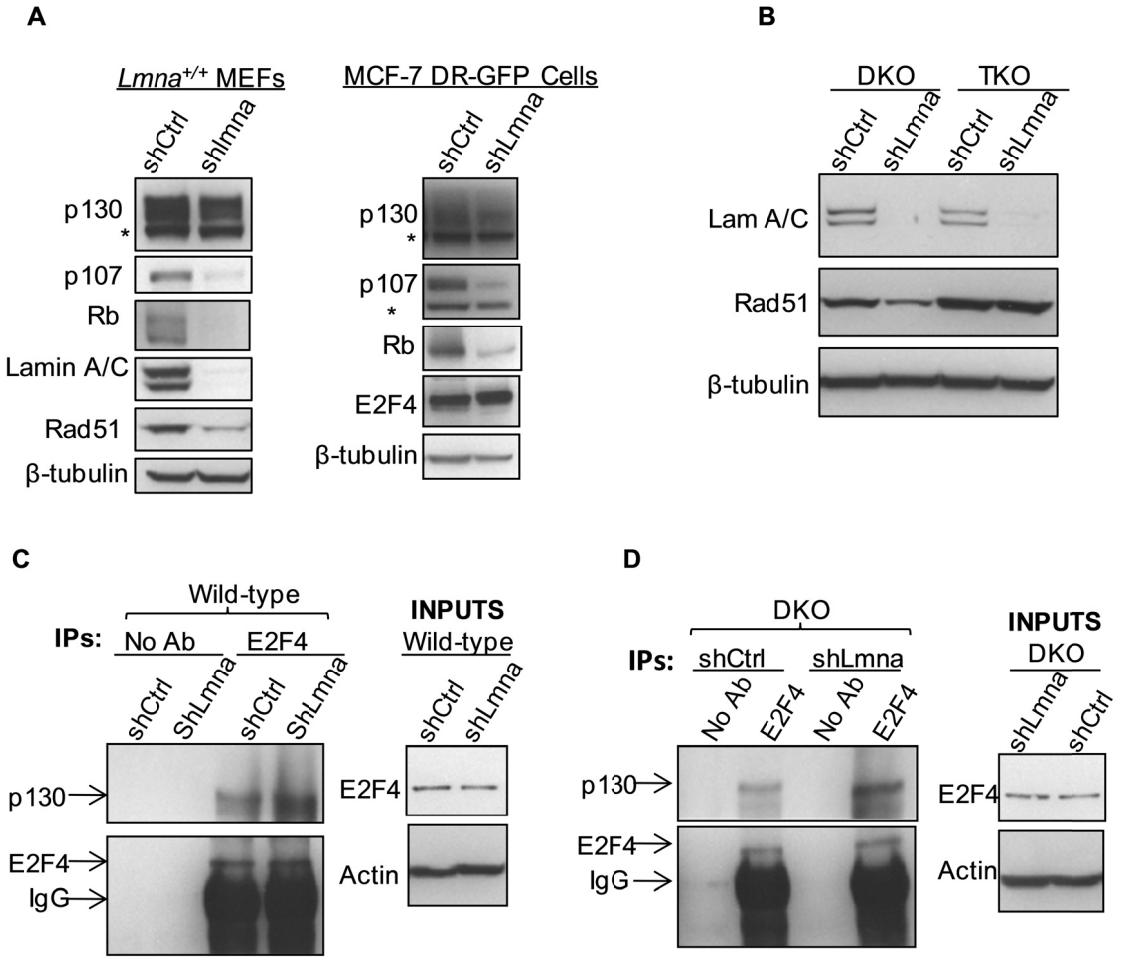

Figure 26. Downregulation of RAD51 in lamin A/C-deficient cells requires p130, a member of the pocket family of proteins. (A) Western blots showing alterations in expression of the pocket family proteins in MCF-7 DR-GFP cells and MEFs upon depletion of lamin A/C. Note significant decreases in Rb and p107, but not p130. Also note that expression of the repressive transcription factor, E2F4, remains unchanged. **(B)** Western blot showing depletion of A-type lamins from MEFs that are null for two (DKO: $Rb^{-/-}$; $p107^{-/-}$) or all three (TKO: $Rb^{-/-}$; $p107^{-/-}$; $p130^{-/-}$) of the pocket family proteins. Loss of lamins leads to a dramatic decrease of RAD51 only in the cells that are p130 proficient (DKO). **(C)** Co-immunoprecipitation of p130 with E2F4. Lysates from lamin A/C –proficient or –deficient MEFs were subjected to immunoprecipitation with an E2F4 antibody. Western blots (left) shows successful immunoprecipitation of E2F4, and co-precipitation of p130. Note how loss of lamins leads to increased pull down of p130. Inputs are on the right. **(D)** Similar to (C), except lysates were obtained from DKO MEFs. *Non-specific bands.

The p130/E2F4 repressor complex is active primarily during G0/G1 phases of the cell cycle. In addition, the levels of RAD51 and BRCA1 fluctuate during the cell cycle, being reduced during G1 and upregulated at late G1, S, and G2 phases of the cycle. Thus we investigated the possibility that p130/E2F4 mediated repression occurs due to changes in the cell cycle profile such that depletion of A-type lamins would induce a growth arrest in G1, which in turn would increase p130/E2F4 repressor complex activity and repression of RAD51 and BRCA1 genes. We used flow cytometry to analyze the cell cycle profile of pre-immortalized MEFs that were lentivirally transduced with a control shRNA or an shRNA specific for A-type lamins. While depletion of A-type lamins led to sharp decreases in RAD51 levels, it was not associated with an accumulation of cells in G1 phase of the cell cycle (Figure 27). These results indicate that the effect of depletion of A-type lamins on components of HR-mediated repair is not due to cell cycle arrest.

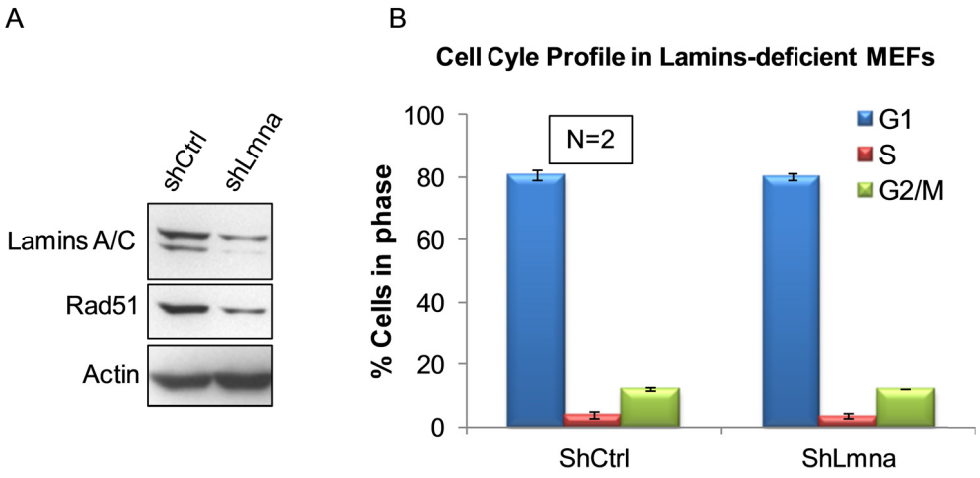

Figure 27. Loss of Lamins and Cell Cycle Profile. (A) Western blots show decreased RAD51 protein in pre-immortalized wild-type MEFs upon depletion of A-type lamins by lentiviral transduction with shLmna. **(B)** Decreased RAD51 in lamins-deficient cells is not due to alterations in cell cycle profile, as flow cytometry analysis demonstrates a similar cell cycle profile in both the shLmna and shCtrl cells.

Altogether, these data demonstrate an unprecedented role for A-type lamins in the transcriptional regulation of two key factors in HR, BRCA1 and RAD51, in both mouse and human cells. Furthermore, neutral comet assays performed in MCF7 DR-GFP cells depleted of A-type

lamins showed that these cells are also defective in fast-phase DNA repair (data not shown). Thus, we demonstrate novel roles for A-type lamins in the maintenance of factors with key roles in the repair of DSBs by both NHEJ and HR.

3.4 Cathepsin L regulates degradation of the retinoblastoma tumor suppressor proteins pRb and p107

Loss of A-type lamins leads to increased degradation of Rb and p107 [148]. This is thought to occur partly through the ability of A-type lamins to bind and regulate the sub-nuclear localization of these proteins. However, the specific mechanism by which Rb and p107 are targeted for degradation remains quite elusive, being independent of both MDM2 and gankyrin, a component of the 19S proteasome subunit which is overexpressed in Lmna KO cells [165]. Given our recent findings that CTSL promotes the degradation of 53BP1, we speculated that this protease could be the missing link between A-type lamins and Rb/p107 degradation. We envisioned a scenario where CTSL-mediated degradation of Rb and p107 alters the balance between the pocket family proteins, leading to increased formation of p130/E2F4 complexes, which can in turn mediate transcriptional repression of BRCA1 and RAD51 and thus inhibit HR.

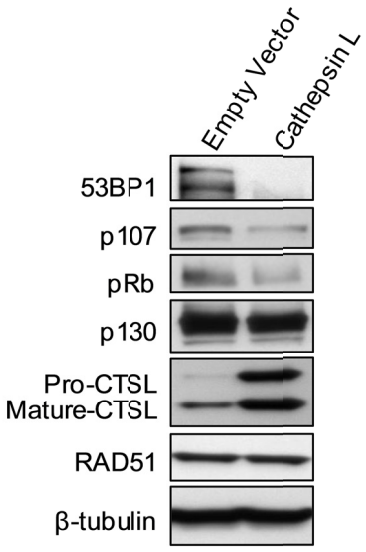

Figure 28. Regulation of Rb family members by CTSL. Western-blots showing that overexpression of CTSL in wild-type MEFs leads to downregulation of the pocket proteins pRb and p107 but has no effect in the levels of p130. Cells were retrovirally transduced with am empty vector as a negative control. As a positive control for increased CTSL activity, we show decreased levels of 53BP1 in the CTSL overexpressing cells.

To test our model we overexpressed CTSL in wild-type MEFs and monitored the levels of Rb family members and RAD51. Indeed, we found that upregulation of CTSL was associated with a substantial decrease in pRb and p107 but little effect on p130, mirroring the phenotype observed in lamins-deficient cells (

Figure 28). These results demonstrate a novel role for CTSL in the regulation of the Rb family of tumor suppressors. However, altering the levels of these proteins was not sufficient to induce transcriptional repression of BRCA1 or RAD51 (data not shown), suggesting that A-type lamins have additional roles in the regulation of transcription of these genes.

3.5 Loss of A-type lamins increases radiosensitivity

Radiation therapy is a common modality in the treatment of cancer. IR preferentially kills repair-compromised cells, which are unable to deal with the extensive DNA damage generated. To determine if loss of A-type lamins and the associated deficiency in 53BP1 and RAD51/BRCA1 affect sensitivity to IR, we performed colony formation assays. $Lmna^{+/+}$ and $Lmna^{-/-}$ MEFs were treated with increasing doses of IR up to 6 Gy, and their clonogenic capability assessed after 10 days in culture. The survival curves shown in (Figure 29) describe the relationship between the radiation dose and the proportion of cells that retain reproductive integrity. In line with severely compromised DNA repair, $Lmna^{-/-}$ MEFs were significantly more sensitive to IR than wild-type controls.

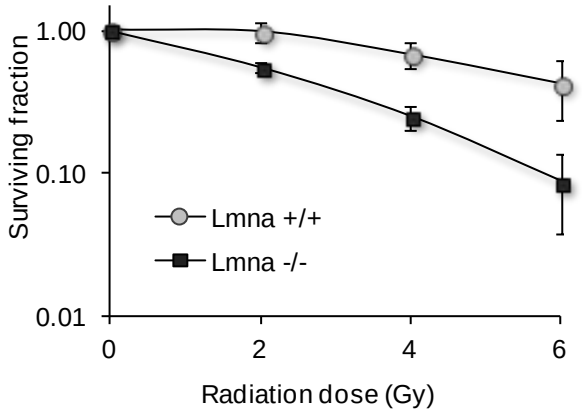

Figure 29 Lmna$^{-/-}$ MEFs display increased sensitivity to ionizing radiation. Clonogenic survival in Lmna$^{+/+}$ and Lmna$^{-/-}$ MEFs in response to increasing doses of radiation (0 to 6 Gy). Shown are the surviving fractions and standard deviation of the mean from three independent experiments.

3.6 DISCUSSION

We have shown that acute loss of A-type lamins leads to a severe compromise in HR. These studies reveal an unprecedented role for A-type lamins in the transcriptional co-regulation of two key factors in HR, RAD51 and BRCA1, by means of formation of p130/E2F4 repressor complexes. Since BRCA1 associates with the MRN complex, which displays nucleolytic activity, it is likely that HR-dependent end-resection itself is afflicted in lamins-deficient cells. This notion is consistent with the defective recruitment of RPA to DNA DSBs in the absence of detectable changes in the global levels of the protein. HR requires nucleolytic degradation of DNA ends to generate 3'-ended ssDNA, a process mediated by MRN, CtIP and BRCA1 proteins. The ssDNA generated by end-resection is rapidly bound by Replication Protein A (RPA), which removes secondary structures in ssDNA and allows the formation of the RAD51 nucleoprotein filament that drives DNA strand invasion and exchanges during HR [213]. BRCA1 also interacts with phosphorylated CtIP, a protein that is involved in DNA end-resection and known to function in

both HR and A-NHEJ [77, 81, 86, 214, 215]. Disrupting the interaction of BRCA1 with CtIP is detrimental to HR, but does not affect A-NHEJ [215]. Thus, consistent with our discussion of C- versus A-NHEJ in lamin A/C deficient cells it is possible that loss of BRCA1 and RAD51 inhibits HR, but does not affect the ability of cells to enact A-NHEJ. Overall, our data indicate a that A-type lamins promote the major mechanisms of DNA repair by contributing to the stability of 53BP1 protein and transcription of BRCA1/RAD51 genes. Unravelling which mutations in A-type lamins affect levels of CTSL, destabilize 53BP1 and Rb family members and/or transcriptionally regulate RAD51/BRCA1 will allow us to predict which lamins-related diseases present with defects in specific mechanisms of DNA repair. The connection between CTSL and cellular levels of Rb and p107 is particularly interesting since upregulation of CTSL has been associated with a number of cancers. It will be useful to determine if CTSL plays a role in regulation of Rb/p107 under normal physiological conditions, and elucidate the exact mechanism by which upregulation of CTSL causes decreased Rb/p107 proteins.

4.0 SUMMARY & DISCUSSION

SUMMARY OF THE THESIS

Several lines of evidence indicate that not only are A-type lamins silenced or upregulated in a variety of human cancers, but that these changes significantly impact patient outcome [14, 15, 150]. Furthermore, mutations in A-type lamins lead to a variety of degenerative diseases, some of which are characterized by premature aging phenotypes and genomic instability. A major challenge is to identify and characterize the molecular mechanisms that underlie lamins-associated pathogenesis. To advance this field, I evaluated the role of A-type lamins in the maintenance of genomic stability in mouse and human cells. Chapter one demonstrated a role for A-type lamins in telomere homeostasis, such that loss of lamin A/C is associated with gross alterations in the nuclear distribution of telomeres, along with telomere attrition and epigenetic changes at the telomeres.

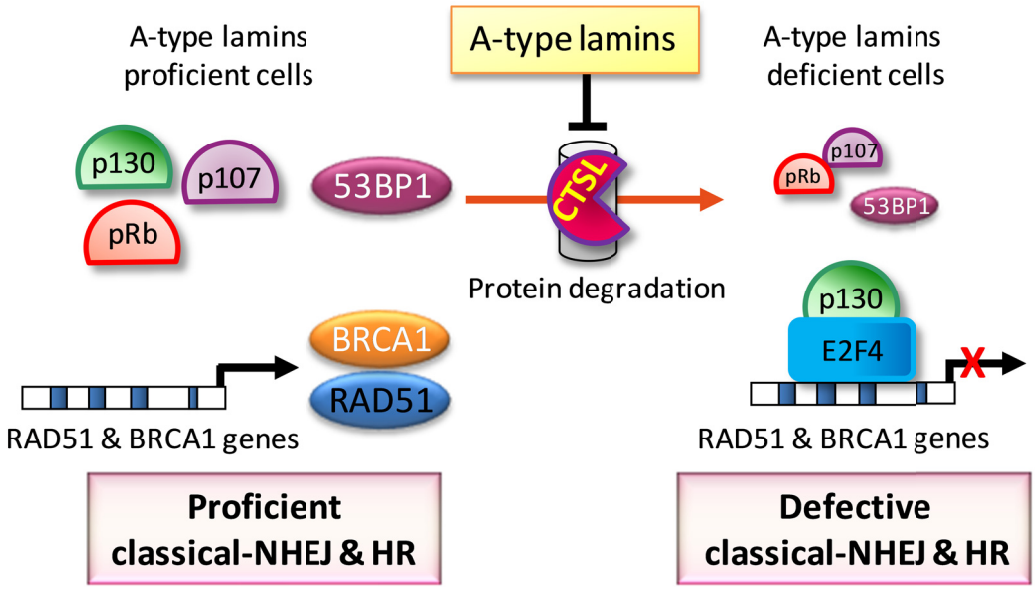

Figure 30. Model depicting the effect of A-type lamins on the DNA damage repair pathways. A-type lamins stabilize the pocket family proteins pRb and p107, as well as the NHEJ protein 53BP1, by inhibiting CTSL-mediated degradation. By stabilizing 53BP1, A-type lamins promote classical-NHEJ. The lamins-associated alterations in the pocket family proteins lead to increased formation of p130/E2F4 complexes, which can in turn bind the RAD51 and BRCA1 gene promoters and inhibit their transcription. Thus, loss of A-type lamins leads to defects in the two major mechanisms of DNA DSBs repair (NHEJ and HR), increased genomic instability and radiation sensitivity.

In chapter two, I focus on the role of A-type lamins in non-homologous end-joining (NHEJ), showing that A-type lamins are necessary for both long- and short-range NHEJ. I demonstrate that the mechanism by which loss A-type lamins inhibits NHEJ is *via* destabilization of 53BP1. In chapter three, I show that loss of A-type lamins leads to inhibition of homologous recombination (HR) of DSBs due to transcriptional repression of BRCA1 and RAD51 by the 130/E2F4 complex. Importantly, these studies led to our discovery of novel roles for the cysteine protease CTSL in regulating the stability of both 53BP1 [187] and the retinoblastoma pocket family proteins. The findings are summarized in the model (Figure 30).

DISCUSSION OF THE THESIS

4.1 Nuclear organization of telomeres

Telomeres are nucleoprotein structures that protect the ends of eukaryotic chromosomes [216-218]. A minimal length of telomeric DNA repeats and proper binding of specialized proteins such as shelterin complex components and DNA repair factors are required for the maintenance of telomere structure and function [40]. Similarly, acquisition of a heterochromatic structure at mammalian telomeres is critical for the control of telomere homeostasis [219]. The importance of telomere compartmentalization for telomere function has been clearly demonstrated in yeast [177]. In *Saccharomyces cerevisiae* or budding yeast, telomeres are clustered in foci at the nuclear periphery [220, 221]. At least two redundant mechanisms have been identified that mediate tethering of telomeres to the periphery. One mechanism involves yKu70/Ku80 heterodimer, which associates with the telomerase complex Est1/Est2/Tlc1, and an integral inner nuclear membrane protein of the SUN domain family, Mps3 [222, 223]. A second mechanism involves the histone deacetylase Sir4, which binds to the inner nuclear membrane-associated protein Esc1 (Enhancer of silent chromatin 1) [224-226]. Importantly, disruption of the tethering of telomeres to the nuclear periphery leads to deprotection and hyper-recombination of telomeres [223], and derepression of subtelomeric genes [177]. In the case of Sir4, inactivating mutations also involve telomere shortening [227], suggesting a link between telomere localization at the nuclear periphery and maintenance of length homeostasis.

Mammalian telomeres do not accumulate at the nuclear periphery, except during meiosis [228]. They are distributed throughout the entire nucleoplasm in G1 and S phases of the cell cycle, while assembling in the center of the nucleus during G2 in preparation for mitosis [166]. It has been proposed that interactions between telomeres and the nuclear matrix determine their localization in the nuclear space [229, 230]. Tracking 3D trajectories of fluorescently labeled

telomeres in a broad time range has provided new information about telomere dynamics within the nucleus. At short time scales, the diffusion of telomeres is anomalous, while at longer time scales a normal diffusion is observed with a wide distribution of diffusion constants. This transient anomalous diffusion was explained by the existence of a local binding or obstruction mechanism to telomere mobility [231]. To date, the molecular mechanisms that orchestrate nuclear tethering and localization of mammalian telomeres, and their relevance for telomere metabolism remain unknown [232].

Interestingly, the 3D organization of telomeres is altered in tumor cells [166, 167], and in senescent cells that present defects in the nuclear lamina [168]. This data suggests a relationship between changes in nuclear distribution of telomeres and the alterations of telomere metabolism observed during senescence and immortality. We have shown that A-type lamins bind to mouse telomeres and participate in their nuclear compartmentalization. Embryonic fibroblasts from LMNA null mice exhibit changes in the nuclear distribution of telomeres towards the nuclear periphery and away from the nuclear center. This was unexpected, since lamins are highly enriched at the nuclear periphery. However, while B-type lamins are exclusively found at the nuclear periphery, lamins A and C are proposed to form part of a filamentous meshwork that expands throughout the entire nucleoplasm. We speculate that A-type lamins actively participate in the distribution of telomeres throughout the nucleus. In the absence of A-type lamins, proteins at the nuclear periphery such as B-type lamins, inner nuclear membrane proteins or nuclear pore complex proteins, could undertake the tethering of telomeres. In this model, the nuclear periphery would represent a default pathway for telomere distribution, which would resemble telomere localization in yeast, which do not express lamins. This model is supported by a 2010 study in which Winnok H. De Vos and colleagues demonstrated hypermobility of telomeres in human fibroblasts that lack expression of lamin A/C. This study supports the idea that A-type lamins help tether telomeres throughout the 3D nuclear space.

Further studies need to characterize the molecular determinants of the association of A-type lamins with telomeres. A-type lamins can bind directly to DNA-chromatin and indirectly via their interaction with lamin-associated proteins such as LAP-2α, emerin and MAN1 [12, 233]. Although we found that A-type lamins bind telomeric sequences by chromatin immunoprecipitation, we do not know whether the interaction is direct or mediated by lamin-associated proteins. LAP-2α is of special interest given that it binds to telomeres during nuclear reassembly after mitosis [234]. In addition, LAP-2α mediates the interaction of Rb with A-type lamins, contributing to the stabilization of Rb family function [235], and is the only member of its family that is localized throughout the nucleoplasm. All these characteristics make LAP-2α a good candidate for mediating tethering of telomeres to A-type lamins. From the telomere end, it is possible that components of the shelterin complex associate with A-type lamins or lamin-associated proteins localized at the nucleoplasm. Alternatively, A-type lamins might recognize heterochromatic features at the telomere. Heterochromatin Protein 1 (HP1) has been shown to form a complex with A-type lamins and LAP-2α [236], and therefore could participate in the tethering of heterochromatic domains such as telomeres and centromeres to the scaffold of A-type lamins.

4.2 A-type lamins and telomere structure, length and function

The first evidence supporting a role for A-type lamins in telomere biology came from studies of patients with Hutchinson Gilford Progeria Syndrome. HGPS or progeria is a premature aging disease caused by a mutation in the LMNA gene that generates a truncated lamin A isoform known as progerin, which is toxic for the cell [140, 155]. HGPS fibroblasts were shown to undergo faster telomere attrition during proliferation than normal counterparts [22, 141]. Fibroblasts from HGPS patients and aged individuals also present defects in epigenetic marks characteristic of constitutive heterochromatin, although the effect on telomeres was not tested [173, 174]. The mechanism by which mutation in the LMNA gene resulting in the expression of progerin leads to telomere shortening remains unknown. Additional evidence of a crosstalk

between A-type lamins and telomeres was provided by studies showing that telomerase rescues proliferative defects of human fibroblasts expressing lamin A mutants [237], and that senescence-associated alterations of the nuclear lamina are accompanied by aggregation of telomeres to the nuclear lamina [168].

Despite the importance of telomere maintenance for cancer progression, the impact that the loss of A-type lamins that characterizes certain tumor types has on telomere biology remained undetermined. Our study using LMNA knock-out mouse fibroblasts as a model revealed that A-type lamins play a key role in the maintenance of telomere structure, length and function. Telomeres in $Lmna^{-/-}$ mice are consistently shorter than the corresponding wild-type controls, and exhibit an increase in signal-free ends (loss of telomeric signals). Furthermore, acute depletion of A-type lamins by shRNAs specific for depletion of lamins A and C, leads to telomere shortening after only a few passages of the cells in culture as determined by Quantitative Fluorescence In Situ Hybridization (Q-FISH) with a telomeric probe. Most importantly, reintroduction of either lamin A, lamin C, or both by retroviral transduction rescued the telomere shortening phenotype. Reintroduction of lamins significantly increased the average telomere length and was associated with a decrease in the pool of short telomeres, and an increase in the pool of long telomeres. These data indicate that A-type lamins play a key role in the control of telomere length. However, we do not know the mechanism behind the telomere shortening phenotype observed in A-type lamins-deficient cells. The levels of telomerase activity and the binding of the shelterin complex components TRF1 and TRF2 were not affected by the loss of A-type lamins. Similarly, we did not observe any evidence of aberrant recombination at telomeres, which could explain the loss of telomeric sequences. It is possible that the binding of other shelterin complex components or DNA repair factors with a function at the telomere could be defective in LMNA null cells. Alternatively or concomitantly, loss of A-type lamins might hinder the accessibility of telomerase or other proteins implicated in telomere metabolism, especially factors implicated in telomere replication.

Maintenance of a heterochromatic structure at telomeres is also critical for the control of telomere length. Previous studies demonstrated that loss of heterochromatic features such as methylation of histones H3 and H4 at different lysine residues and methylation of subtelomeric DNA results in a pronounced telomere elongation phenotype [56, 232, 238, 239]. In most cases, telomere elongation correlated with an increase of telomere sister chromatid exchange (T-SCE) events, characteristic of the activation of Alternative Lengthening of Telomeres (ALT) pathway of telomere maintenance [32, 240]. We found that loss of A-type lamins resulted in decreased levels of the heterochromatic mark H4K20me3 -histone H4 trimethylated at lysine 20-. This defect is likely due to the fact that Rb family members, which have a known role in the stabilization of this chromatin modification, are targeted to degradation by the proteasome upon loss of A-type lamins [148]. However, contrary to the telomere elongation phenotype characteristic of Rb-deficient cells [171, 241] and H4K20me3- deficient cells (Suv4-20h double knock-out) [55], the loss of Rb or decrease in H4K20me3 was not sufficient to trigger telomere elongation in the context of A-type lamins deficiency. Thus, A-type lamins, or a process regulated by these proteins, are necessary for the elongation of telomeres upon loss of Rb family members and decrease of H4K20me3. Interestingly, depletion of A-type lamins in U2OS cells, an osteosarcoma cell line which relies on ALT for telomere maintenance, did not lead to any significant alterations in telomeric sister-chromatid exchange, indicating that loss of A-type lamins is sufficient to inhibit ALT that is associated with alterations in histone methylation.

4.3 Mechanisms of DNA DSBs repair

Repair of damaged DNA is critical for maintenance of genomic stability. Among the various types of DNA damage, DSBs are the most deleterious, leading to mutations, loss of genomic material, and translocations if not properly repaired. The two major pathways of DSBs repair, homologous recombination (HR) and classic non-homologous end-joining (C-NHEJ) are considered to compete for repair substrate [62, 90]. HR is error-free and requires both resection of the 5' DNA ends around the break and the presence of a homologous template. In contrast,

ligation of damaged DNA during C-NHEJ requires neither extensive resection nor homologous templates. C-NHEJ is a fast and error-prone mechanism which can cause translocations and/or loss of genetic material. While C-NHEJ is the predominant repair mechanism in G0/G1 stages of the cell cycle, when the lack of the sister chromatid prevents HR from being used, the slower HR repair mechanism has traditionally been thought to dominate during S and G2 phases of the cell cycle. Recent evidence has challenged the notion of HR dominance in S/G2, suggesting that the need for rapid DNA damage repair makes NHEJ the preferred pathway even when HR is possible [92]. According to this data it is only when the damage cannot be repaired by NHEJ that end-resection is promoted and additional mechanisms undertake DNA repair. Besides HR and C-NHEJ, a less understood pathway, alternative non-homologous end-joining (A-NHEJ), is sometimes used as a backup repair pathway [69, 242]. A-NHEJ involves processing of DNA by end-resection to reveal regions of microhomology which are then ligated. In contrast to HR, resected DNA is not filled in during A-NHEJ, making it a more deleterious process than both C-NHEJ and HR. In line with this notion, A-NHEJ is associated with high frequencies of chromosomal translocations and genomic instability.

4.4 A-type lamins and DNA repair

Expression of mutant lamin A isoforms is associated with defective DNA repair. Fibroblasts from HGPS patients and from a mouse model of progeria generated by depletion of the metalloproteinase responsible for the maturation of prelamin A (Zmpste24 knock-out) [152, 158] have alterations in the DDR. In particular, these cells exhibit increased DNA damage and chromosome aberrations and are more sensitive to DNA-damaging agents. At a molecular level, HGPS and Zmpste24$^{-/-}$ MEFs showed a delayed recruitment of 53BP1 to phosphorylated histone H2AX (γ-H2AX)-labeled DNA repair foci upon induction of DNA damage, and a delayed disappearance of these foci. Zmpste24$^{-/-}$ MEFs also showed impaired recruitment of RAD51 to sites of DNA damage leading to a delayed checkpoint response and defective DNA repair [152]. Furthermore, ectopic expression of mutant forms of lamin A in the presence of wild-type lamin

A/C diminished the cellular ability to form γ-H2AX-labeled DNA repair foci in response to mild doses of cisplatin or UV irradiation, and mislocalized ATR kinase, a key sensor in DDR [161]. More recent studies have demonstrated that fibroblasts from HGPS patients and from Zmpste24$^{-/-}$ MEFs display an activated DNA damage response, as evidenced by enhanced γ-H2AX, and activation of the p53 pathway [160, 173]. All these reports suggest that unprocessed prelamin A and truncated lamin A act in a dominant negative fashion to perturb DNA damage response and repair. Elucidating the specific steps of these processes that are affected in the different laminopathies could bring about new possibilities for treatment.

4.5 A-type lamins affect 53BP1-dependent NHEJ of telomeres

Our study shows that LMNA null fibroblasts exhibit signs of genomic instability: higher incidence of chromosome and chromatid breaks, increased numbers of signal free ends (telomere loss), and basal levels of unrepaired DNA, as shown by the presence of cells labeled with γ-H2AX. These data indicate that not only mutant forms of lamins, but also depletion of A-type lamins affects the ability of cells to properly deal with DNA damage. Nevertheless, the different mutations and the changes in expression of A-type lamins are expected to have different consequences for nuclear function, given the variety of diseases associated with the different alterations. Establishing for example, if tumor cells in which the LMNA promoter is silenced by DNA methylation are defective in DNA repair and more sensitive to DNA damaging agents, would provide valuable information towards the use of lamins as targets for cancer therapeutics.

Loss of telomere integrity activates a classical DDR characterized by the activation of the ATM/p53 pathway and the formation of DNA damage foci at telomeres [185]. These telomere dysfunction-induced foci (TIF) contain many DNA damage response proteins, including γ-H2AX, 53BP1, MDC1, and MRN complex, and are established as a read-out of telomere damage. Activation of ATM/p53 is followed by the processing of dysfunctional telomeres by the NHEJ repair pathway, leading to chromosome end-to-end fusions [186]. Two recent studies have shown

that deprotected telomeres are more mobile and sample larger territories within the nucleus than functional telomeres [51, 243]. Dimitrova et al. presented evidence about 53BP1 playing an active role in chromatin dynamics, such that it facilitates the association and fusion of dysfunctional telomeres that might be far away within the nucleus [51]. Our study shows that chromosome end-to-end fusions of dysfunctional telomeres, induced by the expression of a dominant negative TRF2 protein, require A-type lamins, providing the first link between loss of A-type lamins and defective NHEJ repair. In addition, we demonstrated that the mechanism of inhibition of telomere NHEJ was due to the destabilization of 53BP1 in lamin A/C-deficient cells. It is possible that in addition to maintaining 53BP1 stability, A-type lamins play an active role in the DDR and in the 53BP1-mediated regulation of mobility and NHEJ of dysfunctional telomeres. In 2010 Winnok H. De Vos and colleagues demonstrated intranuclear hypermobility of telomeres in human fibroblasts that lack expression of lamin A/C [244]. Based on this report, increased mobility of telomeres in the $Lmna^{-/-}$ fibroblasts should circumvent the need for 53BP1 for efficient fusion; however we still see decreased telomere fusions in these cells, arguing against the 53BP1-mediated telomere mobility hypothesis.

4.6 A-type lamins affect NHEJ of ionizing radiation-induced DSBs

Despite the increase in genomic instability, similar to what was reported in progeria cells, loss of A-type lamins does not impair activation of the DNA damage response (DDR) when cells are exposed to ionizing radiation. ATM-dependent phosphorylation of H2AX and p53 at Ser15 was not affected in $Lmna^{-/-}$ mouse embryonic fibroblasts (MEFs), and the kinetics of formation and resolution of γ-H2AX ionizing radiation-induced foci (IRIF) was indistinguishable between lamins-deficient and –proficient cells In contrast, lamins-deficient cells showed defective accumulation of 53BP1 at IRIF at all post-irradiation times tested. Importantly, this deficiency was due to the decrease in 53BP1 and not to failed recruitment, since 53BP1 IRIF formed although at a much lower intensity. These data, together with the fact that 53BP1-deficient cells exhibit

increased genomic instability and radiosensitivity suggested that the loss of 53BP1 could be responsible for the DNA repair deficiencies observed in lamin A/C-deficient cells.

Consistent with our hypothesis, lamins-deficient cells treated with ionizing radiation had profound defects in the fast phase of DNA DSBs repair. Fast repair is traditionally associated with C-NHEJ, since similar defects are observed upon depletion or mutation of essential factors in this process such as DNA-PK, Ku80, XRCC4, and DNA ligase IV. Importantly, we found that reconstitution of 53BP1 in lamins-deficient cells rescues the defects in NHEJ of DNA DSBs and dysfunctional telomeres. Overall, these results revealed that 53BP1 deficiency is a major contributor of the DNA repair phenotype observed in lamins-deficient cells. This is a critical observation, since many studies rely on foci formation to determine whether a step in the DDR is functional. Our results indicate that it is important to monitor the levels of DDR proteins at DSBs when assessing deficiencies in DNA repair.

4.7 How are the levels of 53BP1 regulated by A-type lamins?

During our exploration of mechanisms by which A-type lamins affect DNA DSBs repair our group discovered a role for cathepsin L (CTSL) in the stability of 53BP1 protein. The first link between CTSL and A-type lamins was established in a mouse model of progeria [160]. In particular, mice lacking Zmpste24, a metalloprotease that participates in the maturation of lamin A, exhibit a drastic increase in the levels of CTSL mRNA. Although this suggested a relationship between CTSL and the aging phenotype, no association was established between CTSL and the increase in genomic instability displayed by these mice. Our studies showed that $Lmna^{-/-}$ cells also exhibit a marked increase in the levels of CTSL mRNA and protein [187], indicating that loss of A-type lamins induces transcriptional upregulation of CTSL. Furthermore, we show that upregulation of CTSL leads to a dramatic downregulation of 53BP1 protein levels. Since many cancers present with high CTSL expression [190-192, 245, 246], these studies indicate

suppression of DSBs repair as an important mechanism by which CTSL contributes to tumorigenesis.

4.8 Lamins role in DNA DSBs repair by HR

Loss of 53BP1 favors repair of DNA DSBs by HR [89, 90]. However, despite decreased 53BP1 levels, we found that HR was suppressed upon depletion of A-type lamins. Inhibition of HR is explained by the significant reduction in expression of two key factors in this process, BRCA1 and RAD51. In contrast to the CTSL-mediated degradation of 53BP1, decreased levels of BRCA1 and RAD51 were brought about by transcriptional repression. Previous reports had demonstrated transcriptional repression of BRCA1 and RAD51 under certain stressful conditions, such as hypoxia or PARP inhibition, via formation of p130/E2F4 complexes at E2F sites within their promoters [211, 212]. We found that repression RAD51 and BRCA1 genes in lamins-deficient cells was linked to the status of members of the Rb family of tumor suppressors (Rb, p107 and p130) - repression of BRCA1 and RAD51 required p130 and occurred in the context of decreased levels of Rb and p107. Furthermore co-immunoprecipitation studies in cells depleted of A-type lamins showed an increase in the formation of p130/E2F4 complexes. These data suggest activation of a repressive mechanism in lamins-deficient cells, where altering the balance of the pocket proteins favors association of p130 with E2F4, leading to transcriptional inhibition of responsive promoters. However, we cannot rule out the possibility that loss of A-type lamins leads to alterations in the nuclear localization of BRCA1 and RAD51 genes, which might contribute to their transcriptional repression.

It is well established that pocket proteins associate with lamins and that loss of A-type lamins leads to increased degradation of Rb and p107 [148]. This is thought to occur partly through the ability of A-type lamins to regulate the sub-nuclear localization of these proteins. However up until now, the specific mechanism by which Rb and p107 are targeted for degradation remained quite elusive, being independent of both MDM2 and gankyrin, a

component of the 19S proteasome subunit which is overexpressed in Lmna KO cells [165]. Given our recent findings that CTSL promotes the degradation of 53BP1, we speculated that this protease could be the missing link between A-type lamins and Rb/p107 degradation. We envisioned a scenario where CTSL-mediated degradation of Rb and p107 alters the balance between the pocket family proteins, leading to increased formation of p130/E2F4 complexes, which can in turn mediate transcriptional repression of BRCA1 and RAD51 and this inhibit HR. To test our model we overexpressed CTSL in wild-type MEFs and monitored the levels of Rb family members, BRCA1 and RAD51. Indeed, we found that upregulation of CTSL was associated with a substantial decrease in pRb and p107, with little effect on p130, mirroring the phenotype observed in lamins-deficient cells. These results demonstrate a novel role for CTSL in the regulation of the retinoblastoma family of tumor suppressors. However, altering the levels of these proteins was not sufficient to induce transcriptional repression of BRCA1 or RAD51, suggesting that lamins have additional roles in the regulation of transcription of these genes.

Upregulation of CTSL is featured in a variety of cancers. Given the important role of Rb as a tumor suppressor, it is likely that overexpression of CTSL represents yet another mechanism by which tumor cells escape cell-cycle arrest. Furthermore, upregulation of CTSL and the ensuing degradation of 53BP1 would compromise C-NHEJ and lead to genomic instability. Thus upregulation of CTSL increases genomic instability by hindering DDR, yet impedes one of the major cell cycle checkpoints responsible for ensuring genomic stability [247] by promoting degradation of pRb. This double-blow to the integrity of the genome supports a significant role for CTSL in tumorigenesis. Importantly, we have not identified the mechanism by which loss or mutation of A-type lamins leads to transcriptional upregulation of CTSL. Given that alterations in A-type lamins causes gross alterations in 3D distribution of chromatin, it is possible that increased transcription of CTSL is a result of altered nuclear localization. It will be interesting to manipulate nuclear positioning of the CTSL gene and test how this affects its transcription.

4.10 Concluding remarks

While A-type lamins are implicated in wide a variety of human diseases, including premature aging syndromes and cancer, little is known about the molecular mechanisms that contribute to their pathogenesis. Here, I have presented our findings that loss of A-type impacts telomere homeostasis and the two major pathways of repair of DSBs, NHEJ and HR. Additionally, our studies on A-type lamins have led to the discovery of CTSL as a novel regulator of 53BP1 and the retinoblastoma pocket family proteins, suggesting a fundamental role for CTSL in the regulation of cell cycle progression and DNA repair. These novel findings provide a significant contribution to understanding the molecular mechanisms that contribute to genomic stability, and advance our understanding of cancer, aging and laminopathic mutations

The findings that depletion of A-type lamins impairs DNA repair and induces radiosensitivity, along with clinical data indicating that lamins expression can affect prognosis in certain malignancies, introduces the possibility of using these proteins as targets for cancer therapeutics. In addition, identification of 53BP1, RAD51 and BRCA1 as molecular targets of A-type lamins provides new tools to screen disease-associated mutations in the LMNA gene for defects in DNA repair and genomic instability, which could contribute to their pathophysiology

.

5.0 MATERIALS AND METHODS

Cell Culture

$Lmna^{+/+}$ and $Lmna^{-/-}$ MEFs and adult fibroblasts were generated in the laboratory of Colin L Stewart as described by Sullivan et al [151]. Rb family-deficient MEFs were generated in the laboratory of Julien Sage (Stanford University, CA). MCF-7 and U2OS cells were obtained from ATCC (Manassas, VA). The MCF-7 DR-GFP cell line was previously described [248]. All lines were maintained in DMEM-Glutamax (Invitrogen) supplemented with 10% bovine growth serum, antibiotics, and antimycotics. For cycloheximide and proteasome inhibitor treatments, 0.5 106 cells were cultured for 6 h in media containing 10 g/ml cycloheximide, 30 M MG-132 (EMD Biochemicals) or EtOH as control.

Chromatin Immunoprecipitation (ChIP)

ChIP analyzes were carried out exactly as described [54]. Chromatin extracted from Cells cultured to 70-80% confluency in 150mm plates and subjected to immunoprecipitation with various antibodies. Chromatin isolation: Adherent cells were treated for 15minutes at room temperature (rt) with 1% formaldehyde/PBS to crosslink protein and DNA. Crosslinking was terminated by the addition of glycine (final concentration 0.125 – 0.150 M) for 5 minutes. Cells were then washed once with PBS, and then transferred (by scraping with ice-cold PBS/PMSF/protease inhibitor cocktail) to 50ml falcon tubes. Cells were kept on ice from this point on. Cells were pelleted and the lysed with a solution of lysis buffer (below) with PMSF/protease inhibitors for 10 minutes on ice, and then sonicated to obtain DNA fragments between 250 and 1000 base pairs. Sonication was done in a bioruptor at 30 second intervals for 15 minutes at high. After centrifugation of the sonicated mixture (14, 000 rpm for 15 minutes at rt), the supernatant containing the chromatin was collected and the pellet was discarded.

Immunoprecipitation: 200 µl of the lysates was transferred to a 2ml eppendorf tube and diluted 1/10 in dilution buffer (below) with PMSF/protease inhibitors and then pre-cleared with 40µl of salmon sperm/protein A/G agarose beads (Upstate# 16-157) for 5 hours at

4°C on a rotating platform. The supernatant was recovered by centrifuging the mixture at rt for 4 minutes, 4000 rpm. Next, 4µg of the antibody of interest was added to the solution, followed by incubation at 4°C for 1hr. 60 µl protein A/G beads was added to the solution, which was then incubated at 4°C overnight on a rotating platform. The solution was centrifuged and the supernatant stored on ice as the unbound fraction for later use as inputs. The pelleted fraction, containing the beads, was washed with a series of wash buffers (detailed below): once in low salt immune complex wash buffer, once in high salt immune complex wash buffer, once in LiCl immune complex wash buffer, twice in TE buffer. 2ml of the respective buffers was used for the each wash, which was done for 4minutes at rt on a rotating platform. Elution of the immune complexes was done by adding 250µl of elution buffer (below), vortexing at rt slowly for 15, followed by centrifugation at 4000 rpm for 4 minutes. The eluate was transferred to a separate tube, and the elution procedure repeated once more. The eluates were combined to get ≈500ul containing the bound fraction. We then reversed the crosslinks by adding 20µl of 5M NaCl and incubating at 65°C overnight (inputs were included at this step).

DNA Recovery: To remove RNA and proteins we added 10µl of 0.5M EDTA, 20 µl 1M Tris-HCl pH 6.5, 2 µl RNase (10 µg/ µl), 2 µl proteinase K (20 µg/ µl) to each sample, and incubated at 45°C for 1hour. DNA was then recovered by phenol/chloroform extraction and ethanol precipitation. 500 µl chloroform: isoamyl alcohol 24:1 was added and the solution vortexed on high, then centrifuged at rt for 5 minutes at 10, 000 rpm in a tabletop centrifuge. The supernatant was transferred to a 2ml eppendorf tube in which we added 50 µl 5M NaCl, 1.5 ml ethanol and 1 µl glycogen, followed by incubation at -20°C for an hour to precipitate the DNA. After centrifuging this mixture for 15 minutes at 14, 000 rpm we washed the pellet with 70% ethanol. The pellet was allowed to air dry

and then resuspended in 30 µl TE buffer. DNA was then slot-blotted on a Hybond N+ membrane and hybridized to a telomeric probe (gift from T de Lange, Rockefeller University, NY, USA) or a major satellite probe. The quantification of the signal was done using the ImageQuant software (Molecular Dynamics). We calculated the amount of telomeric or pericentric DNA immunoprecipitated relative to the signal of the corresponding inputs. In all cases, we represented the ChIP values as a percentage of the total input telomeric DNA, therefore correcting for differences in the number of telomere repeats.

The following antibodies were used for chromatin immunoprecipitation:

Anti-H3K9me3 (#07-442, Upstate); anti-H4K20me3 (#07-463, Upstate); anti-TRF1 (T1948, Sigma); anti-TRF2 (#05-521, Upstate); or anti-lamin A/C (SC-6215, Santa Cruz).

ChIP solutions:

Lysis buffer: 1% SDS, 10mM EDTA, 50 mM Tris-HCl pH8, protease inhibitor cocktail.

Dilution buffer: 1.1% Triton X-100, 0.01% SDS, 1.2 mM EDTA pH 8.0, 167 mM NaCl, 16.7 mM Tris-HCl pH 8, protease inhibitor cocktail.

Low salt immune complex wash buffer: 0.1% SDS, 1% Triton X-100, 2mM EDTA, 20 mM Tris-HCl pH 8, 150 mM NaCl.

High salt immune complex wash buffer: 0.1% SDS, 1% Triton X-100, 2mM EDTA, 20 mM Tris-HCl pH 8, 500 mM NaCl.

LiCl immune complex wash buffer: 0.25M LcCl, 1% NP-40, 1% deoxycholateNa, 1mM EDTA, 10 mM Tric-Hcl ph 8.

Elution buffer: 1% SDS, 50 mM $NaHCO_3$

Immunoprecipitation, Immunoblotting and Immunofluorescence

Immunoprecipitation of Rb family members.

Cells were lysed in RIPA buffer (0.15 M NaCl, 0.05 M Tris–HCl pH 7.2, 1% Triton-X 100, 1% sodium deoxycholate, and 0.1% SDS), sonicated and 1 mg of total protein immunoprecipitated with antibodies bound to protein A-agarose beads: Rb (IF18), p107 (C-18), and p130 (C-20) from Santa Cruz. Protein detection was carried out using antibodies against Rb (BD Pharmingen), p107 and p130 (Santa Cruz).

Immunoblotting

For immunoblotting, cells were lysed in RIPA buffer. Protein detection was carried out using the following antibodies: Lamin A/C (SC-6215, 20681 Santa Cruz), actin (Clone C4, MPB), -tubulin (Sigma), TRF1 (gift from Maria A Blasco), TRF2 (#05-521, Upstate), POT1 (gift from Qin Yang), 53BP1 (Bethyl Laboratories, A300-272A), MDC1 (gift from Junran Zhang), ATM (GTX7107, GeneTex), DNA-PKcs (MS-423-P, NeoMarkers), Mre11 (Novus, MB100-142), Nbs1 (Cell Signaling, 3002B), Ku70 (SC-1486, Santa Cruz), H2AX (Upstate, 07-164), H2AX (Upstate, 07-164), ERCC1 (SC-17809, Santa Cruz), RPA2 (Calbiochem, NA18), actin (Clone C4, MPB), β-tubulin (Sigma), and BRCA1 (Santa Cruz-6954).

Immunofluorescence

Immunofluorescence was performed with antibodies: γH2AX (1:600, Upstate Biotechnology), 53BP1 (1:600, Novus Biologicals NB100-304), RAD51 (1:100, Santa Cruz sc-8349), or RPA2 (1:100 Calbiochem, NA18). Cells were grown on coverslips until 70–80% confluent and irradiated with a dose of either 0.5 Gy (53BP1 and γH2AX) or 8 Gy (RAD51). At different times post-IR, cells were fixed with 3.7% formaldehyde and 0.2% Triton-X100 for 10 min at RT. Cells were blocked for 1 h at 37°C with 1% goat serum or BSA in PBS and incubated with primary antibodies for 1 h at 37°C. Secondary antibody incubations were performed for 1h at 37°C using Alexa- and Cy3-labeled antibodies. Slides were counterstained using DAPI in

Vectashield (Vector). Fluorescent images were taken using a Nikon 90i upright microscope or with a confocal microscope Zeiss L510.

X-ray irradiation

This was done using a PANTAK pmc1000 X-ray machine with a 0.1 Cu+ 2.5 AL filter at a dose rate of 1.1 Gy/min. For immunofluorescence studies cells were irradiated with 0.5 Gy or 8 Gy, and for comet assays cells were given 8 Gy.

Terminal restriction fragment (TRF) analysis

We prepared cells in agarose plugs and carried out TRF analysis as described [249]. Cells were washed with 1X PBS, pelleted by centrifugation, resuspended in 50 µl PBS and incubated at 50^{o}C for 5 minutes. 50 µl of 2% low-melt agarose/PBS (previously heated at 50^{o}C) was added and the mixture (100 µl) incubated for 5 minutes at 50^{o}C.This mixture was then transferred to a disposable plug mold (Bio-Rad #170-3713) and allowed to solidify by cooling at rt for 5 minutes and then at 4^{o}C for 15 minutes. The plugs were then transferred to eppendorf tubes and 500 µl of proteinase K buffer (2mg/ml proteinase K) added to the tube, which was incubated at 4^{o}C overnight. The next day, plugs were washed with TE buffer (4 x 1 hour each). PMSF was added to the third and fourth washes to inactivate the proteinase K. Samples were then stored at 4^{o}C in TE buffer until digestion. Plugs were washed in water for 1 hour, and then equilibrated for 1 hour in MboI enzyme buffer. Next, the plugs were incubated in 0.3 ml restriction enzyme buffer containing 50U of MboI enzyme solution overnight at 37^{o}C. Following digestion the plugs were washed 30 minutes with water and 30 minutes with 0.5X TBE buffer. Finally, pulse-field gel electrophoresis was performed using 1% low-melt agarose in 0.5X TBE buffer for 23 hours at 6 V/cm^{2}. Following electrophoresis, the gel was denatured 3 x 30 minutes and neutralized 3 x 30 minutes (solutions below). The Whatman TurboBlotter™ system was used to transfer the DNA to nylon membrane. Finally, DNA was crosslinked to the membrane using the Stratalinker® UV crosslinker, and treated with a $(TTAGGG)_n$ probe.

TRF solutions

Denaturing solution: 0.5M NaOH, 1.5M NaCl in water

Neutralizing solution: 0.5M Tris-HCl, 1.5M NaCl in water, adjusted to pH 7.0

Quantitative Fluorescence *in Situ* Hybridization (Q-FISH)

We prepared metaphase stage chromosomal spreads for Q-FISH and hybridized them as described [250].

Metaphase preparation:

Cells were cultured in 10mm dishes to 70% confluence. Colcemid (Sigma #D1925) was added to the culture media (100 µl to every 10 ml media) for 4 hours to arrest cells in metaphase. After collecting the culture media, we washed with 1X PBS (which was also collected), and collected the trypsinized cells. All the fractions were combined and centrifuged to pellet the cells. Supernatant was the aspirated to leave ≈1 ml of media + cell pellet, which was resuspended by gentle flicking. 9 ml of pre-heated (37^{o}C) hypotonic buffer (0.56% KCl) was added then to the cell suspension, which was incubated in a 37^{o}C water bath to allow hypotonic swelling of the cells. A small amount (≈3 drops) of fixing solution (3:1 methanol: acetic acid) was added and the cells were pelleted at 4^{o}C by centrifugation. Cells were kept on ice from this point onwards. After aspirating the supernatant to leave ≈1ml, the cells were resuspended by gentle flicking and 11ml fixing solution was added dropwise. The suspension was centrifuged once more to pellet the cells and fixing solution added in a similar manner. This mixture was stored at -20^{o}C until hybridization.

Metaphase hybridization:

Cells were pelleted, resuspended in 1ml fresh fixing solution, added to microscope slides and allowed to dry at rt overnight. Next, we washed the slides 3 x 5minutes in 1X PBS, fixed in 4$formaldehyde/PBS and washed 3 x 5 minutes in 1X PBS. Slides were treated with pre-heated acidified pepsin (below) for 10 minutes at 37^{o}C and washed 3 x 5 minutes in 1X PBS. After a

second treatment with formaldehyde and PBS washes, the slides were dehydrated by incubating for 5 minutes each in 70%, 90%, then 100% ethanol and allowed to air dry. Two drops (10 µl each) of the probe mixture (below) was then added to each slides and a coverslip applied. Slides were then heated at 80^{o}C for 3 minutes for denaturation, and incubated in a wet chamber away from light for 2 hours at rt. Following incubation, the slides were washed 2 x 15 minutes in buffer#1 (below), and then 3 x 5 minutes in buffer#2 (below). Finally, slides were dehydrated in ethanol as before, air dried and DNA counterstained with DAPI solution. Fluorescent images were taken using a Nikon 90i upright microscope and intensity of telomere fluorescence analyzed using the TFL-Telo program (gift from P Lansdorp, Vancouver, Canada) [251]. Images and telomere fluorescence values were obtained from more than 50 metaphases in all cases.

Q-FISH Solutions

Pepsin solution: 200ml water, 200mg pepsin, 168 µl concentrated HCl (stock 12M).

Probe solution: 2.5µl Tris 1M pH7.4, 21.4µl $MgCl_2$ buffer, 175µl deionized formamide, 5.0µl telomere probe 25 µg/ml, 12.5µl blocking reagent, 33.6µl distilled water.

PNA telomere probe: TelC-Cy3 (Panagene catalog# F1002-5)

Blocking reagent: 10g Boehringer reagent in 100ml maleic acid buffer pH7.5

Maleic acid buffer: 100 mM maleic acid, 150 mM NaCl pH 7.5

$MgCl_2$ buffer: 25 mM $MgCl_2$, 9mM citric acid, 82 mM Na_2HPO_4, adjusted to pH 7.0

Buffer #1: 280 ml Formamide, 4 ml Tris 1M pH 7.2, 4 ml BSA (stock of 10% in water), 112 ml distilled water.

Buffer #2: 0.08% tween-20 in TBS

Viral Transductions

Viral transduction with dominant-negative TRF2, lamin A, lamin C, and shRNAs (shLmna and shLuciferase). A dominant-negative TRF2 mutant (TRF2$^{\Delta B\Delta M}$) cloned into the pLPC vector (gift from Titia de Lange, Rockefeller University) along with packaging and envelope plasmids pUMVC and pCMV-VSV-G (provided by Sheila Stewart, Washington University) were transfected

in 293T packaging cells using Fugene 6® (Roche Applied Science). Virus-containing media collected from the 293T cells and used to infect the target cells. For retroviral transductions the infection was repeated 24 h later. The same procedure was used to introduce lamins A/C into A-type lamins depleted cells. Retroviral vectors for expression of lamins A/C were a gift from Brian Kennedy (University of Washington, Seattle, WA). GFP was used to monitor the efficiency of 293T transfection and MEF infection. Lentiviral transduction of shRNA sequences cloned into pLKO was carried out in the same manner, using the packaging plasmid pHR'8.2ΔR and the envelope plasmid pCMV-VSV-G. Infected cells were subjected to immunoblotting after selection to ensure depletion or overexpression of the target proteins. shLmna and shLuciferase were a gift from Didier Hodzic (Washington University, St Louis, MO), sh53BP1 was a gift from Barry Sleckman (Washington University, St Louis, MO). 53BP1 expression plasmid was obtained from Addgene.

Immuno-FISH

Cells were fixed for 10 min in 3.7% formaldehyde/0.2% Tx-100/PBS at RT, followed by three washes in PBS. After blocking in 10% BGS/PBS for 1 h, cells were incubated with anti-H2AX antibody 1 h at 37°C, washed three times and incubated with secondary antibodies. After washing extensively in PBS, cells were processed for FISH. Cells were fixed in 3.7% formaldehyde/PBS for 10 min at RT, washed in PBS, dehydrated in ethanol (70%, 90%, 100% ethanol, 5min each), and air dried. Hybridization solution containing the cy3-labeled telomeric probe was added to coverslips, which were heated to 80°C for 10 min, and incubated for 3 h in the dark at RT. Coverslips were washed twice for 15 min in washing solution, and three times in PBS. Cells were counterstained with DAPI and coverslips mounted on slides.

CO-FISH

CO-FISH analysis was carried out as described [175]. Briefly, cells were cultured in 20 M BrdU for 22 h and 0.1 g/ml colcemid was added for the last 4 h to enrich for mitotic cells. Metaphase stage chromosomal spreads were prepared as for Q-FISH [250]. The slides were

treated with RNase A (0.5 g ml-1 for 10 min at 37°C), stained with Hoechst 33258 in 2X SSC for 15 min at RT and exposed to 365 nm UV light for 30 min. Exonuclease III (3 U/l) treatment for 20 min at RT was used to digest the BrdU-labeled strands. The slides were then processed as for Q-FISH but with two different probes added sequentially. Hybridizations were carried out first with the G-rich probe (labeling the leading strand) followed by the C-rich probe (labeling the lagging strand).

Histones.

Histones were purified by acid extraction as detailed by Shechter et al [252]. Histone modifications were detected by immunoblotting using anti-H3K9me3 and anti-H4K20me3 (Upstate).

Telomerase Activity

Telomerase activity was determined using the TeloTAGGG Telomerase PCR ELISA* Kit (Roche) following manufacturer's instructions.

Comet Assays

Neutral comet assays were performed using CometSlide assay kits (Trevigen). Cells were irradiated with 8 Gy, and incubated at 37ºC for different periods of time (0, 30, 60, 90, 120 and 150 min) to allow for DNA damage repair. Cells were embedded in agarose, lysed and subjected to neutral electrophoresis. Before image analysis, cells were stained with ethidium bromide and visualized under a fluorescence microscope. Single-cell electrophoresis results in a comet-shaped distribution of DNA. The comet head contains high molecular weight and intact DNA, and the tail contains the leading ends of migrating fragments. Olive comet moment was calculated by multiplying the percentage of DNA in the tail by the displacement between the means of the head and tail distributions, as described 60. We utilized the program CometScore™ Version 1.5 (TriTek) to calculate Olive Comet Moment. A total of 25 to 30 comets were analyzed per sample in each experiment.

X-ray irradiation

This was done with a PANTAK pmc1000 X-ray machine with a 0.1 Cu+ 2.5 AL filter at a dose rate of 1.1 Gy/min. For immunofluorescence studies cells were irradiated with 0.5 Gy or 8 Gy, and for comet assays cells were given 8 Gy.

Homologous recombination assays

Proficiency of HR is monitored by using a chromosomally integrated HR reporter substrate, DR-GFP, in MCF-7 cells 58. The DR-GFP substrate consists of two tandem GFP sequences that have been mutated to abrogate expression of GFP and an I-SceI recognition site in one sequence. Transient expression of the I-SceI produces a DSB at the recognition site. Repair of this break by intragenic HR with the downstream GFP sequence as the homology substrate results in restoration of a functional GFP gene. Thus, expression of GFP is readout of successful HR 58. MCF-7 DR-GFP cells were transfected with an I-SceI expressing plasmid. After 48 hours, flow cytometry was used to determine the percent of cells expressing GFP as an indication of successful HR.

Colony formation assays

Clonogenic analysis was performed as described. Briefly, cells were plated in p60 culture dishes to facilitate formation of 30-40 colonies per plate and allowed to become adherent by incubating at 37°C for 2-3 hours. Cells were immediately treated with 0, 2, 4, or 6 Gy of ionizing radiation, and allowed to grow undisturbed for 7-10 days. Colonies were then counted and the surviving fractions calculated. Colony formation experiments were done three times, with triplicate samples within each experiment.

Quantitative real time PCR

For chapter 2 Quantitative real-time PCR was carried out on a MyiQ Detection system (BIO-RAD, California, USA) using Taqman Universal PCR Master Mix (PE Applied Biosystems,

California, USA). The cDNA was generated from 1 g of total RNA using Geneamp RNA PCR kit (PE Applied Biosystems) following manufacturer's instructions. 53BP1 and GAPDH expression was determined using Taqman Gene expression assays (Mm00658689_m1 and Mm99999915_g1, respectively, PE Applied Biosystems). For the analysis, all reactions (in triplicate) were carried out by amplifying target gene and endogenous controls in the same plate. Relative quantitative evaluation of target gene was determined by comparing the threshold cycles.

For chapter 3. Quantitative real-time PCR was performed using the 7900HT Fast Real-Time PCR system (Applied Biosystems) with the Taqman® Universal PCR Master Mix (Applied Biosystems, California, USA). Generation of cDNA was carried out by reverse transcription of 1µg total RNA using the GeneAmp® RNA PCR kit, also from Applied Biosystems. RAD51, BRCA1 and RPA2 transcripts were detected by TaqMan® Gene Expression Assays (Hs00153418_m1, Hs01556193_m1, and Hs00358315_m1 respectively). All PCR reactions were done in triplicate within experiments to amplify endogenous target genes, with 18S controls in the same plate. Data was analyzed by relative quantitation.

Statistical analysis

A 'two-tailed' Student's t-test, 'two-samples of equal variance' was used to calculate statistical significance of the observed differences in telomere length. Microsoft Excel v.2001 and Graphpad Instat v3.05 were used for the calculations. A paired t-test to determine statistical significance was alternatively used when indicated. In all cases, differences were considered statistically significant when $P<0.05$.

REFERENCES

1. Ferlay J, S.H., Bray F, Forman D, Mathers C and Parkin DM. *GLOBOCAN 2008 v1.2, Cancer Incidence and Mortality Worldwide: IARC CancerBase No. 10 [Internet].* 2008 [cited 2011 10/11/2011]; Available from: http://globocan.iarc.fr.
2. Loeb, L.A., *Cancer cells exhibit a mutator phenotype.* Adv Cancer Res, 1998. **72**: p. 25-56.
3. Hanahan, D. and R.A. Weinberg, *Hallmarks of cancer: the next generation.* Cell, 2011. **144**(5): p. 646-74.
4. Hanahan, D. and R.A. Weinberg, *The hallmarks of cancer.* Cell, 2000. **100**(1): p. 57-70.
5. *Fast Stats: An interactive tool for access to SEER cancer statistics. Surveillance Research Program, National Cancer Institute.* [cited 2011 10/31/2011]; Available from: http://seer.cancer.gov/faststats.
6. Misteli, T., *Beyond the sequence: cellular organization of genome function.* Cell, 2007. **128**(4): p. 787-800.
7. Dechat, T., et al., *Nuclear lamins: major factors in the structural organization and function of the nucleus and chromatin.* Genes Dev, 2008. **22**(7): p. 832-53.
8. Zink, D., A.H. Fischer, and J.A. Nickerson, *Nuclear structure in cancer cells.* Nat Rev Cancer, 2004. **4**(9): p. 677-87.
9. Taddei, A., et al., *The function of nuclear architecture: a genetic approach.* Annu Rev Genet, 2004. **38**: p. 305-45.
10. Goldman, R.D., et al., *Nuclear lamins: building blocks of nuclear architecture.* Genes Dev, 2002. **16**(5): p. 533-47.
11. Gruenbaum, Y., et al., *The nuclear lamina comes of age.* Nat Rev Mol Cell Biol, 2005. **6**(1): p. 21-31.
12. Broers, J.L., et al., *Nuclear lamins: laminopathies and their role in premature ageing.* Physiol Rev, 2006. **86**(3): p. 967-1008.

13. Capell, B.C. and F.S. Collins, *Human laminopathies: nuclei gone genetically awry.* Nat Rev Genet, 2006. **7**(12): p. 940-52.

14. Agrelo, R., et al., *Inactivation of the lamin A/C gene by CpG island promoter hypermethylation in hematologic malignancies, and its association with poor survival in nodal diffuse large B-cell lymphoma.* J Clin Oncol, 2005. **23**(17): p. 3940-7.

15. Prokocimer, M., A. Margalit, and Y. Gruenbaum, *The nuclear lamina and its proposed roles in tumorigenesis: projection on the hematologic malignancies and future targeted therapy.* J Struct Biol, 2006. **155**(2): p. 351-60.

16. Willis, N.D., et al., *Lamin A/C is a risk biomarker in colorectal cancer.* PLoS One, 2008. **3**(8): p. e2988.

17. Willis, N.D., R.G. Wilson, and C.J. Hutchison, *Lamin A: a putative colonic epithelial stem cell biomarker which identifies colorectal tumours with a more aggressive phenotype.* Biochem Soc Trans, 2008. **36**(Pt 6): p. 1350-3.

18. Negrini, S., V.G. Gorgoulis, and T.D. Halazonetis, *Genomic instability--an evolving hallmark of cancer.* Nat Rev Mol Cell Biol, 2010. **11**(3): p. 220-8.

19. Levy, M.Z., et al., *Telomere end-replication problem and cell aging.* J Mol Biol, 1992. **225**(4): p. 951-60.

20. Chan, S.S. and S. Chang, *Defending the end zone: studying the players involved in protecting chromosome ends.* FEBS Lett, 2010. **584**(17): p. 3773-8.

21. Harley, C.B., A.B. Futcher, and C.W. Greider, *Telomeres shorten during ageing of human fibroblasts.* Nature, 1990. **345**(6274): p. 458-60.

22. Allsopp, R.C., et al., *Telomere length predicts replicative capacity of human fibroblasts.* Proc Natl Acad Sci U S A, 1992. **89**(21): p. 10114-8.

23. Shay, J.W. and W.E. Wright, *Senescence and immortalization: role of telomeres and telomerase.* Carcinogenesis, 2005. **26**(5): p. 867-74.

24. Stewart, S.A. and R.A. Weinberg, *Telomeres: Cancer to Human Aging.* Annu Rev Cell Dev Biol, 2006.

25. Greider, C.W. and E.H. Blackburn, *Identification of a specific telomere terminal transferase activity in Tetrahymena extracts.* Cell, 1985. **43**(2 Pt 1): p. 405-13.

26. Greider, C.W. and E.H. Blackburn, *The telomere terminal transferase of Tetrahymena is a ribonucleoprotein enzyme with two kinds of primer specificity.* Cell, 1987. **51**(6): p. 887-98.

27. Greider, C.W. and E.H. Blackburn, *A telomeric sequence in the RNA of Tetrahymena telomerase required for telomere repeat synthesis.* Nature, 1989. **337**(6205): p. 331-7.

28. Vaziri, H. and S. Benchimol, *Reconstitution of telomerase activity in normal human cells leads to elongation of telomeres and extended replicative life span.* Curr Biol, 1998. **8**(5): p. 279-82.

29. Bodnar, A.G., et al., *Extension of life-span by introduction of telomerase into normal human cells.* Science, 1998. **279**(5349): p. 349-52.

30. Bryan, T.M., et al., *Telomere elongation in immortal human cells without detectable telomerase activity.* EMBO J, 1995. **14**(17): p. 4240-8.

31. Bryan, T.M., et al., *Evidence for an alternative mechanism for maintaining telomere length in human tumors and tumor-derived cell lines.* Nat Med, 1997. **3**(11): p. 1271-4.

32. Dunham, M.A., et al., *Telomere maintenance by recombination in human cells.* Nat Genet, 2000. **26**(4): p. 447-50.

33. Zeng, S., et al., *Telomere recombination requires the MUS81 endonuclease.* Nat Cell Biol, 2009. **11**(5): p. 616-23.

34. Hahn, W.C., et al., *Inhibition of telomerase limits the growth of human cancer cells.* Nat Med, 1999. **5**(10): p. 1164-70.

35. Hahn, W.C. and M. Meyerson, *Telomerase activation, cellular immortalization and cancer.* Ann Med, 2001. **33**(2): p. 123-9.

36. Cerone, M.A., J.A. Londono-Vallejo, and C. Autexier, *Telomerase inhibition enhances the response to anticancer drug treatment in human breast cancer cells.* Mol Cancer Ther, 2006. **5**(7): p. 1669-75.

37. Akiyama, M., et al., *Telomerase inhibitors as anticancer therapy.* Curr Med Chem Anticancer Agents, 2002. **2**(5): p. 567-75.

38. Cairns, D., et al., *Design of telomerase inhibitors for the treatment of cancer.* Curr Pharm Des, 2002. **8**(27): p. 2491-504.

39. Moyzis, R.K., et al., *A highly conserved repetitive DNA sequence, (TTAGGG)n, present at the telomeres of human chromosomes.* Proc Natl Acad Sci U S A, 1988. **85**(18): p. 6622-6.

40. de Lange, T., *Shelterin: the protein complex that shapes and safeguards human telomeres.* Genes Dev, 2005. **19**(18): p. 2100-10.

41. Liu, D., et al., *Telosome, a mammalian telomere-associated complex formed by multiple telomeric proteins.* J Biol Chem, 2004. **279**(49): p. 51338-42.

42. Broccoli, D., et al., *Human telomeres contain two distinct Myb-related proteins, TRF1 and TRF2.* Nat Genet, 1997. **17**(2): p. 231-5.

43. Smogorzewska, A., et al., *Control of human telomere length by TRF1 and TRF2.* Mol Cell Biol, 2000. **20**(5): p. 1659-68.

44. van Steensel, B., A. Smogorzewska, and T. de Lange, *TRF2 protects human telomeres from end-to-end fusions.* Cell, 1998. **92**(3): p. 401-13.

45. Kim, S.H., et al., *TIN2 mediates functions of TRF2 at human telomeres.* J Biol Chem, 2004. **279**(42): p. 43799-804.

46. Ye, J.Z., et al., *POT1-interacting protein PIP1: a telomere length regulator that recruits POT1 to the TIN2/TRF1 complex.* Genes Dev, 2004. **18**(14): p. 1649-54.

47. Liu, D., et al., *PTOP interacts with POT1 and regulates its localization to telomeres.* Nat Cell Biol, 2004. **6**(7): p. 673-80.

48. Li, B., S. Oestreich, and T. de Lange, *Identification of human Rap1: implications for telomere evolution.* Cell, 2000. **101**(5): p. 471-83.

49. Li, B. and T. de Lange, *Rap1 affects the length and heterogeneity of human telomeres.* Mol Biol Cell, 2003. **14**(12): p. 5060-8.

50. Smogorzewska, A., et al., *DNA ligase IV-dependent NHEJ of deprotected mammalian telomeres in G1 and G2.* Curr Biol, 2002. **12**(19): p. 1635-44.

51. Dimitrova, N., et al., *53BP1 promotes non-homologous end joining of telomeres by increasing chromatin mobility.* Nature, 2008. **456**(7221): p. 524-8.

52. Peters, A.H., et al., *Loss of the Suv39h histone methyltransferases impairs mammalian heterochromatin and genome stability.* Cell, 2001. **107**(3): p. 323-37.

53. Lachner, M., et al., *Methylation of histone H3 lysine 9 creates a binding site for HP1 proteins.* Nature, 2001. **410**(6824): p. 116-20.

54. Garcia-Cao, M., et al., *Epigenetic regulation of telomere length in mammalian cells by the Suv39h1 and Suv39h2 histone methyltransferases.* Nat Genet, 2004. **36**(1): p. 94-9.

55. Benetti, R., et al., *Suv4-20h deficiency results in telomere elongation and derepression of telomere recombination.* J Cell Biol, 2007. **178**(6): p. 925-36.

56. Gonzalo, S., et al., *DNA methyltransferases control telomere length and telomere recombination in mammalian cells.* Nat Cell Biol, 2006. **8**(4): p. 416-24.

57. Canudas, S., et al., *A role for heterochromatin protein 1gamma at human telomeres.* Genes Dev, 2011. **25**(17): p. 1807-19.

58. Azzalin, C.M., et al., *Telomeric repeat containing RNA and RNA surveillance factors at mammalian chromosome ends.* Science, 2007. **318**(5851): p. 798-801.

59. Schoeftner, S. and M.A. Blasco, *Developmentally regulated transcription of mammalian telomeres by DNA-dependent RNA polymerase II.* Nat Cell Biol, 2008. **10**(2): p. 228-36.

60. Luke, B. and J. Lingner, *TERRA: telomeric repeat-containing RNA.* EMBO J, 2009. **28**(17): p. 2503-10.

61. Luke, B., et al., *The Rat1p 5′ to 3′ exonuclease degrades telomeric repeat-containing RNA and promotes telomere elongation in Saccharomyces cerevisiae.* Mol Cell, 2008. **32**(4): p. 465-77.

62. Hartlerode, A.J. and R. Scully, *Mechanisms of double-strand break repair in somatic mammalian cells.* Biochem J, 2009. **423**(2): p. 157-68.

63. Lieber, M.R., *The mechanism of double-strand DNA break repair by the nonhomologous DNA end-joining pathway.* Annu Rev Biochem, 2010. **79**: p. 181-211.

64. Lieber, M.R., et al., *Nonhomologous DNA end joining (NHEJ) and chromosomal translocations in humans.* Subcell Biochem, 2010. **50**: p. 279-96.

65. Zhou, B.B. and S.J. Elledge, *The DNA damage response: putting checkpoints in perspective.* Nature, 2000. **408**(6811): p. 433-9.

66. Jackson, S.P. and J. Bartek, *The DNA-damage response in human biology and disease.* Nature, 2009. **461**(7267): p. 1071-8.

67. Huen, M.S. and J. Chen, *The DNA damage response pathways: at the crossroad of protein modifications.* Cell Res, 2008. **18**(1): p. 8-16.

68. Bartek, J., J. Bartkova, and J. Lukas, *DNA damage signalling guards against activated oncogenes and tumour progression.* Oncogene, 2007. **26**(56): p. 7773-9.

69. Iliakis, G., et al., *Mechanisms of DNA double strand break repair and chromosome aberration formation.* Cytogenet Genome Res, 2004. **104**(1-4): p. 14-20.

70. Heyer, W.D., K.T. Ehmsen, and J. Liu, *Regulation of homologous recombination in eukaryotes.* Annu Rev Genet, 2010. **44**: p. 113-39.

71. Holthausen, J.T., C. Wyman, and R. Kanaar, *Regulation of DNA strand exchange in homologous recombination.* DNA Repair (Amst), 2010. **9**(12): p. 1264-72.

72. Mimitou, E.P. and L.S. Symington, *Nucleases and helicases take center stage in homologous recombination.* Trends Biochem Sci, 2009. **34**(5): p. 264-72.

73. Mimitou, E.P. and L.S. Symington, *DNA end resection: many nucleases make light work.* DNA Repair (Amst), 2009. **8**(9): p. 983-95.

74. Quennet, V., et al., *CtIP and MRN promote non-homologous end-joining of etoposide-induced DNA double-strand breaks in G1.* Nucleic Acids Res, 2011. **39**(6): p. 2144-52.

75. Eid, W., et al., *DNA end resection by CtIP and exonuclease 1 prevents genomic instability.* EMBO Rep, 2010. **11**(12): p. 962-8.

76. You, Z. and J.M. Bailis, *DNA damage and decisions: CtIP coordinates DNA repair and cell cycle checkpoints.* Trends Cell Biol, 2010. **20**(7): p. 402-9.

77. Sartori, A.A., et al., *Human CtIP promotes DNA end resection.* Nature, 2007. **450**(7169): p. 509-14.

78. Huertas, P. and S.P. Jackson, *Human CtIP mediates cell cycle control of DNA end resection and double strand break repair.* J Biol Chem, 2009. **284**(14): p. 9558-65.

79. You, Z., et al., *CtIP links DNA double-strand break sensing to resection.* Mol Cell, 2009. **36**(6): p. 954-69.

80. Yu, X., et al., *BRCA1 ubiquitinates its phosphorylation-dependent binding partner CtIP.* Genes Dev, 2006. **20**(13): p. 1721-6.

81. Chen, L., et al., *Cell cycle-dependent complex formation of BRCA1.CtIP.MRN is important for DNA double-strand break repair.* J Biol Chem, 2008. **283**(12): p. 7713-20.

82. Buis, J., et al., *Mre11 nuclease activity has essential roles in DNA repair and genomic stability distinct from ATM activation.* Cell, 2008. **135**(1): p. 85-96.

83. Scully, R., et al., *Location of BRCA1 in human breast and ovarian cancer cells.* Science, 1996. **272**(5258): p. 123-6.

84. Scully, R. and D.M. Livingston, *In search of the tumour-suppressor functions of BRCA1 and BRCA2.* Nature, 2000. **408**(6811): p. 429-32.

85. Neuhausen, S.L. and C.J. Marshall, *Loss of heterozygosity in familial tumors from three BRCA1-linked kindreds.* Cancer Res, 1994. **54**(23): p. 6069-72.

86. Schlegel, B.P., F.M. Jodelka, and R. Nunez, *BRCA1 promotes induction of ssDNA by ionizing radiation.* Cancer Res, 2006. **66**(10): p. 5181-9.

87. Feng, Z. and J. Zhang, *A dual role of BRCA1 in two distinct homologous recombination mediated repair in response to replication arrest.* Nucleic Acids Res, 2011.

88. Aly, A. and S. Ganesan, *BRCA1, PARP, and 53BP1: conditional synthetic lethality and synthetic viability.* J Mol Cell Biol, 2011. **3**(1): p. 66-74.

89. Bouwman, P., et al., *53BP1 loss rescues BRCA1 deficiency and is associated with triple-negative and BRCA-mutated breast cancers.* Nat Struct Mol Biol, 2010. **17**(6): p. 688-95.

90. Bunting, S.F., et al., *53BP1 inhibits homologous recombination in Brca1-deficient cells by blocking resection of DNA breaks.* Cell, 2010. **141**(2): p. 243-54.

91. Cao, L., et al., *A selective requirement for 53BP1 in the biological response to genomic instability induced by Brca1 deficiency.* Mol Cell, 2009. **35**(4): p. 534-41.

92. Shibata, A., et al., *Factors determining DNA double-strand break repair pathway choice in G2 phase.* EMBO J, 2011. **30**(6): p. 1079-92.

93. Mladenov, E. and G. Iliakis, *Induction and repair of DNA double strand breaks: the increasing spectrum of non-homologous end joining pathways.* Mutat Res, 2011. **711**(1-2): p. 61-72.

94. Costantini, S., et al., *Interaction of the Ku heterodimer with the DNA ligase IV/Xrcc4 complex and its regulation by DNA-PK.* DNA Repair (Amst), 2007. **6**(6): p. 712-22.

95. Ma, Y., K. Schwarz, and M.R. Lieber, *The Artemis:DNA-PKcs endonuclease cleaves DNA loops, flaps, and gaps.* DNA Repair (Amst), 2005. **4**(7): p. 845-51.

96. Yannone, S.M., et al., *Coordinate 5' and 3' endonucleolytic trimming of terminally blocked blunt DNA double-strand break ends by Artemis nuclease and DNA-dependent protein kinase.* Nucleic Acids Res, 2008. **36**(10): p. 3354-65.

97. Ma, Y., et al., *Hairpin opening and overhang processing by an Artemis/DNA-dependent protein kinase complex in nonhomologous end joining and V(D)J recombination.* Cell, 2002. **108**(6): p. 781-94.

98. Manis, J.P., et al., *53BP1 links DNA damage-response pathways to immunoglobulin heavy chain class-switch recombination.* Nat Immunol, 2004. **5**(5): p. 481-7.

99. Ward, I.M., et al., *53BP1 is required for class switch recombination.* J Cell Biol, 2004. **165**(4): p. 459-64.

100. Difilippantonio, S., et al., *53BP1 facilitates long-range DNA end-joining during V(D)J recombination.* Nature, 2008. **456**(7221): p. 529-33.

101. Stewart, G.S., et al., *RIDDLE immunodeficiency syndrome is linked to defects in 53BP1-mediated DNA damage signaling.* Proc Natl Acad Sci U S A, 2007. **104**(43): p. 16910-5.

102. Buck, D., et al., *Cernunnos, a novel nonhomologous end-joining factor, is mutated in human immunodeficiency with microcephaly.* Cell, 2006. **124**(2): p. 287-99.

103. Zhang, Y. and M. Jasin, *An essential role for CtIP in chromosomal translocation formation through an alternative end-joining pathway.* Nat Struct Mol Biol, 2011. **18**(1): p. 80-4.

104. Simsek, D., et al., *DNA ligase III promotes alternative nonhomologous end-joining during chromosomal translocation formation.* PLoS Genet, 2011. **7**(6): p. e1002080.

105. Iliakis, G., *Backup pathways of NHEJ in cells of higher eukaryotes: cell cycle dependence.* Radiother Oncol, 2009. **92**(3): p. 310-5.

106. Bennardo, N., et al., *Alternative-NHEJ is a mechanistically distinct pathway of mammalian chromosome break repair.* PLoS Genet, 2008. **4**(6): p. e1000110.

107. Iwabuchi, K., et al., *Two cellular proteins that bind to wild-type but not mutant p53.* Proc Natl Acad Sci U S A, 1994. **91**(13): p. 6098-102.

108. Anderson, L., C. Henderson, and Y. Adachi, *Phosphorylation and rapid relocalization of 53BP1 to nuclear foci upon DNA damage.* Mol Cell Biol, 2001. **21**(5): p. 1719-29.

109. Fernandez-Capetillo, O., et al., *DNA damage-induced G2-M checkpoint activation by histone H2AX and 53BP1.* Nat Cell Biol, 2002. **4**(12): p. 993-7.

110. Wang, B., et al., *53BP1, a mediator of the DNA damage checkpoint.* Science, 2002. **298**(5597): p. 1435-8.

111. Iwabuchi, K., et al., *53BP1 contributes to survival of cells irradiated with X-ray during G1 without Ku70 or Artemis.* Genes Cells, 2006. **11**(8): p. 935-48.

112. Adams, M.M. and P.B. Carpenter, *Tying the loose ends together in DNA double strand break repair with 53BP1.* Cell Div, 2006. **1**: p. 19.

113. Nakamura, K., et al., *Genetic dissection of vertebrate 53BP1: a major role in non-homologous end joining of DNA double strand breaks.* DNA Repair (Amst), 2006. **5**(6): p. 741-9.

114. Noon, A.T., et al., *53BP1-dependent robust localized KAP-1 phosphorylation is essential for heterochromatic DNA double-strand break repair.* Nat Cell Biol, 2010. **12**(2): p. 177-84.

115. Noon, A.T. and A.A. Goodarzi, *53BP1-mediated DNA double strand break repair: Insert bad pun here.* DNA Repair (Amst), 2011. **10**(10): p. 1071-6.

116. Ward, I.M., et al., *p53 Binding protein 53BP1 is required for DNA damage responses and tumor suppression in mice.* Mol Cell Biol, 2003. **23**(7): p. 2556-63.

117. Goodarzi, A.A., T. Kurka, and P.A. Jeggo, *KAP-1 phosphorylation regulates CHD3 nucleosome remodeling during the DNA double-strand break response.* Nat Struct Mol Biol, 2011. **18**(7): p. 831-9.

118. Bothmer, A., et al., *53BP1 regulates DNA resection and the choice between classical and alternative end joining during class switch recombination.* J Exp Med, 2010. **207**(4): p. 855-65.

119. Farmer, H., et al., *Targeting the DNA repair defect in BRCA mutant cells as a therapeutic strategy.* Nature, 2005. **434**(7035): p. 917-21.

120. Helleday, T., H.E. Bryant, and N. Schultz, *Poly(ADP-ribose) polymerase (PARP-1) in homologous recombination and as a target for cancer therapy.* Cell Cycle, 2005. **4**(9): p. 1176-8.

121. Allinson, S.L., Dianova, II, and G.L. Dianov, *Poly(ADP-ribose) polymerase in base excision repair: always engaged, but not essential for DNA damage processing.* Acta Biochim Pol, 2003. **50**(1): p. 169-79.

122. Ame, J.C., et al., *PARP-2, A novel mammalian DNA damage-dependent poly(ADP-ribose) polymerase.* J Biol Chem, 1999. **274**(25): p. 17860-8.

123. Satoh, M.S. and T. Lindahl, *Role of poly(ADP-ribose) formation in DNA repair.* Nature, 1992. **356**(6367): p. 356-8.

124. Woodhouse, B.C. and G.L. Dianov, *Poly ADP-ribose polymerase-1: an international molecule of mystery.* DNA Repair (Amst), 2008. **7**(7): p. 1077-86.

125. Ashworth, A., *A synthetic lethal therapeutic approach: poly(ADP) ribose polymerase inhibitors for the treatment of cancers deficient in DNA double-strand break repair.* J Clin Oncol, 2008. **26**(22): p. 3785-90.

126. Guha, M., *PARP inhibitors stumble in breast cancer.* Nat Biotechnol, 2011. **29**(5): p. 373-4.

127. Finkel, T., M. Serrano, and M.A. Blasco, *The common biology of cancer and ageing.* Nature, 2007. **448**(7155): p. 767-74.

128. Lombard, D.B., et al., *DNA repair, genome stability, and aging.* Cell, 2005. **120**(4): p. 497-512.

129. Lowndes, N.F., *The interplay between BRCA1 and 53BP1 influences death, aging, senescence and cancer.* DNA Repair (Amst), 2010.

130. Pichierri, P., et al., *The Werner syndrome protein: linking the replication checkpoint response to genome stability.* Aging (Albany NY), 2011. **3**(3): p. 311-8.

131. Poot, M., et al., *Impaired S-phase transit of Werner syndrome cells expressed in lymphoblastoid cell lines.* Exp Cell Res, 1992. **202**(2): p. 267-73.

132. Gebhart, E., et al., *Spontaneous and induced chromosomal instability in Werner syndrome.* Hum Genet, 1988. **80**(2): p. 135-9.

133. Adelfalk, C., et al., *Nuclear deformation characterizes Werner syndrome cells.* Cell Biol Int, 2005. **29**(12): p. 1032-7.

134. Bonne, G. and N. Levy, *LMNA mutations in atypical Werner's syndrome.* Lancet, 2003. **362**(9395): p. 1585-6; author reply 1586.

135. Chen, L., et al., *LMNA mutations in atypical Werner's syndrome.* Lancet, 2003. **362**(9382): p. 440-5.

136. Vigouroux, C., et al., *LMNA mutations in atypical Werner's syndrome.* Lancet, 2003. **362**(9395): p. 1585; author reply 1586.

137. Pereira, S., et al., *HGPS and related premature aging disorders: from genomic identification to the first therapeutic approaches.* Mech Ageing Dev, 2008. **129**(7-8): p. 449-59.

138. Glynn, M.W. and T.W. Glover, *Incomplete processing of mutant lamin A in Hutchinson-Gilford progeria leads to nuclear abnormalities, which are reversed by farnesyltransferase inhibition.* Hum Mol Genet, 2005. **14**(20): p. 2959-69.

139. Goldman, R.D., et al., *Accumulation of mutant lamin A causes progressive changes in nuclear architecture in Hutchinson-Gilford progeria syndrome.* Proc Natl Acad Sci U S A, 2004. **101**(24): p. 8963-8.

140. De Sandre-Giovannoli, A., et al., *Lamin a truncation in Hutchinson-Gilford progeria.* Science, 2003. **300**(5628): p. 2055.

141. Huang, S., et al., *Accelerated telomere shortening and replicative senescence in human fibroblasts overexpressing mutant and wild-type lamin A.* Exp Cell Res, 2008. **314**(1): p. 82-91.

142. Worman, H.J., *Nuclear lamins and laminopathies.* J Pathol, 2011.

143. Mattout, A., et al., *Nuclear lamins, diseases and aging.* Curr Opin Cell Biol, 2006. **18**(3): p. 335-41.

144. Hutchison, C.J. and H.J. Worman, *A-type lamins: guardians of the soma?* Nat Cell Biol, 2004. **6**(11): p. 1062-7.

145. Constantinescu, D., et al., *Lamin A/C expression is a marker of mouse and human embryonic stem cell differentiation.* Stem Cells, 2006. **24**(1): p. 177-85.

146. Rober, R.A., et al., *Cells of the cellular immune and hemopoietic system of the mouse lack lamins A/C: distinction versus other somatic cells.* J Cell Sci, 1990. **95 (Pt 4)**: p. 587-98.

147. Spann, T.P., et al., *Alteration of nuclear lamin organization inhibits RNA polymerase II-dependent transcription.* J Cell Biol, 2002. **156**(4): p. 603-8.

148. Johnson, B.R., et al., *A-type lamins regulate retinoblastoma protein function by promoting subnuclear localization and preventing proteasomal degradation.* Proc Natl Acad Sci U S A, 2004. **101**(26): p. 9677-82.

149. Lee, D.C., et al., *A-type nuclear lamins act as transcriptional repressors when targeted to promoters.* Exp Cell Res, 2009. **315**(6): p. 996-1007.

150. Prokocimer, M., et al., *Nuclear lamins: key regulators of nuclear structure and activities.* J Cell Mol Med, 2009.

151. Sullivan, T., et al., *Loss of A-type lamin expression compromises nuclear envelope integrity leading to muscular dystrophy.* J Cell Biol, 1999. **147**(5): p. 913-20.

152. Liu, B., et al., *Genomic instability in laminopathy-based premature aging.* Nat Med, 2005. **11**(7): p. 780-5.

153. Ramirez, C.L., et al., *Human progeroid syndromes, aging and cancer: new genetic and epigenetic insights into old questions.* Cell Mol Life Sci, 2007. **64**(2): p. 155-70.

154. Worman, H.J. and G. Bonne, *"Laminopathies": a wide spectrum of human diseases.* Exp Cell Res, 2007. **313**(10): p. 2121-33.

155. Eriksson, M., et al., *Recurrent de novo point mutations in lamin A cause Hutchinson-Gilford progeria syndrome.* Nature, 2003. **423**(6937): p. 293-8.

156. Stewart, C.L., et al., *Mouse models of the laminopathies.* Exp Cell Res, 2007. **313**(10): p. 2144-56.

157. Bergo, M.O., et al., *Zmpste24 deficiency in mice causes spontaneous bone fractures, muscle weakness, and a prelamin A processing defect.* Proc Natl Acad Sci U S A, 2002. **99**(20): p. 13049-54.

158. Pendas, A.M., et al., *Defective prelamin A processing and muscular and adipocyte alterations in Zmpste24 metalloproteinase-deficient mice.* Nat Genet, 2002. **31**(1): p. 94-9.

159. Andres, V. and J.M. Gonzalez, *Role of A-type lamins in signaling, transcription, and chromatin organization.* J Cell Biol, 2009. **187**(7): p. 945-57.

160. Varela, I., et al., *Accelerated ageing in mice deficient in Zmpste24 protease is linked to p53 signalling activation.* Nature, 2005. **437**(7058): p. 564-8.

161. Manju, K., B. Muralikrishna, and V.K. Parnaik, *Expression of disease-causing lamin A mutants impairs the formation of DNA repair foci.* J Cell Sci, 2006. **119**(Pt 13): p. 2704-14.

162. Broers, J.L., et al., *Nuclear A-type lamins are differentially expressed in human lung cancer subtypes.* Am J Pathol, 1993. **143**(1): p. 211-20.

163. Kaufmann, S.H., et al., *Differential expression of nuclear envelope lamins A and C in human lung cancer cell lines.* Cancer Res, 1991. **51**(2): p. 581-6.

164. Genovese, C., et al., *Cell cycle control and beyond: emerging roles for the retinoblastoma gene family.* Oncogene, 2006. **25**(38): p. 5201-9.

165. Nitta, R.T., C.L. Smith, and B.K. Kennedy, *Evidence that proteasome-dependent degradation of the retinoblastoma protein in cells lacking A-type lamins occurs independently of gankyrin and MDM2.* PLoS One, 2007. **2**(9): p. e963.

166. Chuang, T.C., et al., *The three-dimensional organization of telomeres in the nucleus of mammalian cells.* BMC Biol, 2004. **2**: p. 12.

167. Mai, S. and Y. Garini, *The significance of telomeric aggregates in the interphase nuclei of tumor cells.* J Cell Biochem, 2006. **97**(5): p. 904-15.

168. Raz, V., et al., *The nuclear lamina promotes telomere aggregation and centromere peripheral localization during senescence of human mesenchymal stem cells.* J Cell Sci, 2008. **121**(Pt 24): p. 4018-28.

169. Vermolen, B.J., et al., *Characterizing the three-dimensional organization of telomeres.* Cytometry A, 2005. **67**(2): p. 144-50.

170. Gonzalez-Suarez, I., et al., *Novel roles for A-type lamins in telomere biology and the DNA damage response pathway.* Embo J, 2009. **28**(16): p. 2414-27.

171. Garcia-Cao, M., et al., *A role for the Rb family of proteins in controlling telomere length.* Nat Genet, 2002. **32**(3): p. 415-9.

172. Gonzalo, S., et al., *Role of the RB1 family in stabilizing histone methylation at constitutive heterochromatin.* Nat Cell Biol, 2005. **7**(4): p. 420-8.

173. Scaffidi, P. and T. Misteli, *Lamin A-dependent nuclear defects in human aging.* Science, 2006. **312**(5776): p. 1059-63.

174. Shumaker, D.K., et al., *Mutant nuclear lamin A leads to progressive alterations of epigenetic control in premature aging.* Proc Natl Acad Sci U S A, 2006. **103**(23): p. 8703-8.

175. Bailey, S.M., E.H. Goodwin, and M.N. Cornforth, *Strand-specific fluorescence in situ hybridization: the CO-FISH family.* Cytogenet Genome Res, 2004. **107**(1-2): p. 14-7.

176. Iovino, F., et al., *RB acute loss induces centrosome amplification and aneuploidy in murine primary fibroblasts.* Mol Cancer, 2006. **5**: p. 38.

177. Akhtar, A. and S.M. Gasser, *The nuclear envelope and transcriptional control.* Nat Rev Genet, 2007. **8**(7): p. 507-17.

178. Glass, C.A., et al., *The alpha-helical rod domain of human lamins A and C contains a chromatin binding site.* Embo J, 1993. **12**(11): p. 4413-24.

179. Stierle, V., et al., *The carboxyl-terminal region common to lamins A and C contains a DNA binding domain.* Biochemistry, 2003. **42**(17): p. 4819-28.

180. Schermelleh, L., et al., *Subdiffraction multicolor imaging of the nuclear periphery with 3D structured illumination microscopy.* Science, 2008. **320**(5881): p. 1332-6.

181. Nitta, R.T., et al., *Stabilization of the retinoblastoma protein by A-type nuclear lamins is required for INK4A-mediated cell cycle arrest.* Mol Cell Biol, 2006. **26**(14): p. 5360-72.

182. Han, X., et al., *Tethering by lamin A stabilizes and targets the ING1 tumour suppressor.* Nat Cell Biol, 2008. **10**(11): p. 1333-40.

183. Gonzalez-Suarez, I., A.B. Redwood, and S. Gonzalo, *Loss of A-type lamins and genomic instability.* Cell Cycle, 2009. **8**(23): p. 3860-5.

184. Riha, K., M.L. Heacock, and D.E. Shippen, *The role of the nonhomologous end-joining DNA double-strand break repair pathway in telomere biology.* Annu Rev Genet, 2006. **40**: p. 237-77.

185. Takai, H., A. Smogorzewska, and T. de Lange, *DNA damage foci at dysfunctional telomeres.* Curr Biol, 2003. **13**(17): p. 1549-56.

186. De Lange, T., *Telomere-related genome instability in cancer.* Cold Spring Harb Symp Quant Biol, 2005. **70**: p. 197-204.

187. Gonzalez-Suarez, I., et al., *A new pathway that regulates 53BP1 stability implicates Cathepsin L and vitamin D in DNA repair.* Embo J, 2011. **30**(16): p. 3383-96.

188. Katunuma, N., *Mechanisms and regulation of lysosomal proteolysis.* Revis Biol Celular, 1989. **20**: p. 35-61.

189. Reiser, J., B. Adair, and T. Reinheckel, *Specialized roles for cysteine cathepsins in health and disease.* J Clin Invest. **120**(10): p. 3421-31.

190. Gocheva, V. and J.A. Joyce, *Cysteine cathepsins and the cutting edge of cancer invasion.* Cell Cycle, 2007. **6**(1): p. 60-4.

191. Jedeszko, C. and B.F. Sloane, *Cysteine cathepsins in human cancer.* Biol Chem, 2004. **385**(11): p. 1017-27.

192. Miyamoto, K., et al., *Cathepsin L is highly expressed in gastrointestinal stromal tumors.* Int J Oncol. **39**(5): p. 1109-15.

193. Duncan, E.M., et al., *Cathepsin L proteolytically processes histone H3 during mouse embryonic stem cell differentiation.* Cell, 2008. **135**(2): p. 284-94.

194. Goulet, B., et al., *A cathepsin L isoform that is devoid of a signal peptide localizes to the nucleus in S phase and processes the CDP/Cux transcription factor.* Mol Cell, 2004. **14**(2): p. 207-19.

195. Alvarez-Diaz, S., et al., *Vitamin D: Proteases, protease inhibitors and cancer.* Cell Cycle, 2010. **9**(1): p. 32-7.

196. Alvarez-Diaz, S., et al., *Cystatin D is a candidate tumor suppressor gene induced by vitamin D in human colon cancer cells.* J Clin Invest, 2009. **119**(8): p. 2343-58.

197. Rogakou, E.P., et al., *DNA double-stranded breaks induce histone H2AX phosphorylation on serine 139.* J Biol Chem, 1998. **273**(10): p. 5858-68.

198. Rogakou, E.P., et al., *Megabase chromatin domains involved in DNA double-strand breaks in vivo.* J Cell Biol, 1999. **146**(5): p. 905-16.

199. Schultz, L.B., et al., *p53 binding protein 1 (53BP1) is an early participant in the cellular response to DNA double-strand breaks.* J Cell Biol, 2000. **151**(7): p. 1381-90.

200. Shi, W., et al., *Disassembly of MDC1 foci is controlled by ubiquitin-proteasome-dependent degradation.* J Biol Chem, 2008. **283**(46): p. 31608-16.

201. Harrigan, J.A., et al., *Replication stress induces 53BP1-containing OPT domains in G1 cells.* J Cell Biol, 2011. **193**(1): p. 97-108.

202. Glover TW, S.C., *Induction of sister chromatid exchanges at common fragile sites.* Am J Hum Genet., 1987. **41**(5): p. 882-90.

203. Olive, P.L., J.P. Banath, and R.E. Durand, *Heterogeneity in radiation-induced DNA damage and repair in tumor and normal cells measured using the "comet" assay.* Radiat Res, 1990. **122**(1): p. 86-94.

204. Nevaldine, B., J.A. Longo, and P.J. Hahn, *The scid defect results in much slower repair of DNA double-strand breaks but not high levels of residual breaks.* Radiat Res, 1997. **147**(5): p. 535-40.

205. Wang, H., et al., *Genetic evidence for the involvement of DNA ligase IV in the DNA-PK-dependent pathway of non-homologous end joining in mammalian cells.* Nucleic Acids Res, 2001. **29**(8): p. 1653-60.

206. di Masi, A., et al., *The R527H mutation in LMNA gene causes an increased sensitivity to ionizing radiation.* Cell Cycle, 2008. **7**(13): p. 2030-7.

207. Rai, R., et al., *The function of classical and alternative non-homologous end-joining pathways in the fusion of dysfunctional telomeres.* EMBO J, 2010.

208. Chen, L., et al., *Interactions of the DNA ligase IV-XRCC4 complex with DNA ends and the DNA-dependent protein kinase.* J Biol Chem, 2000. **275**(34): p. 26196-205.

209. Zhang, J., et al., *MDC1 interacts with Rad51 and facilitates homologous recombination.* Nat Struct Mol Biol, 2005. **12**(10): p. 902-9.

210. Mekeel, K.L., et al., *Inactivation of p53 results in high rates of homologous recombination.* Oncogene, 1997. **14**(15): p. 1847-57.

211. Hegan, D.C., et al., *Inhibition of poly(ADP-ribose) polymerase down-regulates BRCA1 and RAD51 in a pathway mediated by E2F4 and p130.* Proc Natl Acad Sci U S A, 2010. **107**(5): p. 2201-6.

212. Bindra, R.S. and P.M. Glazer, *Repression of RAD51 gene expression by E2F4/p130 complexes in hypoxia.* Oncogene, 2007. **26**(14): p. 2048-57.

213. Assenmacher, N. and K.P. Hopfner, *MRE11/RAD50/NBS1: complex activities.* Chromosoma, 2004. **113**(4): p. 157-66.

214. Yun, M.H. and K. Hiom, *Understanding the functions of BRCA1 in the DNA-damage response.* Biochem Soc Trans, 2009. **37**(Pt 3): p. 597-604.

215. Yun, M.H. and K. Hiom, *CtIP-BRCA1 modulates the choice of DNA double-strand-break repair pathway throughout the cell cycle.* Nature, 2009. **459**(7245): p. 460-3.

216. de Lange, T., *Protection of mammalian telomeres.* Oncogene, 2002. **21**(4): p. 532-40.

217. Blackburn, E.H., *Switching and signaling at the telomere.* Cell, 2001. **106**(6): p. 661-73.

218. Blackburn, E.H., et al., *Molecular manifestations and molecular determinants of telomere capping.* Cold Spring Harb Symp Quant Biol, 2000. **65**: p. 253-63.

219. Blasco, M.A., *The epigenetic regulation of mammalian telomeres.* Nat Rev Genet, 2007. **8**(4): p. 299-309.

220. Gotta, M., et al., *The clustering of telomeres and colocalization with Rap1, Sir3, and Sir4 proteins in wild-type Saccharomyces cerevisiae.* J Cell Biol, 1996. **134**(6): p. 1349-63.

221. Jin, Q.W., J. Fuchs, and J. Loidl, *Centromere clustering is a major determinant of yeast interphase nuclear organization.* J Cell Sci, 2000. **113 (Pt 11)**: p. 1903-12.

222. Hediger, F. and S.M. Gasser, *Nuclear organization and silencing: putting things in their place.* Nat Cell Biol, 2002. **4**(3): p. E53-5.

223. Schober, H., et al., *Yeast telomerase and the SUN domain protein Mps3 anchor telomeres and repress subtelomeric recombination.* Genes Dev, 2009. **23**(8): p. 928-38.

224. Andrulis, E.D., et al., *Esc1, a nuclear periphery protein required for Sir4-based plasmid anchoring and partitioning.* Mol Cell Biol, 2002. **22**(23): p. 8292-301.

225. Gartenberg, M.R., et al., *Sir-mediated repression can occur independently of chromosomal and subnuclear contexts.* Cell, 2004. **119**(7): p. 955-67.

226. Taddei, A., et al., *Separation of silencing from perinuclear anchoring functions in yeast Ku80, Sir4 and Esc1 proteins.* Embo J, 2004. **23**(6): p. 1301-12.

227. Palladino, F., et al., *SIR3 and SIR4 proteins are required for the positioning and integrity of yeast telomeres.* Cell, 1993. **75**(3): p. 543-55.

228. Scherthan, H., *Factors directing telomere dynamics in synaptic meiosis.* Biochem Soc Trans, 2006. **34**(Pt 4): p. 550-3.

229. de Lange, T., *Human telomeres are attached to the nuclear matrix.* Embo J, 1992. **11**(2): p. 717-24.

230. Luderus, M.E., et al., *Structure, subnuclear distribution, and nuclear matrix association of the mammalian telomeric complex.* J Cell Biol, 1996. **135**(4): p. 867-81.

231. Bronstein, I., et al., *Transient anomalous diffusion of telomeres in the nucleus of mammalian cells.* Phys Rev Lett, 2009. **103**(1): p. 018102.

232. Gonzalez-Suarez, I. and S. Gonzalo, *Crosstalk between chromatin structure, nuclear compartmentalization, and telomere biology.* Cytogenet Genome Res, 2008. **122**(3-4): p. 202-10.

233. Verstraeten, V.L., et al., *The nuclear envelope, a key structure in cellular integrity and gene expression.* Curr Med Chem, 2007. **14**(11): p. 1231-48.

234. Dechat, T., et al., *LAP2alpha and BAF transiently localize to telomeres and specific regions on chromatin during nuclear assembly.* J Cell Sci, 2004. **117**(Pt 25): p. 6117-28.

235. Markiewicz, E., et al., *Lamin A/C binding protein LAP2alpha is required for nuclear anchorage of retinoblastoma protein.* Mol Biol Cell, 2002. **13**(12): p. 4401-13.

236. Lattanzi, G., et al., *Pre-Lamin A processing is linked to heterochromatin organization.* J Cell Biochem, 2007. **102**(5): p. 1149-59.

237. Kudlow, B.A., et al., *Suppression of proliferative defects associated with processing-defective lamin A mutants by hTERT or inactivation of p53.* Mol Biol Cell, 2008. **19**(12): p. 5238-48.

238. Benetti, R., et al., *A mammalian microRNA cluster controls DNA methylation and telomere recombination via Rbl2-dependent regulation of DNA methyltransferases.* Nat Struct Mol Biol, 2008. **15**(3): p. 268-79.

239. Jones, B., et al., *The histone H3K79 methyltransferase Dot1L is essential for mammalian development and heterochromatin structure.* PLoS Genet, 2008. **4**(9): p. e1000190.

240. Muntoni, A. and R.R. Reddel, *The first molecular details of ALT in human tumor cells.* Hum Mol Genet, 2005. **14 Spec No. 2**: p. R191-6.

241. Gonzalo, S. and M.A. Blasco, *Role of Rb family in the epigenetic definition of chromatin.* Cell Cycle, 2005. **4**(6): p. 752-5.

242. Wang, M., et al., *PARP-1 and Ku compete for repair of DNA double strand breaks by distinct NHEJ pathways.* Nucleic Acids Res, 2006. **34**(21): p. 6170-82.

243. Wang, X., et al., *Rapid telomere motions in live human cells analyzed by highly time-resolved microscopy.* Epigenetics Chromatin, 2008. **1**(1): p. 4.

244. De Vos, W.H., et al., *Increased plasticity of the nuclear envelope and hypermobility of telomeres due to the loss of A-type lamins.* Biochim Biophys Acta, 2010. **1800**(4): p. 448-58.

245. Lankelma, J.M., et al., *Cathepsin L, target in cancer treatment?* Life Sci, 2010. **86**(7-8): p. 225-33.

246. Joyce, J.A. and D. Hanahan, *Multiple roles for cysteine cathepsins in cancer.* Cell Cycle, 2004. **3**(12): p. 1516-619.

247. Harrington, E.A., et al., *pRB plays an essential role in cell cycle arrest induced by DNA damage.* Proc Natl Acad Sci U S A, 1998. **95**(20): p. 11945-50.

248. Zhang, J. and S.N. Powell, *The role of the BRCA1 tumor suppressor in DNA double-strand break repair.* Mol Cancer Res, 2005. **3**(10): p. 531-9.

249. Blasco, M.A., et al., *Telomere shortening and tumor formation by mouse cells lacking telomerase RNA.* Cell, 1997. **91**(1): p. 25-34.

250. Herrera, E., E. Samper, and M.A. Blasco, *Telomere shortening in mTR-/- embryos is associated with failure to close the neural tube.* Embo J, 1999. **18**(5): p. 1172-81.

251. Zijlmans, J.M., et al., *Telomeres in the mouse have large inter-chromosomal variations in the number of T2AG3 repeats.* Proc Natl Acad Sci U S A, 1997. **94**(14): p. 7423-8.

252. Shechter, D., et al., *Extraction, purification and analysis of histones.* Nat Protoc, 2007. **2**(6): p. 1445-57.

SUPPLEMENTARY METHODS

SUPPLEMENTARY METHODS

Distribution of the telomeres

To analyze the distribution of the telomeres we have chosen as metric; the shortest distance from the telomere to the edge of the convex hull [1], see figure 1. The fluorescent images of the telomere channel have been deconvolved, using in-house deconvolution software written in MatLab (The Mathworks, Natick, MA, USA). The MAPPG algorithm is chosen for devolving as described in [2]. The point spread function (PSF) used is an analytical PSF implemented according to [3]. After deconvolution, four steps are taken: 1. localization of the telomere signals, 2. computation of the convex hull, 3. computation of the distance transform within the convex hull, 4. extraction of the distance and intensity of the telomere fluorescent signal. All analyses have been done in 3D, but for clarification we have shown an example of the algorithms in 2D in figure 1. To determine the position of the telomeres we have used TeloView [4]. This program is especially designed to locate telomere FISH signals in images of fluorescently labeled nuclei. It uses a set of image processing algorithms from DIPimage, developed at the Quantitative Imaging Group (TU-Delft, The Netherlands, http://www.diplib.org) [5]. Both TeloView and DIPimage are implemented in MatLab. localization of the telomere signal, is performed as described in [6]. In short: after a scale space method, which enhances the contrast of the signal, a threshold is chosen to segment the telomere signals. Using the graphical interface of TeloView missed signals can be added or false signals can be removed. The second step is the calculation of the convex hull [1], which is the smallest convex volume enclosing all the found telomeres. For the next step we transform the hull into a distance matrix using the Euclidian Distance Transform (EDT) [7, 8]. The EDT transforms the binary image (the convex hull image) into an image where the intensity level of the pixel is the shortest distance from this pixel to the edge of the hull.

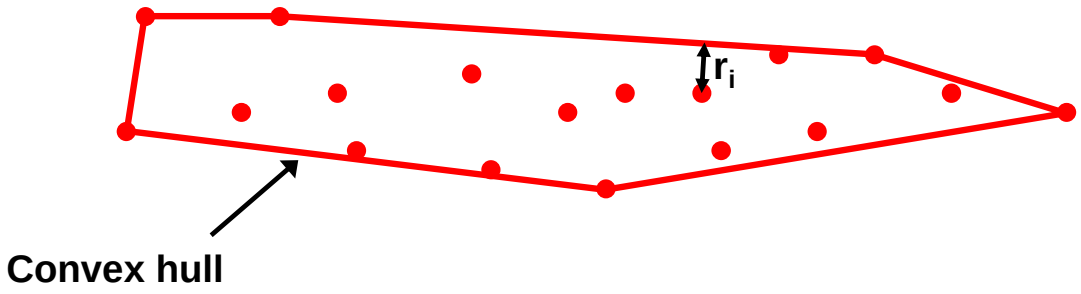

Figure 1: Cartoon showing the distance measure. The red dots represent the telomere signals. The red line represents the convex hull surrounding the telomeres. For every telomere we measure, r_i; the shortest distance from the surface of the convex hull to the telomere.

Distribution of the telomere intensity

The fourth step is to calculate the integrated intensity of the telomere. The integrated intensity is proportional to the size of the telomere because the size is proportional to the amount of fluorochrome that is attached to the telomere and therefore to the telomere length [9]. We create a binary mask with the watershed algorithm [10] of the image data,

g, convolved with a Gaussian profile with $\sigma = 1$ pixel for noise reduction. Now the telomere coordinates (x_n, y_n, z_n), determined above, tell us which objects in this mask are telomere regions. Simply integrating intensities in these regions will also give the wrong answer because background pixels are not excluded from these regions and will bias our calculations. Our solution is to calculate the integrated intensity in a region of interest with (x_n, y_n, z_n) as middle point within this mask resulting from the watershed. The region of interest is a small sphere, with radius r, convolved with a Gaussian profile with width $\sigma = 1$ pixel in the lateral and $\sigma = 3$ pixels in the axial direction, which results in an elongated sphere. We will call this region of interest, which is gray-scale, $sphere_{gray}$ and the region from the watershed, which is binary, we will call *mask*. The next binary region with which we work with is $sphere_{bin}$. This is a binary sphere with radius $r + 3\sigma$ (with $\sigma = 1$ or 3 pixels depending on the direction). Now we define the mean of the grey values of g at the coordinates where *mask* has value one and $sphere_{bin}$ has value zero as our background level, b. Our signal image, g_{signal}, becomes:

$$g_{signal} = g(mask) - b \tag{1}$$

We normalize both $sphere_{gray}$ and g_{signal} for their maximum value and calculate their mean squared difference, ε_{new}, using $sphere_{gray}$ as a weighting function:

$$\varepsilon_{new} = \frac{\sum_i sphere_{gray,i}(sphere_{gray,i} - g_{signal})^2}{\sum_i sphere_{gray,i}} \tag{2}$$

This process starts with $r = 1$. First we rename ε_{new}:

$$\varepsilon_{old} = \varepsilon_{new} \tag{3}$$

Now we grow the region by using $r = r + 1$ for the next iteration and calculate ε_{new} again. The iterative process is stopped when

$$\varepsilon_{new} > \varepsilon_{old} \tag{4}$$

The integrated intensity, I_n, for the n^{th} telomere is now

$$I_n = \sum g_{signal}(sphere_{bin}) \tag{5}$$

In figure 2 we show a flow chart of the algorithm.

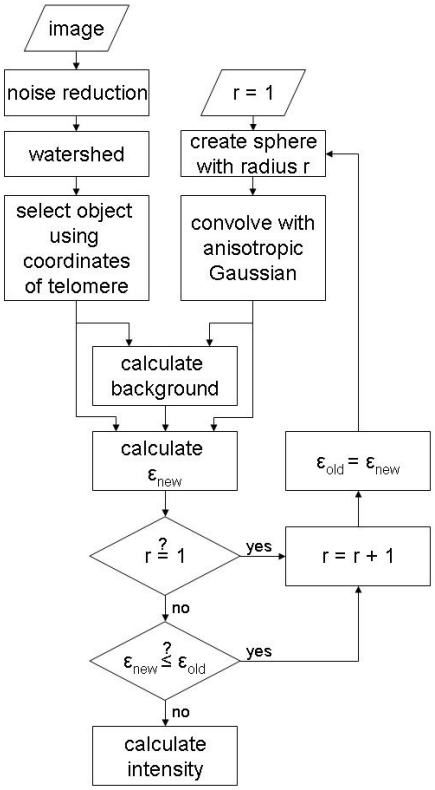

Figure 2: Flow chart showing the algorithm to calculate the integrated intensity of a telomere signal. The basic idea is to calculate the integrated intensity in a growing region of interest until no more intensity is added. The growing is confined by a mask created by a watershed.

References

1. Barber, C.B., D.P. Dobkin, and H. Huhdanpaa, *The Quickhull algorithm for convex hulls.* ACM Transactions on Mathematical Software, 1996. **22**(4): p. 469-483.
2. Verveer, P.J. and T.M. Jovin, *Efficient superresolution restoration algorithms using maximum a posteriori estimations with application to fluorescence microscopy.* Journal of the Optical Society of America a-Optics Image Science and Vision, 1997. **14**(8): p. 1696-1706.
3. Gibson, S.F. and F. Lanni, *DIFFRACTION BY A CIRCULAR APERTURE AS A MODEL FOR 3-DIMENSIONAL OPTICAL MICROSCOPY.* Journal of the Optical Society of America a-Optics Image Science and Vision, 1989. **6**(9): p. 1357-1367.
4. Vermolen, B.J., et al., *3D nuclear organization of telomeres in normal and cancerous mammalian cells.* Cytometry Part A, 2004. **59A**(1): p. 97-97.

5. Luengo Hendriks, C.L., et al., *DIPimage, a scientific image processing toolbox for MATLAB.* 1999, Pattern Recognition Group, Department of Applied Physics, Delft University of Technology.
6. Vermolen, B.J., et al., *Segmentation and Analysis of the Three-Dimensional Redistribution of Nuclear Components in Human Mesenchymal Stem Cells.* Cytometry Part A, 2008. **73A**: p. 816-824.
7. Danielsson, P.E., *EUCLIDEAN DISTANCE MAPPING.* Computer Graphics and Image Processing, 1980. **14**(3): p. 227-248.
8. Mullikin, J.C., *THE VECTOR DISTANCE TRANSFORM IN 2 AND 3 DIMENSIONS.* Cvgip-Graphical Models and Image Processing, 1992. **54**(6): p. 526-535.
9. Lansdorp, P., et al., *Heterogeneity in telomere length of human chromosomes.* Hum. Mol. Genet., 1996. **5**(5): p. 685-691.
10. Verwer, B.J.H., L.J.v. Vliet, and P.W. Verbeek, *Binary and grey-value skeletons: metrics and algorithms.* International Journal of Pattern Recognition and Artificial Intelligence, 1993. **7**(5): p. 1287-1308.